AN ABSTRACT OF THE THESIS OF

Garrett W. Meigs for the degree of Master of Science in Forest Science presented on June 8, 2009.

Title: Carbon Dynamics following Landscape Fire: Influence of Burn Severity, Climate, and Stand History in the Metolius Watershed, Oregon

Abstract approved:

_____

Beverly E. Law

Fire is a fundamental disturbance that drives terrestrial and atmospheric carbon dynamics. Previous studies have quantified fire effects on carbon cycling from local to global scales but have focused nearly exclusively on high-severity, stand-replacement fire. Since 2002, variable-severity wildfires have burned more than 65 000 ha across the east slope of the Oregon Cascades, including 4 large fires that burned *ca.* 50% of the forested area within the Metolius Watershed in 2002 and 2003. This thesis integrates data from 64 field plots, remote-sensing, and an ecosystem process model to investigate the effects of low-, moderate-, and high-severity fire. The primary research objectives were to: (a) quantify combustion and mortality effects on carbon pools, postfire net ecosystem production (NEP), and potential regeneration trajectories at the stand scale; (b) introduce novel remote-sensing datasets into a modeling framework to assess the importance of low- and moderate-severity fire across the landscape and region.

At the stand-scale, the 3 levels of burn severity (overstory tree mortality) resulted in profoundly different impacts on combustion, mortality, postfire carbon balance, and potential regeneration trajectories. Simulated combustion ranged from 16.6 to 32.3 Mg C ha^{-1}, or 13% to 35% of prefire aboveground carbon. C transfers from fire-induced tree mortality were larger in magnitude than combustion, as live aboveground C decreased by >90% from low- to high-severity stands. Despite this decline, total net primary

productivity (NPP) was only 40% lower in high- vs. low-severity stands, reflecting a compensatory effect of non-tree NPP. Dead wood respiratory losses were small relative to C uptake (range: 10-35% of total NPP), suggesting important decomposition lags in this seasonally-arid system. Although soil C, soil respiration, and fine root NPP were conserved across severity classes, NEP declined with increasing severity, driven by trends in aboveground NPP. Postfire conifer seedling density was generally abundant and varied over 5 orders of magnitude (study-wide median: 812, range: 0 – 62 134 seedlings ha^{-1}). Seedling density was negatively correlated with overstory mortality, whereas shrub biomass showed the opposite response, indicating a wide range of potential successional trajectories. Despite substantial combustion and mortality effects on carbon pools and fluxes, the rapid response of postfire vegetation, coupled with conservation of belowground processes, may offset long-term declines in carbon storage, indicating a surprising degree of postfire stability. These stand-scale results describe a broad range of fire effects—a high degree of pyrodiversity—but because burn severity was not evenly distributed across space, the landscape-level fire effects depend on the severity mosaic.

At the landscape-scale, moderate- and low-severity fire contributed 25% and 11% of total estimated pyrogenic carbon emission, respectively (0.66 Tg C total, or *ca.* 2.2% of statewide anthropogenic CO_2 emissions equivalent from the same 2-year period). Moderate- and low-severity fire accounted for 23% and 5% of landscape-level tree mortality, respectively, which resulted in the transfer of 2.00 Tg C from live to dead pools. This carbon transfer was *ca.* 3-fold higher than the one-time pulse from pyrogenic emission, but it will likely take decades for this dead wood to decompose via heterotrophic respiration. The inclusion of moderate-severity fire reduced postfire (2004) mean annual NEP by 39% compared to the high-severity only scenario; low-severity fire influence on NEP was small (additional reduction of 11% in mean NEP), likely because of high tree survivorship and the relatively lower areal coverage of low-severity fire. One year postfire, burned areas were a strong C source (net C exchange across 53 000 ha: -0.065 Tg C y^{-1}; mean ± SD: -123 ± 110 g C m^{-2} y^{-1}) vs. a prefire mean near C neutral (1997-2001 mean NEP ± SD: -5 ± 51 g C m^{-2} y^{-1}). The model has been known to

underestimate carbon uptake in mature and old semi-arid forests, so the prefire value is likely underestimated.

Despite the resurgence of wildfire across western North America, including a substantial increase in the proportion of high-severity fire in the ecoregions studied here, low- and moderate-severity wildfire accounts for the majority of burned area in the Pacific Northwest region. This non-stand-replacement fire has important consequences for carbon loss and uptake at landscape- and regional-scales. The results from this thesis suggest that by accounting for the full gradient of fire effects, carbon modelers can substantially reduce uncertainties in key components of regional and global carbon budgets, particularly pyrogenic emissions, mortality, and NEP. Understanding the effects of disturbance variability on terrestrial carbon cycling will become increasingly important in the context of emerging regional and global carbon policies.

Carbon Dynamics following Landscape Fire: Influence of Burn Severity,
Climate, and Stand History in the Metolius Watershed, Oregon

by
Garrett W. Meigs

A THESIS

submitted to

Oregon State University

In partial fulfillment of
the requirements for the
degree of

Master of Science

Presented June 8, 2009
Commencement June 2010

Master of Science thesis of Garrett W. Meigs presented on June 8, 2009.

APPROVED:

_____

Major Professor, representing Forest Science

_____

Head of the Department of Forest Ecosystems and Society

_____

Dean of the Graduate School

I understand that my thesis will become part of the permanent collection of Oregon State University libraries. My signature below authorizes release of my thesis to any reader upon request.

_____

Garrett W. Meigs, Author

ACKNOWLEDGEMENTS

particularly Cheryll Alex, facilitated an excellent and efficient graduate program. Many faculty members provided valuable feedback and were always willing to share their time and resources, both in and out of the classroom. The graduate students in the College of Forestry cultivated a remarkable community of friends and scholars. And of course, I was catalyzed by the "pyro-maniacs," who kindled many a great discussion and challenged me to delve deeper into the interactions between fire, fuels, and carbon.

My loving family has always fostered my curiosity for the natural world and encouraged me to pursue my disturbance ecology aspirations.

Finally, I am forever grateful for my *ichiban*, Cassie L. Hebel, who tolerated my sleep deficits and idiosyncrasies, supporting me continuously with research feedback, wonderful adventures, and garden-fresh feasts in our happy, peaceful home.

CONTRIBUTION OF AUTHORS

Beverly E. Law assisted with study design, data analysis, and writing of Chapters 2 and 3. Daniel C. Donato, John L. Campbell, and Jonathan G. Martin assisted with study design, data collection, analysis, and writing of Chapter 2. David P. Turner assisted with study design, simulation modeling, and writing of Chapter 3. William D. Ritts and Yang Zhiqiang assisted with simulation modeling and writing of Chapter 3. Manuscripts associated with Chapters 2 and 3 were in the process of peer review at the time this thesis was submitted.

TABLE OF CONTENTS

LIST OF FIGURES

LIST OF FIGURES (continued)

LIST OF TABLES

LIST OF APPENDIX FIGURES

LIST OF APPENDIX TABLES

PREFACE

The stability was of a wildly dynamic sort.

Kurt Vonnegut
<u>Cat's Cradle</u>
1963

CHAPTER 1 || INTRODUCTION

Forest ecosystems are inherently dynamic, defined by change more than constants. In many parts of the world, including western North America, wildfire is the principal disturbance factor—or agent of ecosystem change (Agee 1993). As such, fire is a fundamental driver of carbon dynamics, generating patterns of live and dead carbon pools, as well as periodic pulses of carbon to the atmosphere through combustion. Because fire can drive long-term carbon storage and shift the short-term balance between carbon sink and source, it is increasingly crucial to understand in this era of rapid, unpredictable anthropogenic climate change. As new policies addressing carbon emissions, land use, and forest management emerge, understanding the role of disturbance, and fire in particular, remains an important research frontier (Running 2008).

Though nearly universal as a disturbance factor, fire effects are anything but uniform across time and space. Just as forests are defined by change, fire regimes are defined by variability. The mixed-severity fire regime is widespread and complex, exhibiting high pyrodiversity (*sensu* Martin and Sapsis 1991) and including elements of both surface and stand-replacement fire at irregular frequencies. Although mixed-severity fire is a dominant disturbance process in much of the Pacific Northwest, previous studies have focused primarily on high-severity, stand-replacement fire. This thesis contributes to our growing understanding of the role of disturbance heterogeneity in shaping forest carbon cycling by explicitly comparing low, moderate, and high-severity wildfire.

This project builds on a strong legacy of carbon cycle research in the Metolius River area of Oregon and takes advantage of a large natural experiment resulting from recent landscape-scale wildfires. Specifically, Chapter 2 describes results from an intensive field campaign across 4 fires that burned 35% of the Metolius Watershed (115 000 ha) in 2002 and 2003. This study surveyed 64 inventory plots stratified across 3 landscape gradients: burn severity (overstory mortality), forest type (ponderosa pine and mixed-conifer), and prefire biomass. The research objective was to quantify: (a) combustion and mortality effects on carbon pools; (b) postfire net ecosystem production (NEP); (c) regeneration and potential C trajectories. The stand-scale results describe a

wide range of short-term fire effects and responses that will influence carbon storage for decades. This chapter also highlights the apparent resistance of these disturbance-prone forests to fire-induced state changes, suggesting a surprising degree of ecosystem stability.

Chapter 3 integrates Landsat-based detection of fire extent and severity from the Monitoring Trends in Burn Severity database with the Biome-BGC process model to investigate the impacts of the same large fires at the landscape-scale. Specifically, this chapter focuses on improving the way the Biome-BGC model accounts for disturbance events, comparing 3 scenarios: high severity only (other areas assumed unburned), moderate and high severity, and all severities (low, moderate, and high). After describing the improved disturbance coverage enabled by new model parameterizations, as well as regional patterns of burn severity, Chapter 3 reports on the net effects of the 2002-2003 fires on carbon pools, fluxes, and pyrogenic emission. The chapter concludes with a discussion of remaining uncertainties and future research opportunities for landscape and regional carbon modeling.

Chapter 4 synthesizes emergent themes from Chapters 2 and 3 and concludes the thesis by placing the recent wildfires in a broader context of global change, disturbance ecology, and future research priorities.

CHAPTER 2 || INFLUENCE OF WILDFIRE SEVERITY ON PYROGENIC CARBON TRANSFERS, POSTFIRE CARBON BALANCE, AND REGENERATION TRAJECTORIES IN THE EASTERN CASCADES, OREGON

ABSTRACT

Since 2002, variable-severity wildfires have burned more than 65 000 ha in the Eastern Cascades of Oregon. This study quantifies: (a) combustion and mortality effects on carbon pools; (b) postfire net ecosystem production (NEP); (c) regeneration and potential C trajectories. We surveyed 64 forest stands across four fires that burned 35% of the Metolius Watershed (115 000 ha) in 2002 and 2003, stratifying the landscape by burn severity (overstory mortality), forest type (ponderosa pine [PP] and mixed-conifer [MC]), and prefire biomass. Stand-scale C combustion ranged from 13% to 35% of prefire aboveground C (area-weighted mean = 22%). Across the sampled landscape, total estimated pyrogenic C emission was 0.76 Tg C, equivalent to 2.5% of statewide anthropogenic CO_2 emissions from the same 2-year period. C transfers from fire-induced tree mortality were larger in magnitude than combustion, as live aboveground C decreased by >90% from low- to high-severity stands. Despite this decline, total net primary productivity (NPP) was only 40% lower in high- vs. low-severity stands, reflecting a compensatory effect of non-tree NPP. Dead wood respiratory losses were small relative to C uptake (range: 10-35% of total NPP), suggesting important decomposition lags in this seasonally-arid system. Although soil C, soil respiration, and fine root NPP were conserved across severity classes, NEP declined with increasing severity, driven by trends in aboveground NPP. Postfire conifer seedling density was generally abundant and varied over 5 orders of magnitude (study-wide median: 812, range: 0 – 62 134 seedlings ha^{-1}). Seedling density was negatively correlated with overstory mortality, whereas shrub biomass showed the opposite response, indicating a wide range of potential successional trajectories across the mixed-severity mosaic. Despite substantial combustion and mortality effects on C pools and fluxes, postfire vegetation responded rapidly, potentially reducing long-term declines in C storage in this disturbance-prone system.

INTRODUCTION

Forest ecosystems play a vital role in the global carbon cycle, and spatiotemporal variability due to disturbance remains an active frontier in carbon research (Goward and others 2008; Running 2008). With increasing focus on forests in the context of climate change and potential mitigation strategies for anthropogenic carbon emissions (CCAR 2007; IPCC 2007), it is important to quantify the impacts associated with anthropogenic and natural disturbance regimes, particularly wildfire. Although numerous studies have investigated the effects of fire on carbon dynamics, very few to date have analyzed the full spectrum of burn severity and compared pyrogenic carbon transfers, postfire carbon balance, and regeneration dynamics across multiple forest types in the first few years following disturbance.

Fire's role in the terrestrial carbon (C) cycle has been studied extensively in the boreal zone (*e.g.,* Hicke and others 2003; Kurz and others 2008) and, to a lesser extent, in temperate forests (*e.g.,* Kashian and others 2006; Gough and others 2007), but many uncertainties remain. Like other disturbances (insects, pathogens, large storms), fire alters the distribution of live and dead C pools and associated C fluxes through mortality and regeneration, but fire also causes direct C emission through combustion (Amiro and others 2001; Campbell and others 2007; Bormann and others 2008). Depending on burn severity (defined here as overstory tree mortality), C transfer to the atmosphere, and from live to dead pools can vary substantially. In some cases the amount of C released from necromass decomposition over decades can exceed one-time emissions from combustion (Wirth and others 2002; Hicke and others 2003; this thesis, Chapter 3). One key uncertainty is the magnitude of pyrogenic C emission and the relative combustion of different C pools (Campbell and others 2007). Another important uncertainty is the rate at which postfire vegetation net primary productivity (NPP) offsets the lagged decomposition of necromass pools and their effects on net ecosystem production (NEP; Wirth and others 2002). A third uncertainty is the change in heterotrophic respiration (R_h) and soil C over the first few years postfire. Although fire might increase R_h or facilitate soil C loss, studies in Western Oregon have shown that both can be remarkably conserved following disturbance, buffering potential negative spikes in postfire NEP

(Campbell and others 2004, 2009; Irvine and others 2007). A final uncertainty is the distribution and abundance of understory vegetation—conifer regeneration, shrubs, and herbs—which influence both short-term NPP dynamics and C balance through succession. All of these ecosystem responses and uncertainties might diverge radically in high- vs. low-severity stands, but most fire-carbon studies have been limited to stand-replacement events. For example, regional and continental C models typically ignore low-severity fire, largely due to remote-sensing detection limitations (Turner and others 2007), despite the inherent heterogeneity of fire effects across forest landscapes.

The area burned by wildfire has increased in recent decades across western North America due to an interaction of time since previous fire, forest management, and climate (Westerling and others 2006; Keane and others 2008). Recent fires have also exhibited increasing severity, but low- and moderate-severity fire effects remain an important component of nearly all large wildfires (Schwind 2008; Miller and others 2009). The mixed-severity fire regime, defined by a wide range and high variability of fire frequencies and effects (*i.e.,* high pyrodiversity; Martin and Sapsis 1991), is characteristic of many forest types (Schoennagel and others 2004; Lentile and others 2005; Hessburg and others 2007) and may represent a new fire regime in other types that historically burned with lower severity (Monsanto and Agee 2008). The widespread increase in burned area, combined with the intrinsic variability of mixed-severity fire regimes, represents a potentially dramatic and unpredictable shift in terrestrial C cycle processes. In addition, historically uncharacteristic fires in some systems, including ponderosa pine *(Pinus ponderosa)* forests, can push vegetation into fundamentally different successional pathways and disturbance feedbacks (Savage and Mast 2005; Bradley and others 2006), which may lead to long-term reductions in terrestrial C storage (Dore and others 2008).

Since 2002, large wildfires have burned approximately 65 000 ha in and around the Metolius River Watershed in the Oregon East Cascades (Fig. 2.1). These fires generated a mosaic of variable burn severity across multiple forest types and a wide range of prefire conditions. The extent and variability of these fires, coupled with robust existing datasets on C pools and fluxes in unburned forests in the Metolius area (*e.g.,* Law and others 2001a, 2003), presented a unique opportunity to understand fire's impacts

on the terrestrial C cycle. In this study, we investigated C dynamics and vegetation responses across three levels of burn severity and two forest types 4-5 years postfire. Our research objective was to quantify three related response variables associated with immediate, short-term, and long-term fire effects, respectively:

1. *Pyrogenic C transfers:* combustion and mortality effects on C pools (immediate).

2. *Postfire C balance:* fire effects on C fluxes and net ecosystem production (short-term).

3. *Postfire regeneration:* understory responses and potential C trajectories (long-term).

METHODS

Study area

The Metolius Watershed is located NW of Sisters, OR and delineated by the Cascade Crest to the W and the Deschutes River to the E (Fig. 2.1). The Metolius River is primarily spring-fed from high-elevation precipitation and groundwater on both sides of the Crest (USDA 1996, USDA 2004). The watershed includes approximately 100 000 ha of forest, almost half of which has burned since 2002. Most of the area is administered by the Deschutes National Forest (DNF), with private inholdings and a portion inhabited by the Confederated Tribes of Warm Springs. The postfire landscape is shaped by three important environmental gradients: forest type associated with climate, prefire biomass associated with past disturbance and management, and burn severity from recent fires (defined here as overstory tree mortality).

Forest type and climatic setting. The east slope of the Oregon Cascades is defined by a steep climatic gradient from high-elevation subalpine forests (cool, wet) to low-elevation *Juniperus* woodlands (warm, dry), with several forest types exhibiting an unusually rich assemblage of conifer species (Swedberg 1973). This study focuses on the two most prominent forest types—ponderosa pine (PP) and mixed-conifer (MC)—which encompass the *Pinus ponderosa* and *Abies grandis* forest zones of Eastern Oregon (Franklin and Dyrness 1973). The higher elevation, mesic MC forest is generally more productive and supports higher biomass than the PP forest. In the MC forest type, ponderosa pine, grand fir *(Abies grandis)*, and Douglas-fir *(Pseudotsuga menziesii)* are the dominant trees species, and incense-cedar *(Calocedrus decurrens),* western larch *(Larix occidentalis),* and lodgepole pine *(Pinus contorta)* are also abundant (see Appendix 1 for full woody species list and taxonomy). In the PP forest type, ponderosa pine is dominant, with frequent presence of incense-cedar. Across both forest types, characteristic understory species include shrubs greenleaf manzanita *(Arctostaphylos patula),* snowbrush *(Ceanothus velutinus),* and bitterbrush *(Purshia tridentata)*; forbs fireweed *(Epilobium angustifolium),* bracken fern *(Pteridium aquilinum),* and American vetch *(Vicia americanum)*; and graminoids pinegrass *(Calamagrostis rubescens),* squirreltail grass *(Elymus elymoides)*, and Idaho fescue *(Festuca idahoensis).*

Study area elevation ranges from 600 m to 2000 m (summit of Black Butte). Despite generally gradual slopes (up to 22° in sampled plots), this area is among the steepest precipitation gradients in western North America (Daly and others 2002; PRISM Group, Oregon St. Univ., prismclimate.org), spanning the transition from a maritime to a continental climate (Swedberg 1973). Mean annual precipitation ranges from 400 mm in eastern parts of the PP forest type to 2150 mm at high points in the MC forest type (estimated from a 23 y record of spatially-modeled climate data; Thornton and others 1997, DAYMET 2009). Summers are warm and dry, and most of the annual precipitation falls as snow between October and June (Law and others 2001a). From west to east across the study area, average minimum January temperature ranges from -6 °C to -3.5 °C, and average maximum July temperature ranges from 22 °C to 30 °C (DAYMET 2009). Soils are volcanic in origin (vitricryands and vitrixerands), well-drained sandy loams/loamy sands. Additional study area characteristics are summarized in Table 2.1, and characteristic postfire stands are shown in Fig. 2.2.

Historic disturbance and prefire biomass. The Metolius Watershed spans a range of historic fire regimes, from frequent, low-severity fire in PP to infrequent, high-severity fire in subalpine forests. Historic fire return intervals ranged from 3 to 38 y in PP forests (Weaver 1959; Soeriaatmadhe 1966; Bork 1985; Fitzgerald 2005), from 9 to 53 y in the MC forest type (Bork 1985; Simon 1991), and up to 168 y in subalpine forests *(Tsuga mertensiana)* (Simon 1991). Given the abundance of lightning ignitions (Rorig and Ferguson 1999), lack of prominent topographic barriers, and high vegetation connectivity, it is likely that historic fires burned through multiple forest types and exhibited high spatial and temporal variability in fire behavior. Thus, mixed-severity fire effects have likely been a component of all forest types in the area; this complex disturbance regime is widespread in Western North America but is not well understood (Schoennagel and others 2004).

In addition to fire, several other disturbance agents have shaped these forests, including volcanoes, insects, severe drought, ice storms, and pre-European anthropogenic management, and the prefire landscape was a mosaic of stand ages associated with these legacies. During the 20th Century, fire suppression, grazing, timber harvest, and road

construction resulted in effective fire exclusion. By 2002, many low-elevation PP stands were outside the range of historic fire return intervals, and high-elevation forests were reaching the upper limits of their range. Anthropogenic disturbance dominated landscape pattern and process. Dispersed patch clearcutting was the primary disturbance in recent decades, and most low biomass areas were young plantations (DNF silvicultural GIS data). Relatively dry years between 1985 and 1994 (DAYMET 2009, Thomas and others, 2009) contributed to regional drought stress, and beginning in 1986, an outbreak of Western spruce budworm *(Choristoneura occidentalis)* and bark beetles (Family *Scolytidae*) defoliated and killed trees across a substantial portion of mid- to high-elevation MC forest (Waring and others 1992; Franklin and others 1995; Filip and others 2007). In addition, the Metolius Watershed experienced anomalously dry and warm years from about 2000 to 2007, with 2001, 2003, and 2005 being 3 of the most severe drought years (Fig. 2.3). All of these interacting factors—time since previous fire, forest management, climate, and insect activity—likely contributed to high fuel accumulations and horizontal and vertical connectivity, setting the stage for landscape-scale wildfire. Recognizing the potential threats, the DNF and general public identified stands at high risk of "catastrophic" wildfire and had initiated a process of active fuels management and forest restoration (USDA 2003b).

Recent large wildfires. Since 2002, more than 10 large (>400 ha), variable-severity wildfires have burned about half of the forested area in the Metolius Watershed. The landscape fires burned across multiple forest types and land ownerships and a wide range of fuel, weather, and topographic conditions. Surface, torching, and active crown fire behavior yielded a heterogeneous spatial pattern of tree mortality and survival at stand- and landscape-scales, initiating diverse postfire C trajectories (Fig. 2.2). This study focused on the four major fires that burned *ca.* 35% of the watershed in 2002-2003 (Fig. 2.1, Table 2.2).

Sampling design and scope

We measured postfire C pools and fluxes and vegetation regeneration at 64 independent forest stands across the Metolius Watershed (Fig. 2.1), sampling burned stands in 2007 (4-5 y postfire) and unburned stands in 2008. We employed a stratified

random factorial sampling design with two factors—forest type and burn severity—and included prefire biomass as a continuous covariate. We stratified the postfire landscape using remotely-sensed imagery from the US Forest Service DNF and Laboratory for Applications of Remote Sensing in Ecology (LARSE, www.fsl.orst.edu/larse). We used a plant association group layer to delineate ponderosa pine and mixed-conifer forest types and combined dry and wet ponderosa pine into one type and dry and wet mixed-conifer into the other type. For burn severity, we used DNF burned area reflectance classification (BARC) maps, which were derived from the Landsat differenced normalized burn ratio (dNBR; Key and Benson 2006), a measure of pre- to post-fire change, from which the DNF identified four severity classes (unburned/very low, low, moderate, high) corresponding to overstory tree mortality. For each combination of burn severity and forest type, we used GIS to generate randomized points and establish 8 survey plots from these lists in random order ($n = 64$; Table 2.1, Fig. 2.1). We used GPS to establish permanent plot centers after field-validating each point with respect to forest type and burn severity and recorded elevation (m), slope (°), and aspect (°). All plots were on DNF non-wilderness land at least 50 m from roads, non-forest, salvage-logged, and riparian areas. In addition, we used a live, aboveground biomass map from 2001 to sample the full range of prefire biomass and to ensure comparability between type*severity treatments. This biomass map was derived from random forests regression tree analysis of Landsat spectral data and biophysical predictors (S. Powell and others, USDA Forest Service, in prep.).

We used standard biometric methods described previously (Law and others 2001a, 2003; Campbell and others 2004; Irvine and others 2007). Here, we summarize these methods and provide details specific to postfire measurements. Each plot encompassed a 1 ha stand of structurally homogenous forest, which we sampled with a plot design similar to the USDA Forest Inventory and Analysis protocol (USDA 2003a) with enhanced C budget measurements including tree increment, litter, fine and coarse dead pools, and soil CO_2 effluxes (protocols in Law and others 2008). We scaled all measurements to slope-corrected per-ha or per-m^2 units for comparison across study treatments.

Like other fire studies (*e.g.,* Turner and others 2004, Donato and others, in press), the current project sampled a particular set of fires on a specific landscape. This natural experiment precluded detailed prefire data, but remotely-sensed prefire biomass, GIS databases, and plot attributes allowed us to account for pre-existing differences to the extent possible. In addition, the spatial pattern of forest type, burn severity, and prefire biomass on the landscape was not randomly assigned, so we limited statistical inference and interpretations to the sampled forest types within the study area. To minimize potential confounding effects of spatial and temporal autocorrelation (Hurlbert 1984), we located random plots at least 500 m apart, maximized interspersion within study area gradients, and sampled multiple fires from two different years. As such, we assume each plot to be an independent sample from the population of forest type-burn severity stands from which it was drawn. The experimental unit was the 1 ha plot. For brevity, we refer to the factorial combinations of forest type and burn severity as 'treatments.'

Ecosystem measurements

Aboveground biomass and productivity. We quantified aboveground biomass and productivity for all live vegetation—trees, shrubs, forbs, and graminoids—in four circular, regularly-spaced, non-overlapping subplots. For trees between 10 cm and 69.9 cm diameter at breast height (DBH; 1.37 m), subplot area ranged from 154 to 907 m^2 (7-17 m radius), depending on tree density (min. 60 trees sampled ha^{-1}). We measured trees larger than 70 cm DBH throughout the 1 ha plot (56.4 m radius from plot center) and saplings (DBH from 1.0-9.9 cm) in 78.5 m^2 (5 m radius). For the 5284 trees surveyed, we recorded species, DBH, height, and percent bark and wood char (ocular estimate of surface area). We estimated tree biomass with allometric equations compiled in a database of species- and ecoregion-specific volume equations and density values (BIOPAK; Means and others 1994; Van Tuyl and others 2005; Hudiburg 2008; Hudiburg and others 2009) and computed bole, bark, branch, and foliage mass for each tree from DBH and height. We used congeneric parameters when species-specific parameters were not available. We adjusted tree biomass estimates for reductions due to charring after Donato and others (in press), broken status, and severity-specific estimates of bark, wood, and foliage combustion from Campbell and others (2007). We assumed that the carbon

content of all pools was 0.51 by mass except for forest floor, which we assumed was 0.40 (SD = 0.08) based on Dumas combustion (Campbell and others 2007).

We determined annual aboveground net primary production (NPP) at the 48 burned plots. We estimated bolewood NPP from radial increment measurements of current and previous live tree biomass (Van Tuyl and others 2005; Hudiburg and others 2009). We stratified plots by species and DBH and collected increment cores at 1.37 m from 20 live trees in each low- and moderate-severity plot (and up to 20 dead trees at high-severity plots, depending on bole decay). Cores were mounted on wood blocks, sanded, scanned, measured using the WinDendro[TM] image analysis software (Woolley and others 2007), and digitally archived. Bolewood NPP was the primary application of these data (but see Appendix 2: postfire growth response of dominant tree species). We scaled radial increment measurements to all inventoried trees using the mean from each DBH quartile within a plot (Van Tuyl and others 2005). We modeled current and previous height from DBH using a study-wide exponential regression between measured height and DBH (height (m) = 58.79 * (1 - e$^{(-0.0114 * DBH (cm))}$), adj. R^2 = 0.86, n = 4604; fitted using the exponential rise to maximum statistical program in SigmaPlot [Version 11.0, SPSS Science, IL]). To account for climatic variability, researchers typically average radial increment from the previous 5-10 y (*e.g.,* Reich and others 2001; Law and others 2003). Because disturbance influences interannual variability in tree growth (*e.g.,* Mutch and Swetnam 1995), and we could not assume a steady state condition for annual radial increment 4-5 y postfire, we used only the last full year of radial growth to estimate bolewood NPP. The years influencing the measured radial growth (2006-2007) were not anomalous climate years (Fig. 2.3; Thomas and others 2009). Additionally, the time period of this estimate is on the same temporal scale as biometric estimates of foliage, fine root, and herbaceous NPP. For the few live trees surviving at high-severity plots (n = 23 trees among 3 plots; <0.5% of inventoried trees), we applied forest type species-specific averages of increment data from low- and moderate- severity stands. We calculated foliage NPP as the product of specific leaf mass per unit area (SLA), leaf retention time (LRT), and plot-level leaf area index (LAI). We estimated SLA and LRT from representative canopy shoots with full retention, stratified by species and overstory

class (n = 5-8 samples per plot, collected via shotgun and stored below 5 °C until processing). We measured LAI optically using a Sunfleck ceptometer (Decagon Devices, Inc., Pullman, WA) after Law and others (2001b) and Pierce and Running (1988). We sampled transmitted photosynthetically active radiation (PAR) within two hours of local solar noon under uniform sky conditions and placed an automated unit in a large opening within 10 km of field plots. We collected 20 measurements at 35 points located systematically throughout each plot at 1.37 m (total of 56 000 optical observations per plot). We calculated LAI with the equation (Campbell 1991):

$$(1) \quad LAI = \frac{[f_b (1 - \cos \theta) - 1] \ln (Q_t / Q_o)}{A (1 - 0.47 f_b)}$$

where A is 0.84 for leaf absorptivity (a) of 0.90 in the PAR band ($A = 0.283 + 0.785a - 0.159a^2$), f_b is the fraction direct beam measured concurrently at a forest canopy flux tower within 15 km, and θ is the solar zenith angle calculated from latitude (44.5°N) and hour of day. Because moderate- and high-severity fire substantially altered tree crowns through consumption and mortality, and LAI measurements would be biased by dead canopy light interception, we scaled LAI measurements from low-severity plots using a regression of LAI with live tree basal area (LAI = 3.85 * (1 - e$^{(-0.0311 * \text{live basal area})}$), adj. R^2 = 0.54, n = 16; fitted using the exponential rise to maximum statistical program in SigmaPlot [Version 11.0, SPSS Science, IL]).

     We sampled shrubs, forbs, graminoids, ground cover, and conifer regeneration in four 78.5 m^{-2} (5 m radius) subplots nested within the tree survey subplots. We estimated live shrub percent cover in three height classes (0-0.5 m, 0.5-1.0 m, 1.0-2.0 m) and converted shrub volume to biomass with species-specific allometric equations (Hudiburg and others 2009). We computed shrub wood and foliage NPP from annual radial increment and leaf retention time respectively (Hudiburg 2008). In addition to shrub biomass and NPP, we analyzed postfire shrub community dynamics (Appendix 3). We estimated the percent cover of graminoids, forbs, litter, woody detritus, cryptogams, rocks, and mineral soil and converted graminoid and forb cover to biomass using mass per unit area measurements from 0.25 m^2 clip plots of dominant species sampled across the study area (n = 68, ≥ 8 per species). We assumed herbaceous vegetation mass

equaled annual NPP. We recorded postfire seedling species, age, 5 cm height class, and live/dead status. We identified seedlings established before fire in 0.5 m, 1.0 m, and 2.0 m height classes when age exceeded time since fire. Based on seedling age, vigor, and DNF GIS data, we determined if seedlings were planted and excluded these from natural regeneration analyses. To assess initial understory regeneration dynamics 4-5 y postfire, we compared conifer seedling density and shrub biomass.

  Aboveground necromass and decomposition. We surveyed aboveground dead biomass (hereafter 'necromass') in multiple strata: standing dead wood (snags), dead shrubs, stumps, coarse woody detritus (CWD), fine woody detritus (FWD), and forest floor. We measured snags with the live tree survey, dead shrubs with live shrubs, and stumps within 314 m^2 (10 m radius) subplots. For all tree components, we recorded species, diameter, height, decay class (DC 1-5; Maser and others 1979; Cline and others 1980), and whether or not trees were broken and/or dead prior to 2002 (dead prefire; determined by advanced decay, lack of bark, and heavy wood char). We estimated CWD and FWD volume using line intercepts (Van Wagner 1968; Brown 1974; Harmon and Sexton 1996; Law and others 2009) on four 75 m transects per plot (ordinal directions from plot center), sampling CWD (all pieces $\geq$ 7.62 cm diameter) along the full 300 m and FWD <0.64 cm, 0.65-2.54 cm, and 2.55-7.62 cm along 20 m, 60 m, and 120 m, respectively. We converted volume to necromass with species- and decay class-specific density values (Hudiburg and others 2009) after accounting for volume reduction due to charring (Donato and others, in press). Because we could not identify species for most FWD, we used the 'unknown conifer' species density values. Dead shrubs were widespread in the study area. We measured the average number, length, and diameter of dead shrub stems within the 78.5 m^{-2} (5 m radius) subplots and converted volume to mass using the average (decay class 1) wood density of three locally-abundant hardwood genera *(Acer, Alnus, Castanopsis)* from an allometry database (Hudiburg and others 2009). We sampled forest floor (litter and duff) to mineral soil with 10.2 cm diameter pvc corers at 16 randomized locations at each plot (four samples ~2 m from each subplot center in cardinal directions) and oven-dried samples at 60°C for >72 hrs to determine mass.

We computed aboveground heterotrophic respiration of all dead woody pools by multiplying necromass times decomposition constants from a regional database for CWD (Harmon and others 2005). When species-specific constants were not available and for unknown species, we substituted congeneric constants and a study-wide species average, respectively (3 dominant species: Douglas-fir, grand fir, and ponderosa pine). Because snags decay much more slowly than CWD in this semi-arid system, we assumed that snag decomposition was 10% of CWD decomposition (Irvine and others 2007), but we used the published CWD decomposition rates for stumps, for which microbial decay processes are less moisture-limited (M. Harmon, Oregon St. Univ., 2009, personal communication). We estimated FWD decomposition from McIver and Ottmar (2007) and applied a study-wide average (Douglas-fir, grand fir, and ponderosa pine) for pieces between 2.55-7.62 cm diameter. For dead shrub decomposition, we used the decay constant for *Alnus rubra* (Harmon and others 2005). We assumed that annual mass loss of forbs and graminoids was 50% (Irvine and others 2007).

Belowground carbon pools, productivity, and soil respiration. At the 48 burned plots, we collected soil and fine roots at 16 randomized locations per plot (four samples located ~2 m from each subplot center) using a 7.3 cm diameter auger. Standard sampling depth was 20 cm with one core up to 100 cm per plot (sampled maximum depth = 86 cm). At a subset of plots with very rocky soil, we sampled to 10 cm or 15 cm ($n = 7$ and $n = 3$, respectively) and scaled estimates to 20 cm with a study-wide simple linear regression. We used deep soil samples to derive correction factors to estimate C, N, and fine roots to 100 cm. We assumed that 49% (SD = 14) of soil C, 48% (SD = 17) of soil N, and 62% (SD = 20) of fine roots were in the top 20 cm, within the fine root variation reported by Law and others (2003). All samples were sorted through 2 mm sieves, bench-dried, mixed by subplot, subsampled, and analyzed for mass fraction of C and N (LECO CNS 2000 analyzer, Leco Corp., St. Joseph, MI), texture (hydrometer method), and pH (Oregon St. Univ. Central Analytical Laboratory; see Appendix 4 for soil N, pH, texture, and depth results). We measured the volume of all stones by displacement to calculate bulk density for the sieved soil and separated fine roots (FR: <2 mm diameter) and other organic matter. We combusted a representative FR subsample ($n = 7$ plots) in

a muffle furnace at 550°C for 5 h to determine organic content (74.24%), which we applied to all FR samples to estimate total organic matter. Based on published estimates of regional FR decomposition (Chen and others 2002) and mortality (Andersen and others 2008), we assumed that less than 40% of fire-killed FR remained at the time of sampling, that far fewer were retained by 2 mm sieves, and that the vast majority of sampled FR was newly recruited postfire, even in high-severity stands. We estimated that live roots were 61% of total FR mass in PP stands (O. Sun, Oregon St. Univ., unpublished data; Irvine and others 2007) and 87% of FR mass in MC stands (P. Schwarz, Oregon St. Univ., unpublished data). We computed fine root NPP as the product of total organic mass and a root turnover index from multi-year rhizotron measurements in a nearby unburned ponderosa pine forest (Andersen and others 2008). We estimated live and dead coarse root (CR: >10 mm diameter) mass from the tree, snag, and stump surveys as a function of tree DBH (Santantonio and others 1977) and computed CR NPP from modeled current and previous live tree diameters (from increment cores). This equation is applied widely to North American conifers due to a lack of published species- and region-specific equations (Campbell and others 2009), and reported trends in CR mass and production are solely a function of tree patterns. Because the median stump height was 30 cm, we applied a correction factor of 0.9 to account for bole taper to 1.37 m for stump CR estimates (adapted from D. Donato, unpublished data).

We measured soil CO_2 efflux and adjacent soil temperature at 12 randomized locations per plot using a Li-6400 infrared gas analyzer with Li-6000-9 soil chamber (Li-Cor Biosciences, Lincoln, NE) following established protocols (Law and others 1999; Campbell and Law 2005; Irvine and others 2007, 2008). We estimated annual soil respiration (R_{soil}) by matching point measurements with concurrent, hourly, automated soil respiration measurements at a nearby unburned AmeriFlux PP tower site (within 20 km) (Irvine and others 2008). A plot-specific correction factor was computed based on the ratio of the mean soil respiration for a given plot divided by the concurrent automated rate and scaled to the automated chamber annual data set; correction factors ranged from 0.4 to 1.7 (range of type*severity means: 0.8-1.02). This approach sampled the spatial variability of respiration within each plot to determine base rates and leveraged the long-

term, intensive measurements of temperature- and moisture-driven variability. Similar automated measurements were made in previous years (2002-2003) in a MC stand that subsequently burned in the B&B fire. A comparison of MC and PP continuous respiration datasets during the overlapping measurement period indicated near identical diel amplitudes and seasonal patterns between the two sites (data not shown). Given this similarity, we concluded that annual, plot-specific R_{soil} estimates based on the PP automated soil respiration would adequately represent the spatial and temporal variation within and among all plots. We computed the heterotrophic fraction of soil respiration (R_{hsoil}) based on previous measurements at vegetation-excluded automated chambers at high-severity and unburned AmeriFlux tower sites within the study area (0.56 for high-severity [value from high-severity sites], 0.52 for moderate-severity [mean of high-severity and unburned sites], and 0.48 for low-severity plots [value from unburned sites]; Irvine and others 2007).

Net ecosystem production. We estimated net ecosystem production (NEP: the difference between gross primary production and ecosystem respiration; Chapin and others 2006) using the mass balance approach (Law and others 2003, Campbell and others 2004a, Irvine and others 2007). This method combines the above and belowground fluxes described above:

(2) $NEP = (NPP_A - R_{hWD}) + (NPP_B - R_{hsoil})$

where NPP_A is aboveground NPP (wood and foliage growth of trees, shrubs, and herbs), R_{hWD} is heterotrophic respiration of aboveground woody detritus (decomposition of coarse and fine wood, snags, and stumps), NPP_B is belowground NPP (growth of fine and coarse roots), and R_{hsoil} is heterotrophic soil surface CO_2 efflux (decomposition of soil organic matter and forest floor). NEP is the appropriate C balance metric at the spatiotemporal scale of our measurements, whereas net ecosystem carbon balance (*i.e.,* Net Biome Production) describes landscape- to regional-scale C balance and longer-term effects of fire and other fluxes (*e.g.,* erosion, leaching, timber harvest; Chapin and others 2006). Here, we assume these other fluxes to be negligible at during the sampling period, and we account for combustion losses independently of NEP.

Pyrogenic C emissions from combustion. Before-after measurement of C pools is the most certain method to measure pyrogenic C emission (PE; Campbell and others 2007), but in this study, co-located prefire measurements were not available, and it was not possible to establish a paired plot for every burned condition across the study gradients. We estimated C loss from combustion using a standard simulation program (Consume 3.0; Prichard and others 2006), augmented with field estimates of tree consumption. Consume predicts aboveground fuel consumption, emissions, and heat release based on weather data, fuel moisture, and fuelbed inputs from the Fuel Characteristic Classification System (FCCS 2.0; Ottmar and others 2007) both models available at: www.fs.fed.us/pnw/fera/). We selected representative fuelbeds for PP and MC stands (Table 2.3) using GIS and modified these to develop custom fuelbeds based on field measurements at the 16 unburned plots. We simulated low-, moderate-, and high-severity fire by adjusting canopy combustion and fuel moisture content for woody fuels and duff (Table 2.3; R. Ottmar, US Forest Service, 2009, personal communication). Because Consume 3.0 does not account for consumption of live tree stems and bark, we used field measurements to calculate the changes in mass and density due to charring (Donato and others, in press). We assessed combustion at the stand-scale and scaled stand-level combustion to the sampled landscape with forest type and burn severity GIS data.

Statistical and uncertainty analysis

We used multiple linear regression and analysis of covariance to compare response variables across the study gradients. Because one- and two-way ANOVA (forest type and burn severity tested separately and combined) revealed a significant difference in prefire biomass between the two forest types ($P < 0.001$) but no significant difference among burn severities within either forest type ($P > 0.5$), we conducted analyses separately by forest type. We derived test statistics (coefficients and standard errors) from a multiple linear regression model of the response variable as a function of prefire biomass (continuous) and burn severity (categorical) within a given forest type. Regression analysis showed no significant interactions among explanatory variables; coefficient estimates were calculated from additive models with an assumption of parallel lines among type*severity treatments. We log-transformed data when necessary to satisfy model assumptions. We accounted for multiple comparisons and reported statistical significance as the highest significant or lowest non-significant Tukey-adjusted P-value ($\alpha = 0.05$) common to all groups (*e.g.,* severity classes) in a given comparison (PROC GLM lsmeans multiple comparisons; SAS 9.1, SAS Institute, Inc., Cary, NC).

We take a pragmatic view of uncertainty analysis after Irvine and others (2007). Many scaling assumptions are necessary to estimate plot-level metrics from components sampled at varying spatiotemporal scales. Further, given the wide range of sampled prefire biomass and variability across the postfire landscape, it is possible to commit Type II statistical errors (*i.e.,* fail to reject false null hypothesis) when important differences exist but are confounded by additional factors. We thus focus on the trends and proportions across type*severity treatments rather than absolute magnitudes. To estimate NEP uncertainty, we used a Monte Carlo procedure with the four major fluxes described in equation 1 for each type*severity treatment (NEP uncertainty expressed as $\pm$ 1 SE after 10 000 iterations based on the standard normal distribution with mean, standard deviation, and between-flux covariance in R [R Development Core Team 2009]). We also tested the sensitivity of NEP by varying the key component fluxes by the range of sampled conditions (analysis not shown).

RESULTS AND DISCUSSION

Pyrogenic C transfers: combustion and mortality effects on C pools

Simulated pyrogenic C emission. The two fire-induced pathways of C transfer to the atmosphere are combustion (pyrogenic emission [PE]) and vegetation mortality with subsequent decomposition. Simulated mean PE was 25.5 Mg C ha^{-1} (range: 16.6-32.3 Mg C ha^{-1}) and was very similar between forest types, suggesting equivalent surface fuel loading. Because prefire biomass was lower in PP stands, the % consumed was substantially higher (range: 23-35% vs. 13-24% for PP vs. MC stands respectively, Table 2.4). Stand-scale PE from low-severity fire was 51% and 65% of high-severity emissions in MC and PP stands, respectively, indicating that the largest fraction of PE was from combustion of surface and ground fuels. This result is consistent with Campbell and others (2007), who determined that >60% of total combustion was from litter, foliage, and small downed wood, and that these high surface area:volume ratio pools were readily consumed (>50% combusted) in all burn severities in SW Oregon mixed-conifer forests. Our field-based estimate of live tree stem consumption was on average 1.24% (range: 0.23-2.77%) of live bark and bole mass, a trivial amount compared to other PE uncertainties. The largest remaining uncertainty is that the Consume 3.0 model does not account for belowground C loss due to combustion, erosion, or other fire effects, which can be substantial in some cases (Bormann and others 2008). Without detailed prefire measurements, we were unable to address this issue directly, but our soil C surveys did not show any significant declines in high-severity stands (described below).

Scaled to the sampled landscape (*ca.* 30 000 ha of burned area), simulated total PE was 0.76 Tg C (Table 2.4). High-severity MC stands, with the largest per unit area emissions and landscape area, contributed a disproportionate amount of PE (42% of the total), whereas all PP forests combined released 26% of total PE. These proportions underscore the importance of incorporating landscape patterns of vegetation and fire effects (*i.e.,* the severity mosaic) into modeling and policy analyses. On a per unit area basis, total PE from these fires was 33% higher than the 3.8 Tg C estimated for the 200 000 ha Biscuit Fire (25.5 vs. 19 Mg C ha^{-1}, Campbell and others 2007). This C transfer represents a substantial pulse to the atmosphere relative to annual net C fluxes from

unburned forests in the Metolius area (mean annual net C uptake at a mature PP site: 4.7 ± 1.2 Mg C ha^{-1} y^{-1} ; Thomas and others, 2009). Conversely, 0.76 Tg C is *ca.* 2.5% of Oregon statewide anthropogenic CO_2 emissions for the 2-y period 2002-2003 (30.62 Tg C equivalent; http://oregon.gov/energy/gblwrm/docs/ccigreport08web.pdf). It is important to note that the study scope burned area is *ca.* 60% of the area burned in and around the Metolius Watershed in 2002 and 2003 (49 000 ha, 19 000 beyond this study scope) and that these were large fire years regionally. Thus, PE from our study area represents a relatively small proportion of total C emissions from wildfire. Although further refinements are possible, the current analysis provides a reasonable constraint for regional modeling efforts.

Mortality and postfire C pools. Because large C pools (*e.g.,* live tree boles) were largely unaffected by combustion but were readily killed, fire-induced mortality was the most important overall C transformation, larger in magnitude than total combustion. The distribution of live and dead C pools changed predictably with burn severity, dominated by the shift from live trees to dead wood mass (Table 2.5). Aboveground live tree and dead wood mass (g C m^{-2}) both encompassed wide ranges (live tree range: 0-9302, PP high severity to MC low severity; dead wood range: 924-6252, PP low severity to MC high severity), the latter range encompassing dead wood estimates from Washington East Cascades high-severity stands (*ca.* 3000; Monsanto and Agee 2008). Mean basal area mortality ranged from 14% in low-severity PP stands to 100% in high-severity PP stands, with parallel patterns in MC stands (Table 2.1, Fig. 2.5). Across both forest types in low- vs. high-severity stands, this mortality resulted in a >90% reduction in live aboveground C ($P < 0.005$), coupled with a near tripling of dead wood aboveground C (Table 2.5). Trends in non-tree live mass (*e.g.,* shrubs, forbs) were inverse to live trees, with significantly higher mass in high- vs. low-severity stands ($P < 0.03$) due to regenerating vegetation. Across both forest types, forest floor mass exhibited the largest absolute and relative difference between burned and unburned stands (mean: 1588 and 232 g C m^{-2}, respectively), consistent with near-complete combustion of these pools. Whereas the difference between burned and unburned forest floor mass was highly significant (85% reduction; $P < 0.001$), there were no significant differences among low-, moderate-, and

high-severity stands in either forest type ($P > 0.85$). Because of the decline in forest floor and high tree survival, low-severity stands exhibited lower aboveground necromass than unburned stands (Table 2.5).

Total aboveground C and total ecosystem C declined with increasing burn severity in both forest types (Table 2.5), although total ecosystem C was not significantly different among severities in MC forests ($P > 0.67$). In both types, fine root mass and soil C to 20 cm depth were not significantly different among severities ($P > 0.33$). Scaled to 100 cm, mean soil C stocks (g C m^{-2}, ±1 SE from regression) were 6556 ± 348 and 5903 ± 195 for burned MC and PP stands, respectively (Table 2.5). These values are similar to nearby unburned stands (7057 g C m^{-2}) and substantially lower than soil C in more mesic Oregon forests (14 244 and 36 174 g C m^{-2} in the West Cascades and Coast Range, respectively; Sun and others 2004). The lack of significant differences among severities furthers the evidence that soil C can be conserved with disturbance (Campbell and others 2009), including high-severity fire (Irvine and others 2007). Without site-specific prefire data we were unable to directly measure changes in soil C, and in applying a fixed-depth approach, a limitation of most postfire studies, we could not fully preclude the possibility of fire-induced soil C loss due to combustion, plume transport, or erosion (Bormann and others 2008). Unlike that study, in steep terrain that experienced stand-replacing fire, we did not observe severe erosion or changes in the soil surface between burned and unburned stands, and we detected no significant differences in mean or maximum soil depth among severities (Appendix 4).

Our aboveground and total ecosystem C pool estimates are consistent with previous estimates for PP in the Metolius area. Total aboveground C values for unburned and low-severity PP stands are similar to mature and young pine stands, respectively, whereas moderate- and high-severity stands fall between the values reported for initiation and young stands in a PP chronosequence (Law and others 2003). Our estimates of total ecosystem C in moderate- and high-severity PP stands are consistent with those reported by Irvine and others (2007). No analogous studies exist for the East Cascades MC forest type; the current study provides the first such estimates. The trends with burn severity were generally similar in both forest types, and the forest types differed consistently only

in the magnitude of C pools. Total ecosystem C was 47% greater in MC forests than in PP forests (derived from Table 4).

Postfire C balance: fire effects on C fluxes and net ecosystem production

Aboveground C fluxes. Aboveground C fluxes followed the trends of live and dead C pools; NPP_A declined with increasing tree mortality (Fig. 2.4a). In both forest types, NPP_A was significantly lower ($P < 0.015$) in high-severity vs. moderate- and low-severity stands, which were not significantly different from each other ($P > 0.21$; overall range: 84-214 g C m^{-2} y^{-1}). Although NPP_A declined monotonically with burn severity, the sum of shrub and herbaceous NPP_A was about 2-fold higher in moderate- and high-severity vs. low-severity stands, resulting in a dramatic increase in the non-tree proportion of NPP_A (Table 2.6). Thus, despite a reduction in live aboveground C of over 90% in both forest types in high-severity compared to low-severity stands, NPP_A was only 55% lower on average (Table 2.6). This trend, coupled with NPP_B (described below), resulted in a mean reduction of total NPP of about 40% from low- to high-severity, consistent with a strong compensatory effect of non-tree vegetation NPP_A. Previous studies in clearcut, thinned, and burned forests have shown the same pattern of rapid recolonization by non-trees contributing disproportionately to NPP (Campbell and others 2004; Gough and others 2007; Irvine and others 2007; Campbell and others 2009), and this study furthers the evidence across the full severity gradient in two forest types. These findings suggest that a tree-only perspective (*e.g.,* Hurteau and others 2008) is likely to result in significant biases and that ecosystem models and C policies (*e.g.,* CCAR 2007) should encompass the full suite of ecosystem components and processes, including understory vegetation and rapid belowground recovery following disturbance.

Heterotrophic respiration of aboveground necromass (R_{hWD}), computed from C pools and decomposition constants, was a substantial component of C balance across both forest types but showed weak trends among severities (Fig. 2.4b, Table 2.7). Despite the increase in dead wood mass with severity (Table 2.5), there were no significant differences in MC stands and only suggestive increases of R_{hWD} with severity in PP stands ($P = 0.031$-0.051). We attribute this surprising result to several factors: differing species- and decay-class specific constants and high variability among plots and

severities; high retention and slow decomposition of snags; relatively high snag and dead shrub R_{hWD} in low-severity MC stands; relatively low CWD and dead shrub R_{hWD} in high-severity PP stands (Table 2.7). Although we expected that the immediate postfire period would exhibit maximum necromass over successional time (Wirth and others 2002; Hicke and others 2003), our R_{hWD} estimates were well less than both NPP_A and NPP_B (R_{hWD} <35% of total NPP). These findings suggest that postfire woody detritus decomposition contributes a protracted C loss that is more than counterbalanced by NPP. In addition, R_{hWD} 4-5 y postfire constituted about 15% of total R_h across both forest types; R_{hsoil} (below) accounted for *ca.* 85% (Table 2.7), demonstrating that belowground respiration processes are the predominant drivers of C loss.

Our range of R_{hWD} across the two forest types (28-75 g C m^{-2}, Table 2.7) is higher than estimates 2 y postfire in PP forest (Irvine and others 2007), similar to young PP stands in the Metolius area (Sun and others 2004) and an old-growth *Pseudotsuga-Tsuga* forest about 100km away (Harmon and others 2004), and much less than untreated and thinned PP stands in Northern California (Campbell and others 2009). Our relatively low R_{hWD} estimates, particularly compared to the C uptake from NPP, underscore the importance of decomposition lags in seasonally-arid ecosystems, where microbial snag decomposition is moisture-limited. Other systems, such as tropical or sub-tropical humid zones where decomposition is not moisture- or temperature-limited and disturbance rapidly generates CWD (*e.g.,*hurricanes; Chambers and others 2007) may experience a much more rapid pulse of C emission from necromass. The notion that fire-killed necromass represents a large, short-term C loss is unfounded, however, and warrants further investigation.

Woody detritus decomposition is a highly uncertain process, particularly in burned forests, where charring and snag fall play important, contrasting roles. For these R_{hWD} estimates, we used decomposition constants derived from unburned forests rather than measurements of postfire detritus respiration. We believe that charring would likely reduce decomposition rates (DeLuca and Aplet 2008; Donato and others 2009a) but tested the sensitivity of our estimates by assuming snag decay rates equivalent to CWD. In this scenario, estimated snag R_h would be 1 order of magnitude higher, and mean R_{hWD}

would be *ca.* 125% and 50% higher in MC and PP stands, respectively, pushing all burned stands into a net C source (negative NEP, although mean R_{hWD} would remain <50% of R_{hsoil} in both forest types). Our use of the 10% fraction is consistent with previous studies (Irvine and others 2007); other studies have ignored snag decomposition entirely (*e.g.,* Wirth and others 2002). Our short-term study precluded the assessment of snag fall, a stochastic process dependent on burn severity, topography, climate, and tree species, size, crown scorch, decay stage, and density (Russel and others 2006). That Idaho study, in unlogged stands across a gradient of burn severity, estimated snag half-lives for ponderosa pine and Douglas-fir of 9-10 and 15-16 y, respectively (Russel and others 2006), suggesting that the majority of snags generated in the Metolius fires will last for at least 10 y postfire. R_{hWD} may increase with accelerating snag fall (particularly in high-severity stands) but will remain small relative to R_{hsoil}, and NPP will likely increase over the same time period. Future studies are necessary to reduce the uncertainty of decomposition and snag dynamics in this area.

Belowground C fluxes. Belowground C fluxes were by far the largest and most variable components of the annual C budget and drove the overall magnitude of NEP (Fig. 2.4). Belowground NPP (NPP$_B$) was not significantly different across the entire study (overall mean: 284 g C m^{-2} y^{-1}; $P > 0.68$ in both forest types). Fine root NPP$_B$ to 1 m, based on total fine root mass and a constant turnover rate, accounted for about 90% of NPP$_B$, with increasing importance in high-severity stands, where very few live tree coarse roots survived. The apparent rapid establishment of fine roots in high-severity stands contributed to the strong NPP compensatory effect of non-tree vegetation (Table 2.6). NPP$_B$ accounted for *ca.* 50% of total NPP averaged across all severities and forest types, but high-severity stands in both forest types exhibited higher NPP$_B$ than NPP$_A$ (NPP$_B$ = 58 and 54% of total NPP in MC and PP, respectively), indicating belowground C allocation values between those reported for grasslands and shrublands (67 and 50%, respectively; Chapin and others 2002). These estimates of fine root NPP$_B$ are very similar to those reported for moderate- and high-severity PP by Irvine and others (2007), even though that study accounted for fire-induced fine root mortality and computed fine root NPP from live rather than total fine root stocks. Our estimated FR NPP is higher

than a thinned PP forest in Northern California (Campbell and others 2009) and lower than a mixed-deciduous forest in Michigan (Gough and others 2007). Our estimates of total NPP (*ca.* 200-400 g C m^{-2} y^{-1}) and NPP$_A$:NPP$_B$ ratio (overall mean: 1.15; Table 2.6) are within the range of previous studies in the area (Law and others 2003; Campbell and others 2004) and consistent with the postfire C allocation patterns described by Irvine and others (2007).

Heterotrophic soil respiration (R_{hsoil}) was not significantly different among burn severities and forest types ($P > 0.2$; Fig. 2.4b, Table 2.7), consistent with the trends of forest floor, fine roots, and soil C (Table 2.5). Mean annual R_{hsoil} (g C m^{-2} y^{-1}, ±1 SE from regression) was 294 ± 12 and 274 ± 15 in MC and PP stands, respectively, very similar to previous estimates in mature unburned PP stands (Law and others 2003; Sun and others 2004). The lack of R_{hsoil} differences among severity classes and similarity to unburned forest suggests that this flux is resistant to disturbance-induced changes and supports the findings of previous studies (Irvine and others 2007; Campbell and others 2009). R_{hsoil} chamber measurements 1 y postfire in a nearby high-severity site on the 2006 Black Crater fire were also similar to unburned PP forest and the values in the current study (J. Martin, unpublished data), indicating the lack of a large R_{hsoil} pulse from 1-5 y postfire. Although we did not find evidence of this postfire pulse in the absolute magnitude of R_{hsoil}, the conservation of R_{hsoil} across severities, coupled with declines in NPP, resulted in a dramatic decline of the NPP:R_h ratio (*ca.*0.55 in high-severity stands, both forest types; Table 2.7). This increase in relative R_{hsoil} equated to a muted postfire pulse that is reflected in our NEP estimates.

Implications for NEP. In both forest types, NPP$_A$ was the principal driver of NEP trends, whereas R_{hsoil} controlled NEP magnitudes (Fig. 2.4, Table 2.7). NEP was significantly lower in high- vs. low-severity stands in both forest types ($P < 0.035$). In MC stands, mean NEP (g C m^{-2} y^{-1}, ±1 SE from Monte Carlo simulations) varied from a slight sink (21 ± 48 and 21 ± 55) in low- and moderate-severity stands to a substantial source in high-severity stands (-174 ± 32). In PP forest, mean NEP varied from C neutral in low-severity stands (0 ± 33) to an intermediate source in moderate-severity stands (-87 ± 35) and substantial source in high-severity stands (-142 ± 37). Thus, mean annual NEP

was similar in high-severity stands of both forest types 4-5 years after fire. These results are consistent with previous estimates of NPP, R_h, and NEP in unburned, moderate-, and high-severity PP stands within the study area (Irvine and others 2007), although our NEP estimate for high-severity stands is lower.

Previous studies quantified a NEP recovery period to a net sink of 20-30 y in PP forest following stand-replacement clearcutting (Law and others 2003, Campbell and others 2004). Longer term measurements are necessary to determine the NEP fate of these postfire stands, but <30 y seems appropriate for high-severity stands, which are already closer to zero than initiation stands described by Law and others (2003), despite the removal of necromass via timber harvest in that study and higher R_{hWD} reported here. In both forest types, low-severity NEP was not significantly different from 0 (Table 2.7, SE includes zero), which may be explained by relatively rapid recovery of NEP and/or limited fire effects. Although not a large C source to the atmosphere, C neutral stands represent a substantial decline from prefire NEP (unburned PP mean ± 1 SE: 50 ± 14 g C m^{-2} y^{-1}, Irvine and others 2007). Management actions that mimic low-severity fire via prescribed burning or thinning (thus removing C) will likely reduce short-term NEP and long-term average C storage (Campbell and others 2009; Mitchell and others 2009).

Postfire regeneration: understory responses and potential C trajectories

Conifer and shrub regeneration. In the first 5 y following fire, postfire conifer regeneration was patchy but generally abundant in most type*severity treatments (Fig. 2.5b). Median seedling density (seedlings ha^{-1}) varied over 5 orders of magnitude (study wide range: 0 – 62 134). Conifer regeneration was higher in MC than PP stands, and both forest types showed a negative correlation with overstory tree mortality (Fig. 2.5); for low-, moderate-, and high-severity stands, median seedling density was 10 223, 5111, 414 and 1338, 844, 0 in MC and PP stands, respectively. Seedling density was significantly higher in low- vs. high-severity MC stands ($P = 0.036$) and significantly lower in high-severity PP stands than all other PP stands ($P < 0.003$). Given that a density of 500 seedlings ha^{-1} is considered adequate stocking (Oregon Forest Practices Act: www.leg.state.or.us/ors/527.html), all treatments except for high-severity PP

(median: 0 seedlings ha^{-1}) exhibited a robust regeneration pulse in the immediate postfire period. The large range of variability we observed is similar to conifer regeneration 2-4 y postfire in high-severity SW Oregon MC (5 orders of magnitude; Donato and others 2009b) and 11 y postfire in high-severity Rocky Mountain lodgepole pine (6 orders of magnitude; Turner and others 2004). PP seedling densities were higher in low- and moderate-severity stands than analogous patches in the Black Hills, South Dakota, and consistent with the near absence of regeneration in high-severity patches beyond the dispersal range of surviving seed trees (Lentile and others 2005).

Like conifers, shrub regeneration was generally abundant and highly variable across type*severity treatments, and responses were much stronger in MC forests (Fig. 2.5c). Shrubs showed the opposite relationship with burn severity, however, increasing in abundance with tree mortality; in both forest types, live shrub mass was significantly higher in high- vs. low-severity stands ($P < 0.015$). Shrub biomass was not significantly different among unburned, low-, and moderate-severity stands ($P > 0.14$), indicating rapid recolonization to prefire levels 4-5 years postfire. In some cases, shrubs appeared to have survived fire, but in general, almost all of the shrubs we observed established postfire, predominantly from seed banks but also vegetative resprouts. These results suggest strong shrub resilience in both forest types, where shrubs are an important component of mature stands (Franklin and Dyrness 1973). Fire appears to have played a dual role of initially reducing shrub mass and then enabling rapid shrub growth via overstory tree mortality, as demonstrated by the positive relationship with severity. Whereas shrubs have recovered to prefire levels in low- and moderate-severity stands in both forest types, shrubs in high-severity stands have achieved substantially higher standing biomass, which will likely influence conifer regeneration dynamics and associated successional trajectories.

Carbon trajectory implications. Postfire understory regeneration is a small component of the stand-scale C budget but initiates long-term trajectories of C loss and accumulation (Gough and others 2007). Postfire NPP and NEP may diverge widely in stands dominated by shrubs vs. seedlings (Hicke and others 2003), depending on the establishment, growth rates, and relative abundance of tree and non-tree vegetation.

Because seedlings and shrubs were strongly correlated with overstory mortality, the mixed-severity mosaic could influence C dynamics for decades, as illustrated by the two extremes of conifer regeneration across the study. Abundant regeneration in low-severity MC stands could bolster overstory NPP and NEP in the near term. Alternatively, hyperdense stands (*sensu* Savage and Mast 2005) could exacerbate drought stress on mature trees and facilitate (via ladder fuels) stand-replacement wildfire, yielding a C source for years to decades. In high-severity PP stands, the near absence of conifer regeneration, coupled with 100% tree mortality, suggests a possible state change to non-forest conditions with lasting C impacts. Dense shrubs and the widespread presence of non-native cheatgrass *(Bromus tectorum)* could facilitate subsequent reburn and substantial short- and long-term reductions in C storage (Bradley and others 2006; Dore and others 2008). Although it is possible that some sites could remain in shrubland/grassland conditions for decades (Savage and Mast 2005), the region is now transitioning from an anomalously warm/dry period (Fig. 2.3) to a negative Pacific Decadal Oscillation (cool/wet; Oregon Climate Service: www.ocs.oregonstate.edu). PP regeneration is strongly linked to climate, particularly summer rainfall (Barrett 1979), and because establishment can occur over many years postfire if seed sources persist (Shatford and others 2007), conifer regeneration is still possible.

The widespread presence of shrubs, particularly in high-severity stands, may initially reduce seedling growth through competition (Zavitkovski and Newton 1968), but over the long-term, understory shrubs play an important role in maintaining soil quality (C, N, microbial biomass C) in this ecoregion (Busse and others 1996). In addition, Keyes and Maguire (2008) quantified positive associations between PP seedling survival and the microclimate beneath shrubs (reduced soil temperature and increased shade), and Tappeiner and Helms (1971) documented MC regeneration associated with the low-lying shrub *Ceanothus prostratus* in the Sierra Nevada, an association we observed with *Calocedrus decurrens* (data not shown). These and other studies (*e.g.,* Shatford and others 2007) suggest that even where conifer seedling densities are currently low, shrub presence may enable protracted conifer regeneration and long-term productivity. On shorter time-scales, shrubs contribute to the compensatory effect of non-tree vegetation

NPP, potentially bridging a productivity gap until trees recover to prefire levels of LAI. Other factors such as climate, management, and recurrent disturbance will influence long-term successional trajectories and are beyond the scope of this study.

The importance of scale-dependence and landscape pattern

The C patterns and processes measured here are dependent on the spatiotemporal scales of measurement. This short-term study provides a measurement of direct fire effects and establishes an important baseline for long-term monitoring. Current trends may continue over time, but they will likely evolve. For example, Busse and others (1996) assessed shrub/tree interactions over a 35 y period, and 20 y elapsed before evidence emerged of positive understory effects on tree growth and soil quality. With predictions of accelerating climate change and increasing fire extent and severity in western forests (IPCC 2007; Balshi and others 2009; Miller and others 2009), long-term field measurements are essential to determine ecosystem resistance to fundamental state changes. Federal inventories provide important long-term data but should integrate some of the methods described here to quantify surface fuels (understory, forest floor) and soil C, as well as fire effects such as combustion and charring.

Complex spatial heterogeneity is inherent to wildfire disturbance, and although the stand-scale results presented here are illustrative, the net effect of fire on C pools and fluxes depends on the landscape pattern of type*severity treatments across the study area. For example, the high-severity MC treatment accounted for 33% of the sampled landscape, whereas all severities of PP forest accounted for only 25% combined (Table 2.1). Thus, although high-severity PP stands could represent a state change from forest to non-forest with lasting C consequences, that condition represents only 9% of the study scope. Previous studies have shown that the spatial heterogeneity from disturbance can result in as much variability in ecosystem processes (*e.g.,* NPP) as temporal variation through succession (Campbell and others 2004; Turner and others 2004). Depending on fire frequency and the arrangement of burn severity, the landscape may prove to be surprisingly resistant to lasting reductions in C uptake and storage (Kashian and others 2006).

CONCLUSION

This study quantifies the carbon consequences of wildfire severity and underscores the importance of accounting for the full range of disturbance effects on carbon pools and fluxes. Recent wildfires across the Metolius Watershed caused large, direct carbon transfers from live to dead pools and from terrestrial pools to the atmosphere, and our estimates of these fluxes provide new constraints for regional carbon modeling and policy frameworks. In both forest types, the rapid response of early successional vegetation offset declines in NPP and NEP, reducing potential long-term fire effects on stand and landscape C storage, particularly when combined with the lagged decomposition of necromass and conservation of belowground components (soil C, R_{hsoil}, and NPP_B). Mean annual NEP was highly variable and declined with increasing burn severity, resulting in a substantial C source in high-severity stands of both forest types 4-5 years postfire. Regeneration of conifers and shrubs was generally abundant and highly variable, but the two functional types showed opposite responses to tree mortality, suggesting a wide range of potential postfire carbon trajectories. Because non-stand-replacement fire account for a large percentage of the annual burned area (58% in this study), modeling efforts that focus exclusively on high-severity fire systematically underestimate pyrogenic emission, mortality, and declines in NEP, factors which are likely to play an increasingly important role in regional and global carbon cycling.

REFERENCES

Agee JK. 1993. Fire ecology of Pacific Northwest forests. Island Press, Washington, D.C.

Amiro BD, Todd JB, Wotton BM, Logan KA, Flannigan MD, Stocks BJ, Mason JA, Martell DL, Hirsch KG. 2001. Direct carbon emissions from Canadian forest fires, 1959-1999. Canadian Journal of Forest Research 31:512-525.

Andersen CP, Phillips DL, Rygiewicz PT, Storm MJ. 2008. Fine root growth and mortality in different-aged ponderosa pine stands. Canadian Journal of Forest Research 38:1797-1806.

Balshi MS, McGuire AD, Duffy P, Flannigan M, Walsh J, Melillo JM. 2009. Assessing the response of area burned to changing climate in western boreal North America using a Multivariate Adaptive Regression Splines (MARS) approach. Global Change Biology 15:578-600.

Barrett JW. 1979. Silviculture of ponderosa pine in the Pacific Northwest: the state of our knowledge. USDA Forest Service General Technical Report PNW-97. Portland, OR.

Bork BJ. 1985. Fire history in three vegetation types on the eastern side of the Oregon Cascades. PhD Thesis. Oregon State University. 94 p.

Bormann BT, Homann PS, Darbyshire RL, Morrissette BA. 2008. Intense forest wildfire sharply reduces mineral soil C and N: the first direct evidence. Canadian Journal of Forest Research 38:2771-2783.

Bradley BA, Houghton RA, Mustard JF, Hamburg SP. 2006. Invasive grass reduces aboveground carbon stocks in shrublands of the Western US. Global Change Biology 12:1815-1822.

Brown JK. 1974. Handbook for inventorying downed woods material. USDA Forest Service General Technical Report INT-GTR-16. Ogden, UT.

Busse MD, Cochran PH, Barren JW. 1996. Changes in ponderosa pine site productivity following removal of understory vegetation. Soil Science Society of America Journal 60:1614-1621.

Campbell GS, 1991. Application note: canopy LAI from Sunfleck Ceptometer PAR measurements. Decagon Devices, Inc., Pullman, WA.

Campbell JL, Alberti G, Martin JG, Law BE. 2009. Carbon dynamics of a ponderosa pine plantation following a thinning treatment in the northern Sierra Nevada. Forest Ecology and Management 257:453-463.

Campbell JL, Donato DC, Azuma DL, Law BE. 2007. Pyrogenic carbon emission from a large wildfire in Oregon, United States. Journal of Geophysical Research 112.

Campbell JL, Law BE 2005. Forest soil respiration across three climatically distinct chronosequences in Oregon. Biogeochemistry 73:109-125.

Campbell JL, Sun OJ, Law BE. 2004. Disturbance and net ecosystem production across three climatically distinct forest landscapes. Global Biogeochemical Cycles 18.

CCAR. 2007. Forest sector protocol version 2.1. California Climate Action Registry (CCAR). http://www.climateregistry.org/tools/protocols/industry-specific-protocols.html.

Chambers JQ, Fisher JI, Zeng HC, Chapman EL, Baker DB, Hurtt GC. 2007. Hurricane Katrina's carbon footprint on U. S. Gulf Coast forests. Science 318:1107.

Chapin FS III, Matson PA, Mooney HA. 2002. Principles of Terrestrial Ecosystem Ecology. Springer, New York, NY.

Chapin FS III, Woodwell GM, Randerson JT, Rastetter EB, Lovett GM, Baldocchi DD, Clark DA, Harmon ME, Schimel DS, Valentini R, Wirth C, Aber JD, Cole JJ, Goulden ML, Harden JW, Heimann M, Howarth RW, Matson PA, McGuire AD, Melillo JM, Mooney HA, Neff JC, Houghton RA, Pace ML, Ryan MG, Running SW, Sala OE, Schlesinger WH, Schulze ED. 2006. Reconciling carbon-cycle concepts, terminology, and methods. Ecosystems 9:1041-1050.

Chen H, Harmon ME, Sexton JM, Fasth B. 2002. Fine-root decomposition and N dynamics in coniferous forests of the Pacific Northwest, USA. Canadian Journal of Forest Research 32:320-331.

Cline SP, Berg AB, Wight HM. 1980. Snag characteristics and dynamics in Douglas-fir forests, western Oregon. Journal of Wildlife Management 44:773-786.

Daly C, Gibson WP, Taylor GH, Johnson GL, Pasteris P. 2002. A knowledge-based approach to the statistical mapping of climate. Climate Research 22:99-113.

DAYMET. 2009. Distributed climate data, http://www.daymet.org/.

DeLuca TH, Aplet GH. 2008. Charcoal and carbon storage in forest soils of the Rocky Mountain West. Frontiers in Ecology and the Environment 6:18-24.

Donato DC, Campbell JL, Fontaine JB, Law BE. 2009a. Quantifying char in postfire woody detritus inventories. Journal of Fire Ecology, in press.

Donato DC, Fontaine JB, Campbell JL, Robinson WD, Kauffman JB, Law BE. 2009b. Early conifer regeneration in stand-replacement portions of a large mixed-severity wildfire in the Siskiyou Mountains, Oregon. Canadian Journal of Forest Research, in press.

Dore S, Kolb TE, Montes-Helu M, Sullivan BW, Winslow WD, Hart SC, Kaye JP, Koch GW, Hungate BA. 2008. Long-term impact of a stand-replacing fire on ecosystem CO2 exchange of a ponderosa pine forest. Global Change Biology 14:1801-1820.

Eyre FH (editor).1980. Forest cover types of the United States and Canada. Society of American Foresters, Washington, DC.

Filip GM, Maffei H, Chadwick KL. 2007. Forest health decline in a central Oregon mixed-conifer forest revisited after wildfire: A 25-year case study. Western Journal of Applied Forestry 22:278-284.

Fitzgerald, S.A. 2005. Fire ecology of ponderosa pine and the rebuilding of fire-resilient ponderosa pine ecosystems. Proceedings of the Symposium on Ponderosa Pine: Issues, Trends, and Management, 2004 October 18-21, Klamath Falls, OR. USDA Forest Service General Technical Report PSW-GTR-198. Albany, CA.

Franklin JF, Dyrness CT. 1973. Natural vegetation of Oregon and Washington. USDA Forest Service General Technical Report PNW-GTR-8. Portland, OR.

Goward SN, Masek JG, Cohen WB, Moisen G, Collatz GJ, Healey SP, Houghton RA, Huang C, Kennedy RE, Law BE, Powell SL, Turner DP, Wulder MA. 2008. Forest disturbance and North American carbon flux. Eos, Transactions, American Geophysical Union 89:105-116.

Gough CM, Vogel CS, Harrold KH, George K, Curtis PS. 2007. The legacy of harvest and fire on ecosystem carbon storage in a north temperate forest. Global Change Biology 13:1935-1949.

Harmon ME, Bible K, Ryan MG, Shaw DC, Chen H, Klopatek J, Li X. 2004. Production, respiration, and overall carbon balance in an old-growth *Pseudotsuga-tsuga* forest ecosystem. Ecosystems 7:498-512.

Harmon ME, Fasth B, Sexton JM. 2005. Bole decomposition rates of seventeen tree species in Western U.S.A.: A report prepared for the Pacific Northwest Experiment Station, the Joint Fire Sciences Program, and the Forest Management Service Center of WO Forest Management Staff.
http://andrewsforest.oregonstate.edu/pubs/webdocs/reports/decomp/cwd_decomp_web.htm.

Harmon ME, Sexton JM. 1996. Guidelines for measurements of woody detritus in forest ecosystems. U.S. Long Term Ecological Research Program Network Vol. 20. Albuquerque, NM.

Hessburg PF, Salter RB, James KM. 2007. Re-examining fire severity relations in pre-management era mixed conifer forests: inferences from landscape patterns of forest structure. Landscape Ecology 22:5-24.

Hicke JA, Asner GP, Kasischke ES, French NHF, Randerson JT, Collatz GJ, Stocks BJ, Tucker CJ, Los SO, Field CB. 2003. Postfire response of North American boreal forest net primary productivity analyzed with satellite observations. Global Change Biology 9:1145-1157.

Hudiburg T. 2008. Climate, management, and forest type influences on carbon dynamics of West-Coast US forests. M.S. Thesis. Oregon State University. 86 p.

Hudiburg T, Law BE, Turner DP, Campbell JL, Donato DC, Duane M. 2009. Carbon dynamics of Oregon and Northern California forests and potential land-based carbon storage. Ecological Applications 19:163-180.

Hurlbert, S.H. 1984. Pseudoreplication and the design of ecological field experiments. Ecological Monographs 54:187-211.

Hurteau MD, Koch GW, Hungate BA. 2008. Carbon protection and fire risk reduction: toward a full accounting of forest carbon offsets. Frontiers in Ecology and the Environment 6:493-498.

IPCC. 2007. Climate Change 2007: The physical science basis: Contribution of Working Group I to the Fourth Assessment Report of the Intergovernmental Panel on Climate Change (IPCC) [Solomon S, Qin D, Manning M, Chen Z, Marquis M, Averyt KB, Tignor M, Miller HL. (eds.)]. Cambridge University Press, Cambridge, United Kingdom and New York, NY, USA. http://www.ipcc.ch.

Irvine J, Law BE, Hibbard KA. 2007. Postfire carbon pools and fluxes in semiarid ponderosa pine in Central Oregon. Global Change Biology 13:1748-1760.

Irvine J, Law BE, Martin JG, Vickers D. 2008. Interannual variation in soil CO_2 efflux and the response of root respiration to climate and canopy gas exchange in mature ponderosa pine. Global Change Biology 14:2848-2859.

Kashian DM, Romme WH, Tinker DB, Turner MG, Ryan MG. 2006. Carbon storage on landscapes with stand-replacing fires. Bioscience 56:598-606.

Keane RE, Agee JK, Fule P, Keeley JE, Key C, Kitchen SG, Miller R, Schulte LA. 2008. Ecological effects of large fires on US landscapes: benefit or catastrophe? International Journal of Wildland Fire 17:696-712.

Key CH, Benson NC. 2006. Landscape assessment: Ground measure of severity, the Composite Burn Index; and remote sensing of severity, the Normalized Burn Ratio. In FIREMON: Fire effects monitoring and inventory system. USDA Forest Service General Technical Report RMRS-GTR-164-CD. Fort Collins, CO.

Keyes CR, Maguire DA. 2008. Some shrub shading effects on the mid-Summer microenvironment of ponderosa pine seedlings in Central Oregon. Northwest Science 82:245-250.

Kurz WA, Stinson G, Rampley GJ, Dymond CC, Neilson ET. 2008. Risk of natural disturbances makes future contribution of Canada's forests to the global carbon cycle highly uncertain. Proceedings of the National Academy of Sciences of the United States of America 105:1551-1555.

Law BE, Arkebauer T, Campbell JL, Chen J, Sun O, Schwartz M, van Ingen C, Verma S. 2009. Terrestrial carbon observations: Protocols for vegetation sampling and data submission. Report 55, Global Terrestrial Observing System. FAO, Rome. 87 pp.

Law BE, Ryan MG, Anthoni PM. 1999. Seasonal and annual respiration of a ponderosa pine ecosystem. Global Change Biology 5:169-182.

Law BE, Sun OJ, Campbell JL, Van Tuyl S, Thornton PE. 2003. Changes in carbon storage and fluxes in a chronosequence of ponderosa pine. Global Change Biology 9:510-524.

Law BE, Thornton PE, Irvine J, Anthoni PM, Van Tuyl S. 2001a. Carbon storage and fluxes in ponderosa pine forests at different developmental stages. Global Change Biology 7:755-777.

Law BE, Van Tuyl S, Cescatti A, Baldocchi DD. 2001b. Estimation of leaf area index in open-canopy ponderosa pine forests at different successional stages and management regimes in Oregon. Agricultural and Forest Meteorology 108:1-14.

Lentile LB, Smith FW, Shepperd WD. 2005. Patch structure, fire-scar formation, and tree regeneration in a large mixed-severity fire in the South Dakota Black Hills, USA. Canadian Journal of Forest Research 35:2875-2885.

Martin RE, Sapsis DB. 1991. Fires as agents of biodiversity: pyrodiversity promotes biodiversity. In: Harris RR, Erman DE, Kerner HM, technical coordinators (Ed.), Proceedings of the symposium on biodiversity of northwestern California. Wildland Resources Center, Santa Rosa, CA, pp. 150-157.

Maser, C., Anderson, R.G., Cromack Jr, K., Williams, J.T., Martin, R.E. 1979. Dead and down woody material. Wildlife habitats in managed forests of the Blue Mountains of Oregon and Washington, USDA Forest Service Agriculture Handbook No. 553.

McIver JD, Ottmar RD. 2007. Fuel mass and stand structure after post-fire logging of a severely burned ponderosa pine forest in northeastern Oregon. Forest Ecology and Management 238:268-279.

Means JE, Hansen HA, Koerper GJ, Alaback PB, Klopsch MW. 1994. Software for computing plant biomass-BIOPAK users guide. USDA Forest Service General Technical Report PNW-GTR-340. Portland, OR.

Miller JD, Safford HD, Crimmins M, Thode AE. 2009. Quantitative evidence for increasing forest fire severity in the Sierra Nevada and Southern Cascade Mountains, California and Nevada, USA. Ecosystems 12:16-32.

Mitchell SR, Harmon ME, O'Connell KEB. 2009. Forest fuel reduction alters fire severity and long-term carbon storage in three Pacific Northwest ecosystems. Ecological Applications 19:643-655.

Monsanto PG, Agee JK. 2008. Long-term post-wildfire dynamics of coarse woody debris after salvage logging and implications for soil heating in dry forests of the eastern Cascades, Washington. Forest Ecology and Management 255:3952-3961.

Mutch LS, Swetnam TW. 1995. Effects of fire severity and climate on ring-width growth of giant sequoia after burning. USDA Forest Service General Technical Report INT-GTR-320. Ogden, UT.

OFRI. 2006. Forests, Carbon, and Climate Change: A Synthesis of Science Findings. Oregon Forest Resources Institute (OFRI). Portland, OR.

Ottmar RD, Sandberg DV, Riccardi CL, Prichard SJ. 2007. An overview of the Fuel Characteristic Classification System - Quantifying, classifying, and creating fuelbeds for resource planning. Canadian Journal of Forest Research 37:2383-2393.

Pierce LL, Running SW. 1988. Rapid estimation of coniferous forest leaf-area index using a portable integrating radiometer. Ecology 69:1762-1767.

Prichard SJ, Ottmar RD, Anderson GK. 2006a. Consume 3.0 user's guide. Pacific Wildland Fire Sciences Laboratory, USDA Forest Service, Pacific Northwest Research Station. Seattle, WA.
http://www.fs.fed.us/pnw/fera/research/smoke/consume/index.shtml.

Prichard SJ, Riccardi CL, Sandberg DV, Ottmar RD. 2006b. FCCS user's guide. Pacific Wildland Fire Sciences Laboratory, USDA Forest Service, Pacific Northwest Research Station. Seattle, WA. http://www.fs.fed.us/pnw/fera/fccs/index.shtml.

Reich, P.B., Bakken, P., Carlson, D., Frelich, L.E., Friedman, S.K., Grigal, D.F. 2001. Influence of logging, fire, and forest type on biodiversity and productivity in southern boreal forests. Ecology 82:2731-2748.

Rorig ML, Ferguson SA. 1999. Characteristics of lightning and wildland fire ignition in the Pacific Northwest. Journal of Applied Meteorology 38:1565-1575.

Running SW. 2008. Ecosystem disturbance, carbon, and climate. Science 321:652-653.

Russell RE, Saab VA, Dudley JG, Rotella JJ. 2006. Snag longevity in relation to wildfire and postfire salvage logging. Forest Ecology and Management 232:179-187.

Santantonio D, Hermann RK, Overton WS. 1977. Root biomass studies in forest ecosystems. Pedobiologia 17:1-31.

Savage M, Mast JN. 2005. How resilient are southwestern ponderosa pine forests after crown fires? Canadian Journal of Forest Research 35:967-977.

Schoennagel T, Veblen TT, Romme WH. 2004. The interaction of fire, fuels, and climate across Rocky Mountain forests. Bioscience 54:661-676.

Shatford JPA, Hibbs DE, Puettmann KJ. 2007. Conifer regeneration after forest fire in the Klamath-Siskiyous: How much, how soon? Journal of Forestry 105:139-146.

Schwind B (Compiler). 2008. Monitoring Trends in Burn Severity: Report on the Pacific Northwest and Pacific Southwest fires -- 1984 to 2005. Available online: http://mtbs.gov.

Simon SA. 1991. Fire history in the Jefferson Wilderness area of east of the Cascade Crest. A final report to the Deschutes National Forest Fire Staff.

Soeriaatmadhe RE. 1966. Fire history of the ponderosa pine forests of the Wam Springs Indian Reservation Oregon. Ph.D. Thesis. Oregon State University.

Sun OJ, Campbell JL, Law BE, Wolf V. 2004. Dynamics of carbon stocks in soils and detritus across chronosequences of different forest types in the Pacific Northwest, USA. Global Change Biology 10:1470-1481.

Swedberg, KC. 1973. Transition coniferous forest in the Cascade Mountains of Northern Oregon. American Midland Naturalist 89:1-25.

Tappeiner, JC, Helms JA. 1971. Natural regeneration of Douglas fir and white fir on exposed sites in the Sierra Nevada of California. American Midland Naturalist:358-370.

Thomas CK, Law BE, Irvine J, Martin JG, Pettijohn JC, Davis KJ. 2009. Seasonal hydrology explains inter-annual and seasonal variation in carbon and water exchange in a semi-arid mature ponderosa pine forest in Central Oregon. Journal of Geophysical Research, Biogeosciences, in press.

Thornton PE, Running SW, White MA. 1997. Generating surfaces of daily meteorological variables over large regions of complex terrain. Journal of Hydrology 190:214-251.

Turner DP, Ritts WD, Law BE, Cohen WB, Yang Z, Hudiburg T, Campbell JL, Duane M. 2007. Scaling net ecosystem production and net biome production over a heterogeneous region in the western United States. Biogeosciences 4:597-612.

Turner MG, Tinker DB, Romme WH, Kashian DM, Litton CM. 2004. Landscape patterns of sapling density, leaf area, and aboveground net primary production in postfire lodgepole pine forests, Yellowstone National Park (USA). Ecosystems 7:751-775.

USDA. 1996. Metolius Watershed Analysis. Deschutes National Forest, Sisters Ranger District. Sisters, OR.

USDA. 2003a. Field instructions for the annual inventory of Washington, Oregon, and California. Forest Inventory and Analysis Program. USDA Forest Service Pacific Northwest Research Station. Portland, OR.

USDA. 2003b. Metolius Basin Forest Management Project FEIS. Deschutes National Forest, Sisters Ranger District. Sisters, OR.

USDA. 2004. Metolius Watershed Analysis – Update. Deschutes National Forest, Sisters Ranger District. Sisters, OR.

Van Tuyl S, Law BE, Turner DP, Gitelman AI. 2005. Variability in net primary production and carbon storage in biomass across Oregon forests: An assessment integrating data from forest inventories, intensive sites, and remote sensing. Forest Ecology and Management 209:273-291.

Van Wagner CE. 1968. The line intersect method in forest fuel sampling. Forest Science 14:20-26.

Waring RH, Savage T, Cromack K Jr, Rose C. 1992. Thinning and nitrogen fertilization in a grand fir stand infested with western spruce budworm. Part IV: An ecosystem management perspective. Forest Science 38:275-286.

Weaver H. 1959. Ecological changes in the ponderosa pine forest of the Warm Springs Indian Reservation in Oregon. Journal of Forestry 57:15-20.

Westerling AL, Hidalgo HG, Cayan DR, Swetnam TW. 2006. Warming and earlier spring increase western US forest wildfire activity. Science 313:940-943.

Wirth C, Czimczik CI, Schulze ED. 2002. Beyond annual budgets: Carbon flux at different temporal scales in fire-prone Siberian Scots pine forests. Tellus Series B-Chemical and Physical Meteorology 54:611-630.

Woolley TJ, Harmon ME, O'Connell KB. 2007. Estimating annual bole biomass production using uncertainty analysis. Forest Ecology and Management 253:202-210.

Zavitkovski J, Newton M. 1968. Ecological importance of snowbrush *Ceanothus velutinus* in the Oregon Cascades. Ecology 49:1134-1145.

FIGURES AND TABLES
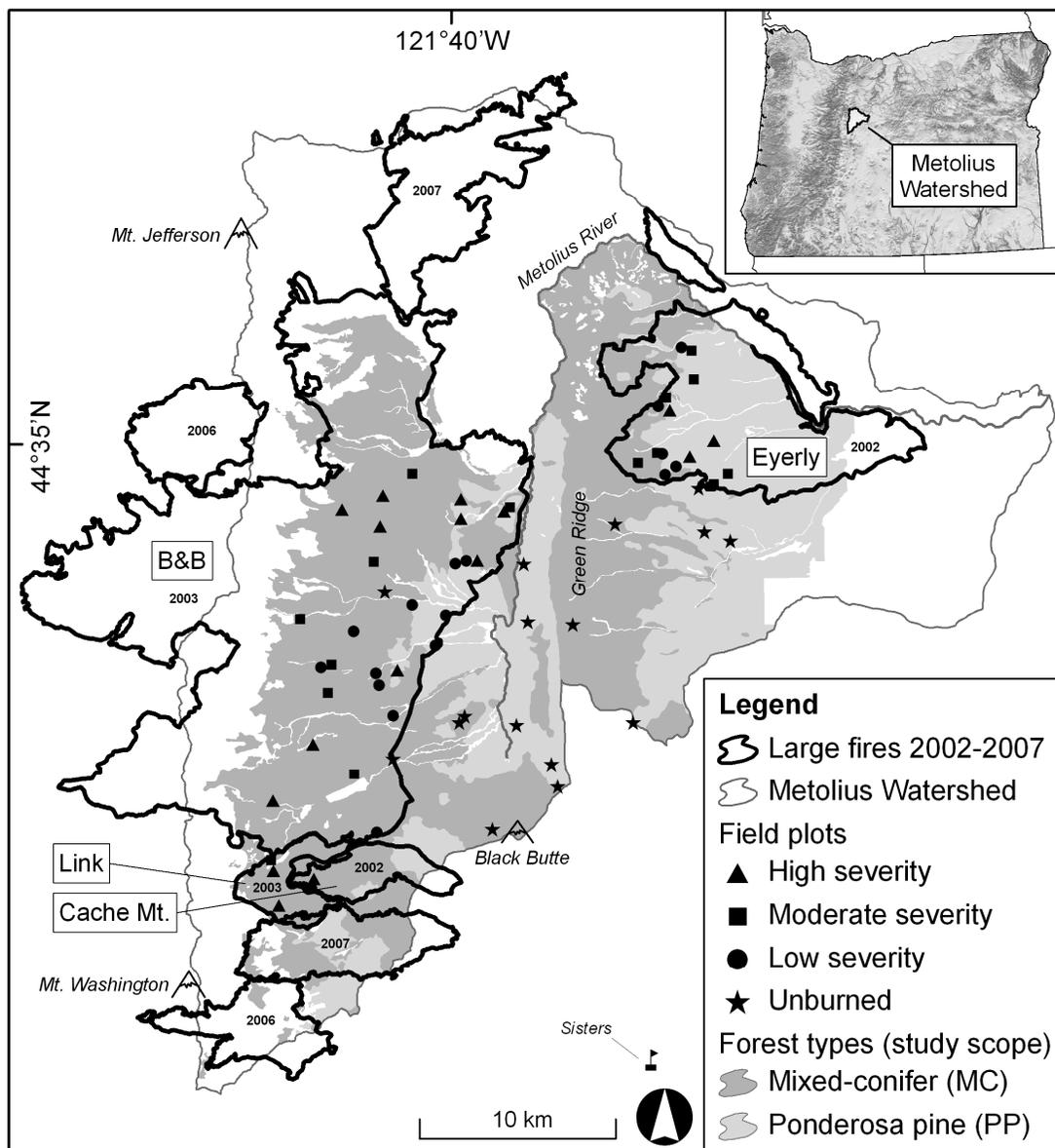
Figure 2.1. Metolius fire study area on the east slope of the Oregon Cascades. Point symbols denote survey plots ($n = 64$), labeled fires are the four surveyed (Table 2.2), and shaded areas are the sampled forest types. Other fires are outside the study scope and are labeled by fire year only. Forest type layer clipped to study scope: two types (MC and PP) on the Deschutes National Forest (DNF) within the Metolius Watershed. Other types (unshaded area within fires) include subalpine forests on the western margin, *Juniperus* woodlands to the east, non-forest, and riparian areas. Inset map shows study area location within Oregon elevation gradients. Fire perimeter and forest type GIS data from DNF. Other GIS data from archives at Oregon State University. Projection: UTM NAD 83. See also the color map in Figure A2.1 (Appendix 2).

Figure 2.2. Characteristic forest stands across the Metolius Watershed study gradients. Clockwise from top-left: (a) unburned MC, (b) low-severity PP, (c) moderate-severity MC, (d) high-severity PP. Unburned stands contain heavy fuel accumulations and high tree and understory vegetation density; low-severity stands show partial bole scorching, high tree survivorship, and rapid recovery of surface litter; moderate-severity stands show increased bole scorch heights and overstory mortality; high-severity stands show near 100% tree mortality and generally thick understory vegetation (shrubs and herbs). Note that almost all fire-killed trees remain standing 4-5 y postfire.
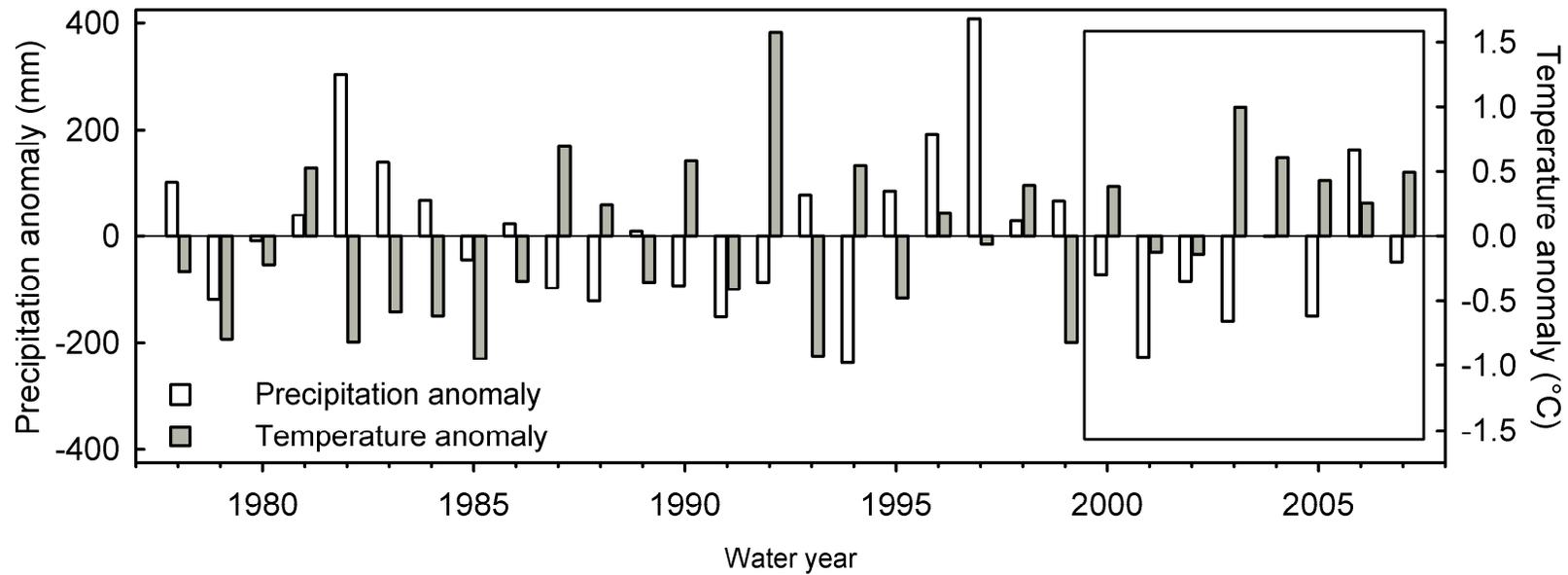
Figure 2.3. Climate anomalies in the Metolius Watershed. Anomalies in precipitation (mm) and temperature (°C) are in reference to the 30-y mean (1978-2007) from PRISM data (prismclimate.org) extracted at a central location in the watershed (described by Thomas and others, 2009). Water year is defined as the 12-mo period from October-September. The 2000 water year marked the beginning of an anomalously warm and dry period, coincident with a positive phase of the Pacific Decadal Oscillation (Thomas and others, 2009). These anomalies contributed to drought stress and set the stage for wildfires and potentially harsh conifer regeneration conditions.
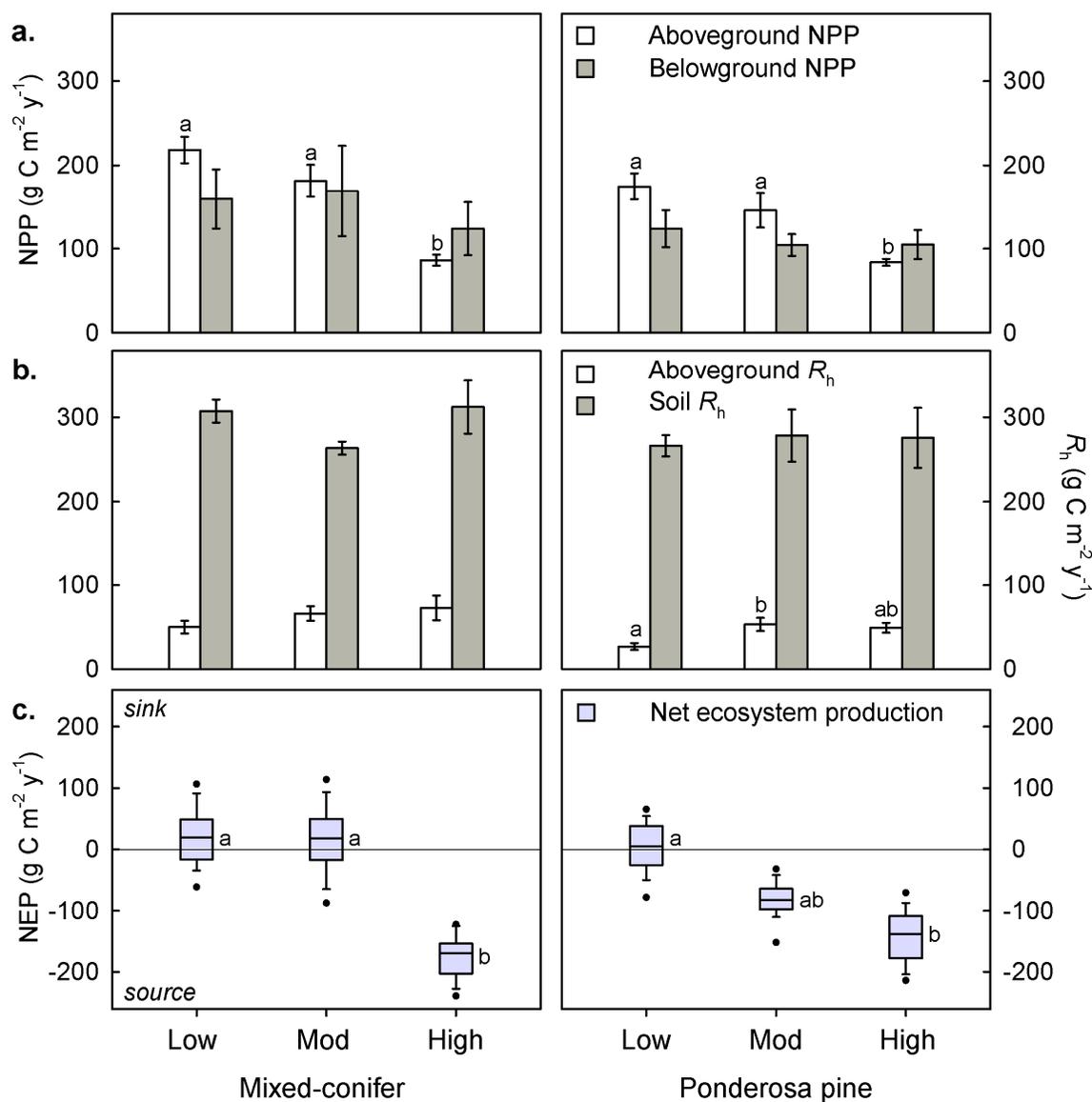
Figure 2.4. (a) Net primary productivity (NPP), (b) heterotrophic respiration (Rh), and (c) net ecosystem production (NEP) by forest type and burn severity in the Metolius Watershed. Bars in (a) and (b) denote means; error bars denote ± 1 SE from 8 plots in each forest type*burn severity treatment. Boxplots in (c) from Monte Carlo uncertainty propagation (see Methods); line denotes median, box edges denote 25th and 75th percentiles, error bars denote 10th and 90th percentiles, and points denote 5th and 95th percentiles. Aboveground R_h includes all dead wood, shrubs, and herbaceous vegetation (Table 2.7). Soil R_h fractions from Irvine and others 2007. Lowercase letters denote statistically significant differences (Tukey-adjusted $P < 0.05$) among severities, tested with regression of each response variable given prefire biomass and severity.
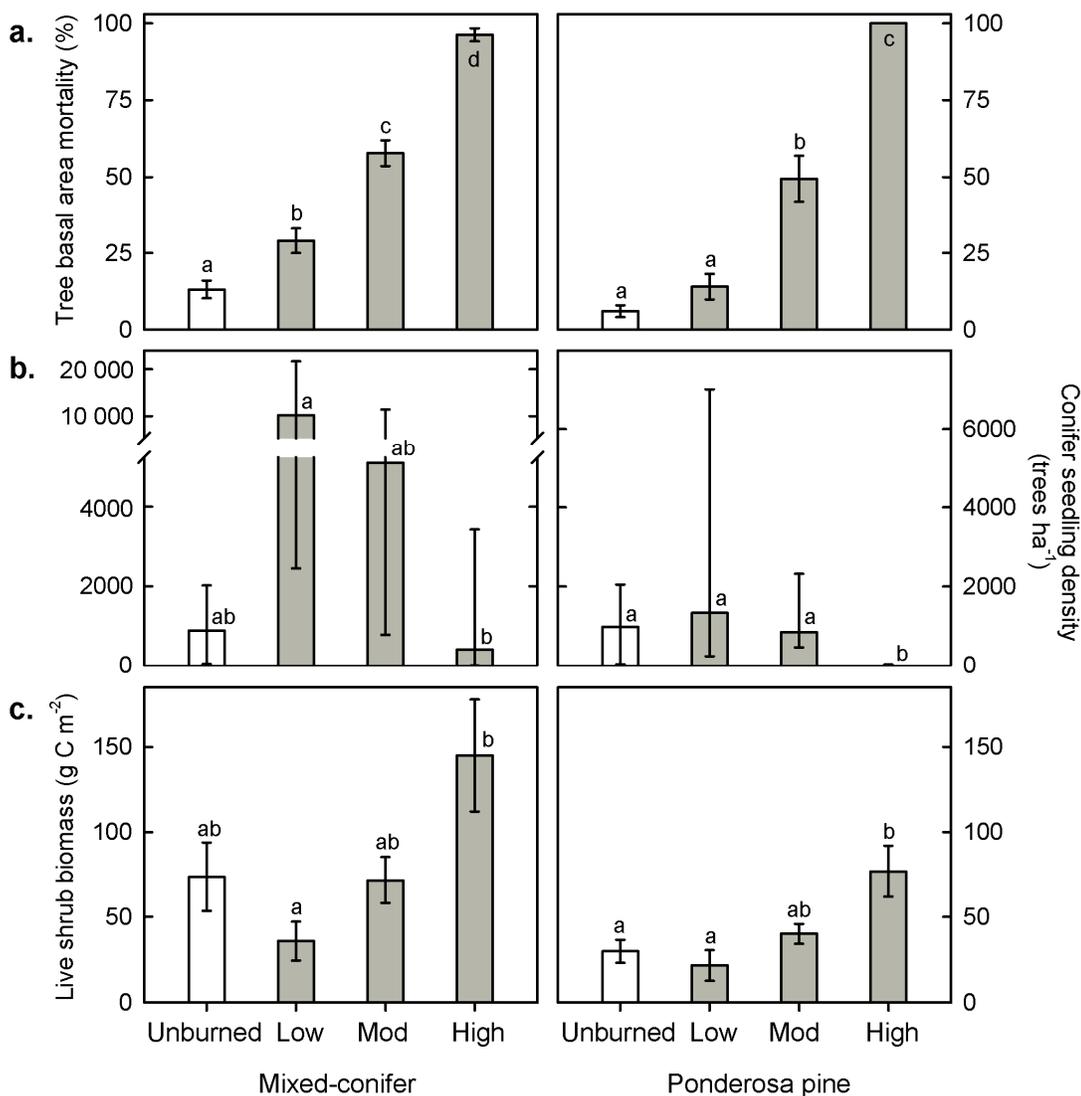
Figure 2.5. (a) Tree basal area (BA) mortality, (b) conifer seedling regeneration, and (c) live shrub biomass 4-5 years postfire by forest type and burn severity in the Metolius Watershed. Bars in (a) and (c) denote means; error bars denote ± 1 SE from 8 plots in each forest type*burn severity treatment. Due to skewness, bars in (c) denote medians and error bars denote 25th and 75th percentile. Note the different scales between forest types above y-axis break in (c). Tree mortality in (a) is % BA mortality due to fire in burned stands and total % dead BA in unburned stands. Lowercase letters denote statistically significant differences (Tukey-adjusted $P < 0.05$) among severities. Statistical tests for (a) used total % BA mortality, a metric common to all treatments. Statistical tests for (b) used $\log_e$-transformed data. (a) and (b) excluded the prefire biomass covariate. Seedlings are live, non-planted trees from the postfire time period only. Note that high-severity PP stands included 100% tree mortality in all 8 plots and a median seedling density of zero.

Table 2.1. Metolius Watershed study area characteristics.

Forest type[a] Burn severity[b]	Number of plots	Burned area (ha) within study scope	Burned area %	Elevation (m) (mean, range)		Slope (degrees) (mean, range)		Total tree basal area (mean m^{-2} ha^{-1}, SE)[c]		Total tree density (mean trees ha^{-1}, SE)[c]		Tree % mortality (mean, SE)[d]	
Mixed-conifer (MC)[a]	32	21 952	74	1160	(910-1558)	8.4	(1-22)	36	(3)	874	(103)	*61*	*(6)*
Unburned	8	na	na	1139	(910-1558)	4.9	(1-22)	35	(7)	911	(255)	13	(3)
Low severity	8	7236	25	1045	(972-1128)	6.8	(2-14)	40	(5)	1041	(252)	*29*	*(4)*
Moderate severity	8	4810	16	1155	(1068-1291)	10.5	(5-22)	35	(4)	1068	(142)	*58*	*(4)*
High severity	8	9906	33	1300	(1136-1479)	11.6	(8-14)	33	(7)	477	(81)	*96*	*(2)*
Ponderosa pine (PP)[a]	32	7821	26	1004	(862-1247)	5.2	(1-22)	21	(2)	643	(91)	*54*	*(8)*
Unburned	8	na	na	1035	(862-1247)	5.5	(1-17)	24	(4)	1020	(247)	6	(2)
Low severity	8	2371	8	977	(910-1074)	5.5	(1-22)	27	(5)	515	(122)	*14*	*(4)*
Moderate severity	8	2827	9	1046	(921-1092)	4.1	(1-7)	14	(3)	461	(122)	*49*	*(7)*
High severity	8	2623	9	957	(902-1063)	5.8	(1-15)	18	(5)	578	(168)	*100*	*(0)*
Overall	64	29 773	100	1082	(862-1558)	6.8	(1-22)	28	(2)	759	(70)	*58*	*(5)*

Notes:
Study scope was the area available for field sampling: Deschutes National Forest (DNF) non-wilderness land at least 50 m from roads, non-forest, and riparian areas. These area estimates are also used for landscape-scaling of pyrogenic emissions (Table 2.3). Note the uneven distribution of severity*type treatments across the sampled landscape.
[a] Determined from DNF plant association group GIS data. Forest type rows describe sum or mean values as applicable.
[b] Determined from DNF BARC burn severity GIS data.
[c] Mean basal area and density of all trees with DBH >1 cm, including live and dead. SE in parentheses.
[d] Mean % basal area mortality due to fire for burned stands (indicated by italics), mean % dead tree basal area for unburned plots. SE in parentheses.

Table 2.2. Four large fires selected for study in the Metolius Watershed.

Fire name	Fire size (ha) within watershed	Fire year	Ignition source
B&B Complex[a]	28 640	2003	lightning
Eyerly Complex	9362	2002	lightning
Link	1453	2003	human
Cache Mt.	1376	2002	lightning
Fire total	40 831		
Fire within MC and PP forest types (scope)	29 773		
Metolius Watershed area	115 869		

Notes:
[a] Booth and Bear Butte Complex: two large fires that merged into one.

Table 2.3. Consume 3.0 severity parameterization and FCCS fuelbeds to estimate pyrogenic C emission.

| FCCS fuelbed[a] | Forest type | Total aboveground C (Mg C ha^{-1})[b] | Burn severity[c] | Severity parameterization[c] | | | |
				10-hr fuel moisture[d] (%)	1000-hr fuel moisture[d] (%)	Duff moisture[e] (%)	Canopy Consumption[f] (%)
Grand fir -- Douglas-fir forest (fire suppression) (SAF 213)	Mixed-conifer	132.6	Unburned				
			Low severity	15	40	120	12.5
			Mod severity	2	20	70	50
			High severity	3	10	30	87.5
Pacific ponderosa pine forest (fire suppression) (SAF 237)	Ponderosa pine	87.2	Unburned				
			Low severity	15	40	120	12.5
			Mod severity	2	20	70	50
			High severity	3	10	30	87.5

Notes:
[a] Fuel Characteristic Classification System (FCCS) fuelbeds determined using GIS data and descriptions from US Forest Service FERA group: www.fs.fed.us/pnw/fera/. SAF codes are Society of American Foresters cover types (Eyre 1980).
[b] Total aboveground C from unburned stands, used for parameterizing FCCS fuelbed inputs for Consume modeling. Multiply by 2 for Mg ha^{-1} mass or by 100 for g C m^{-2}.
[c] Consume severity from fuel moisture and canopy consumption (moisture estimates from R. Ottmar, US Forest Service, 2009, personal communication).
[d] Surface fuel time lag diameter classes: 10-hr = 0.65-2.54 cm; 1000-hr ≥ 7.62 cm.
[e] Duff defined by FCCS as "partially to fully decomposed organic material between the litter-lichen-moss stratum and mineral soil" (Prichard and others 2006b).
[f] Canopy consumption: midpoint of standard burn severity classes (0-25%, 25-75%, 75-100% tree mortality for low, moderate, and high severity, respectively; http://mtbs.gov).

Table 2.4. Pyrogenic C emission (PE) from Consume 3.0 simulations and field measurements of consumption.

Forest type Burn severity	Stand scale			Landscape scale	
	Stand-scale PE (Mg C ha^{-1})[a]	% consumption, aboveground C[b]	% consumption, live tree stems[c]	Total PE (Tg C)[d]	Landscape % of total PE[d]
Mixed-conifer					
Low severity	16.6	13	0.23	0.120	16
Mod severity	25.3	19	0.71	0.122	16
High severity	32.3	24	2.01	0.320	42
Ponderosa pine					
Low severity	19.7	23	0.27	0.047	6
Mod severity	25.6	29	1.43	0.072	10
High severity	30.2	35	2.77	0.079	10
Across sampled burn area (29 773 ha)	**25.5**[e]	**22**[e]	**1.24**[e]	**0.760**	100

Notes:
[a] Pyrogenic C emission (PE) computed from simulated biomass combustion in Consume and field measurements of bark and bole charring calculated after Donato and others (2009a) and Campbell and others (2007).
[b] % of unburned plot aboveground C (Table 2.3, 3rd column).
[c] % of live tree bark and bole bark mass estimated from charring (mean, weighted by tree mass).
[d] Stand-scale PE scaled to the sampled landscape based on area of type*severity treatments (Table 2.1).
[e] Mean, weighted by area of type*severity treatments (Table 2.1).

Table 2.5. Carbon pools of stands in the Metolius Watershed

Forest type[a] Burn severity	Aboveground					Belowground			Ecosystem C[i]	
	Live tree mass	Non-tree live mass[b]	Dead wood mass[c]	FWD[d]	Forest floor[e]	Coarse root[f]	Fine root[g]	Soil C[h]		
Mixed-conifer[a]	5153 (807)	156 (12)	4080 (537)	171 (15)	610 (135)	3115 (232)	*185 (34)*	*6556 (348)*	***18 648 (1213)***
Unburned	a9302 (1146)	a140 (22)	2884 (1008)	205 (31)	a1610 (180)	3588 (480)	na (na)	na (na)	**na** (na)
Low severity	ab7268 (1147)	ab105 (22)	2813 (1009)	166 (31)	b374 (180)	3162 (481)	172 (62)	5960 (611)	**20 414** (2189)
Mod severity	bc3071 (1140)	a181 (22)	4371 (1003)	162 (30)	b289 (179)	2931 (478)	211 (61)	6434 (604)	**17 884** (2163)
High severity	c973 (1141)	ac200 (22)	6252 (1003)	153 (30)	b169 (179)	2780 (478)	172 (61)	7225 (604)	**17 727** (2166)
Ponderosa pine[a]	3178 (538)	104 (9)	1898 (300)	112 (16)	531 (151)	1713 (142)	*135 (10)*	*5903 (195)*	***12 677 (648)***
Unburned	a5110 (714)	abc78 (14)	a1517 (543)	ab179 (29)	a1566 (219)	1842 (276)	na (na)	na (na)	**na** (na)
Low severity	a5576 (716)	ab67 (14)	ab924 (544)	a75 (29)	b234 (219)	2131 (276)	128 (18)	6035 (353)	**ab15 244** (922)
Mod severity	b2098 (724)	bcd126 (14)	a1934 (551)	a130 (30)	b258 (222)	1563 (280)	141 (18)	5899 (359)	**a12 089** (937)
High severity	b0 (0)	d146 (14)	ac3218 (542)	ac64 (29)	b67 (218)	1317 (275)	137 (18)	5775 (351)	**ac10 677** (918)

Notes:
Values: mean C pools (g C m^{-2}). SE from regression in parentheses. Subscript letters indicate significant differences (Tukey-adjusted $P < 0.05$) between severities within each forest type. To convert values to Mg biomass ha^{-1}, divide by 50.
[a] Forest type row: non-italics denote all stands (unburned and burned, $n = 32$); italics denote burned stands only ($n = 24$, unburned stands not surveyed [na]).
[b] Other live pools: shrubs, seedlings, graminoids, forbs.
[c] Dead wood mass: sum of snags, stumps, and CWD (dead down wood ≥7.63 cm diameter).
[d] FWD: all woody fuels <7.63 cm diameter.
[e] Forest floor: sum of litter and duff.
[f] Coarse roots ≥10 mm diameter (modeled from diameter of live and dead trees and stumps).
[g] Fine roots <2 mm diameter (live and dead), scaled from 20 cm depth (62% [SD = 20] of fine roots assumed in top 20 cm)
[h] Soil C to 100 cm depth, scaled from 20 cm depth (49% [SD = 14] of soil C assumed in top 20 cm).
[i] Ecosystem C: sum of all C pools. Includes dead shrubs (not included in other columns).

Table 2.6. Annual net primary productivity (NPP) of burned stands in the Metolius Watershed.

Forest type[a] Burn severity	Aboveground						Belowground						Total NPP[h]		Non-tree[i] % of NPP_A	NPP_A:NPP_B ratio
	Tree[b]		Shrub		Herbaceous[c]		NPP_A[d]		Coarse root[e]		Fine root[f]		NPP_B[g]				
Mixed-conifer[a]	*93*	*(15)*	*20*	*(5)*	*46*	*(4)*	**159**	*(13)*	*18*	*(3)*	*132*	*(24)*	**150**	*(24)*	**309**	*(29)*	*42*	*1.06*
Low severity	ₐ173	(11)	8	(9)	33	(7)	ₐ**214**	(15)	ₐ36	(3)	122	(44)	**159**	(44)	**372**	(47)	19	1.35
Mod severity	ᵦ99	(11)	25	(9)	54	(7)	ₐ**178**	(15)	ᵦ18	(3)	151	(44)	**169**	(43)	**347**	(46)	44	1.05
High severity	ᵪ12	(11)	27	(9)	51	(7)	ᵦ**90**	(15)	ᵪ2	(3)	122	(44)	**125**	(43)	**215**	(46)	87	0.72
Ponderosa pine[a]	*68*	*(13)*	*10*	*(2)*	*57*	*(6)*	**135**	*(11)*	*10*	*(2)*	*96*	*(7)*	**107**	*(7)*	**242**	*(16)*	*50*	*1.26*
Low severity	ₐ135	(11)	3	(4)	ₐ34	(10)	ₐ**172**	(15)	ₐ22	(2)	91	(13)	**113**	(13)	ₐ**285**	(24)	22	1.52
Mod severity	ᵦ69	(12)	10	(4)	ᵦ71	(10)	ₐ**151**	(15)	ᵦ9	(2)	101	(13)	**110**	(13)	ₐᵦ**260**	(24)	54	1.37
High severity	ᵪ0	(0)	16	(4)	ₐᵦ68	(10)	ᵦ**84**	(15)	ᵪ0	(0)	97	(13)	**97**	(13)	ᵦ**180**	(24)	100	0.87

Notes:
Values: mean NPP (g C m^{-2} y^{-1}). SE from ANCOVA in parentheses. Subscript letters indicate significant differences (Tukey-adjusted $P < 0.05$) between severities within each forest type. Summary fluxes bold.
[a] Forest type row: italics denote values from burned stands only ($n = 24$; most NPP components not surveyed in unburned stands).
[b] Tree: sum of bole and foliage NPP_A. Coarse roots modeled from live tree DBH in separate column.
[c] Herbaceous: sum of graminoid and forb NPP_A, equal to dry mass.
[d] NPP_A: Annual aboveground net primary productivity (bold, shown in Fig. 2.4).
[e] Fine root NPP_B to 100 cm depth based on published turnover index (Andersen and others 2008) and total fine root mass scaled from 20 cm depth.
[f] NPP_B: Annual belowground net primary productivity (bold, shown in Fig. 2.4).
[g] Total NPP: sum of all above- and belowground fluxes entering the system (bold).
[h] Non-tree NPP_A: sum of shrub and herbaceous NPP_A.

Table 2.7. Annual heterotrophic respiration (R_h) and NEP of stands in the Metolius Watershed.

Forest type[a] Burn severity	Aboveground (R_{hWD})						Belowground		Total R_h[g]		NEP[h]		NPP:R_h ratio[h]
	Snag[b]	Stump[b]	CWD[c]	Dead shrub	Herbaceous[d]	R_{hWD}[e]	R_{hsoil}[f]	$R_{hsoil}:R_{soil}$ ratio[f]					
Mixed-conifer[a]	7 (1)	5 (1)	24 (4)	3 (2)	22 (2)	**61** (6)	*294 (12)*	*na*	***357*** *(12)*		*-44* *(28)*	*0.87*	
Unburned	3 (2)	7 (1)	29 (9)	1 (4)	19 (4)	**59** (12)	na (na)	(na)	**na** (na)		na (na)	(na)	
Low severity	7 (2)	3 (1)	14 (9)	7 (4)	17 (4)	**48** (12)	305 (21)	0.48	**353** (20)		ₐ21 (48)	1.05	
Mod severity	9 (2)	5 (1)	22 (9)	1 (4)	27 (4)	**64** (12)	261 (21)	0.52	**327** (19)		ₐ21 (55)	1.06	
High severity	9 (2)	5 (1)	32 (9)	3 (4)	26 (4)	**75** (12)	314 (21)	0.56	**388** (19)		₆-174 (32)	0.55	
Ponderosa pine[a]	2 (1)	3 (1)	9 (2)	2 (1)	26 (3)	**42** (3)	*274 (15)*	*na*	***317*** *(17)*		*-76* *(20)*	*0.76*	
Unburned	ₐᵦ0 (1)	4 (1)	ₐᵦ18 (3)	2 (2)	ₐ16 (4)	ₐ**40** (6)	na (na)	(na)	**na** (na)		na (na)	(na)	
Low severity	ₐ1 (1)	3 (1)	ₐ𝒸5 (3)	2 (2)	ₐ17 (4)	ₐᵦ**28** (6)	262 (28)	0.48	**290** (30)		ₐ0 (33)	0.98	
Mod severity	ₐ2 (1)	3 (1)	ₐ8 (3)	4 (2)	ᵦ36 (4)	ₐ𝒸**53** (6)	286 (28)	0.52	**338** (31)		ₐᵦ-87 (35)	0.77	
High severity	ₐ𝒸5 (1)	3 (1)	ₐ7 (3)	1 (2)	ᵦ34 (4)	ₐ**50** (6)	274 (28)	0.56	**324** (30)		ᵦ-142 (37)	0.56	

Notes:
Values: mean R_h (g C m^{-2} y^{-1}). SE from ANCOVA in parentheses, except NEP SE from Monte Carlo simulation (see Methods). Subscript letters indicate significant differences (Tukey-adjusted $P < 0.05$) between severities within each forest type. Summary fluxes bold.
[a] Forest type row: non-italics denote all stands (unburned and burned, $n = 32$); italics denote burned stands only ($n = 24$, unburned stands not surveyed [na]).
[b] Snag R_h uses 10% of CWD decay rate and stump R_h uses 100% of CWD decay rate.
[c] CWD R_h includes FWD R_h, which was less than 0.15% of CWD R_h in all treatments.
[d] Herbaceous: forb and graminoid combined (assumed 50% of dry mass).
[e] R_{hWD}: sum of aboveground components (bold). Includes herbaceous annual turnover (50% of dry mass).
[f] R_{hsoil}: heterotrophic soil respiration, based on total soil efflux and heterotrophic fractions from Irvine and others (2007). Moderate severity fraction is mean of unburned and high severity fractions.
[g] Total R_h: sum of all above- and belowground fluxes from land to atmosphere (bold).
[h] Net ecosystem production: sum of NPP (Table 2.5) and R_h fluxes. SE from Monte Carlo uncertainty propagation. NPP:R_h ratio <1 if negative NEP.

CHAPTER 3 ‖ BEYOND STAND-REPLACEMENT DISTURBANCE: SIMULATION OF LANDSCAPE CARBON DYNAMICS ACROSS A WILDFIRE SEVERITY GRADIENT IN THE EASTERN CASCADE RANGE, OREGON, USA

ABSTRACT

Low- and moderate-severity wildfire influences terrestrial carbon dynamics in forest ecosystems worldwide, but previous carbon modeling efforts have focused primarily on high-severity, stand-replacement fire. Here, we integrate Landsat-based detection of fire extent and severity from the Monitoring Trends in Burn Severity database with the Biome-BGC process model to investigate the impacts of large, variable-severity wildfires on carbon pools, fluxes, and pyrogenic emission across a 250 000 ha landscape in the Oregon Cascade Range. We focused on the effects of 4 fires that burned *ca.* 50 000 ha in 2002 and 2003, comparing 3 scenarios: high-severity only (other areas assumed unburned), moderate and high severity, and all severities (low, moderate, high). At the landscape-scale, moderate- and low-severity fire contributed 25% and 11% of total estimated pyrogenic carbon emission, respectively (0.66 Tg C total, or *ca.* 2.2% of statewide anthropogenic CO_2 emissions equivalent from the same 2-year period). Moderate- and low-severity fire accounted for 23% and 5% of landscape-level tree mortality, respectively, which resulted in the transfer of 2.00 Tg C from live to dead pools. This carbon transfer was *ca.* 3-fold higher than the one-time pulse from pyrogenic emission, but it will likely take decades for this dead wood to decompose via heterotrophic respiration. The inclusion of moderate-severity fire reduced postfire (2004) mean annual NEP by 39% compared to the high-severity only scenario; low-severity fire influence on NEP was small (additional reduction of 11% in mean NEP), likely because of high tree survivorship and the relatively lower areal coverage of low-severity fire. One year postfire, burned areas were a strong C source (net C exchange across 53 000 ha: -0.065 Tg C y^{-1}; mean ± SD: -123 ± 110 g C m^{-2} y^{-1}) vs. a prefire mean near C neutral (1997-2001 mean NEP ± SD: -5 ± 51 g C m^{-2} y^{-1}). The model has been known to underestimate carbon uptake in mature and old semi-arid forests, so the prefire value is likely underestimated. Despite the recent rise in annual burned area across western North

America, including a substantial increase in the proportion of high-severity fire in the ecoregions studied here, low- and moderate-severity wildfire accounts for the majority of burned area in the Pacific Northwest region. This non-stand-replacement fire has important consequences for carbon loss and uptake at the landscape- and regional-scales, even though high-severity fire impacts are greater at the stand scale. These results suggest that by utilizing novel remote-sensing datasets to account for low-, moderate-, and high-severity fire, carbon modelers can substantially reduce uncertainties in key components of regional and global carbon budgets, particularly pyrogenic emissions and mortality.

INTRODUCTION

Given the pivotal role of forests in terrestrial carbon storage and mitigation strategies for anthropogenic greenhouse gas emissions (CCAR 2007, IPCC 2007), accurate modeling of disturbance processes is an increasingly important scientific frontier (Körner 2003, Goward *et al.* 2008, Running 2008). Fire is a fundamental, global phenomenon that has influenced carbon cycling, vegetation, and climate for millions of years (Cope & Chaloner 1985, Bowman *et al.* 2009). Though pervasive, fire is highly variable across space and time. Stand-replacement wildfire is a vital ecological process, but low- and mixed-severity fire regimes are characteristic of many forest types, particularly in western North America (Schoennagel *et al.* 2004, Hessburg *et al.* 2007). Despite the widespread occurrence of non-lethal fire and other partial disturbances (Agee 1993), most carbon model research focuses solely on stand-replacement disturbance. This study presents a novel remote-sensing and modeling framework to quantify the carbon consequences of recent variable-severity wildfires in the eastern Cascades of Oregon.

Numerous carbon (C) modeling efforts have investigated stand-replacement fire, particularly in boreal forests (*e.g.,* Kang *et al.* 2006, Bond-Lamberty *et al.* 2007, Kurz *et al.* 2008), yet many uncertainties remain. One key challenge is the detection of disturbance extent and severity (defined here as remotely-sensed vegetation mortality). Studies to date have been limited by remote-sensing datasets of high-severity disturbance over a relatively short time period (*i.e.,* Landsat MSS since 1972 [Cohen *et al.* 1996], AVHRR since 1982 [Potter *et al.* 2003]). For longer-term analyses, researchers have typically measured chronosequences, substituting stand age for time since disturbance (Law *et al.* 2003, Law *et al.* 2004). These approaches are appropriate where disturbance results in stand-replacement and generally even-aged forests, such as fire in the boreal zone and clearcut harvest (*e.g.,* Amiro *et al.* 2001, Bond-Lamberty *et al.* 2007), but few studies have addressed the effects of nonlethal fires, which are widespread in many regions. By definition, low-severity fire does not dramatically alter the distribution of live and dead C pools, but it does have important impacts on C cycling, particularly

pyrogenic emission, understory vegetation, and net ecosystem production (Meigs *et al.* 2009, this thesis, Chapter 2). In a time of rapid climate change and correlated increases in fire extent and severity (Westerling *et al.* 2006, Miller *et al.* 2009), accounting for the full disturbance gradient is crucial to reduce uncertainty in regional and global C budgets. Yet, to our knowledge, no modeling studies have explicitly assessed the effects of low-, moderate-, and high-severity fire on C pools and fluxes.

Ecosystem process models have been used extensively to investigate the interactive effects of disturbance, climate, CO_2 fertilization, and N deposition on C dynamics (*e.g.,* Thornton *et al.* 2002, Law *et al.* 2003, Smithwick *et al.* 2009), and recent advances in remote-sensing enable enhanced disturbance accounting. Because they are based on mechanistic relationships, process models allow robust hypothesis testing (Mäkela *et al.* 2000) and evaluation of variable disturbance regimes (Balshi *et al.* 2007). The Biome-BGC process model integrates diverse, high resolution data inputs and enables spatially-explicit, seamless mapping of C pools and fluxes (Thornton *et al.* 2002, Bond-Lamberty *et al.* 2007, Turner *et al.* 2007), including measures of C uptake: net primary production, net ecosystem production, and net biome production (NPP, NEP, and NBP, respectively; Chapin *et al.* 2006). It also provides flexibility in disturbance parameterization and can simulate multiple disturbance events derived from remote-sensing datasets. In the current study, we use two emerging change detection datasets— Monitoring Trends in Burn Severity (MTBS; http://mtbs.gov/) and LandTrendr time-series change detection (Kennedy *et al.*, in prep.)—to characterize carbon cycle responses along a gradient of burn severity.

Following a relatively fire-free period, recent wildfires have burned *ca.* 65 000 ha as a variable-severity mosaic in and around the Metolius River Watershed (Figs. 3.1 and 3.2), altering the landscape C balance and emitting a regionally important C pulse through combustion and lagged decomposition of necromass (this thesis, Chapter 2). The large spatial extent and variability in fire effects, combined with previous field, modeling, and remote-sensing studies in burned and unburned forests in the area (*e.g.,* Law *et al.* 2003, Irvine *et al.* 2007), provided an unprecedented opportunity to investigate the role of

wildfire severity in landscape-scale C cycling. This study compliments previous modeling efforts—including extensive site-specific evaluation of the Biome-BGC model (Thornton *et al.* 2002, Law *et al.* 2004, Turner *et al.* 2007)—by introducing new remote-sensing datasets and improved combustion estimates. Our specific objectives were to:

1. Describe burn severity patterns at the landscape and regional scales to assess the importance of non-stand-replacing wildfire.

2. Test the sensitivity of carbon cycle impacts to 3 burn severity scenarios: High severity only; moderate and high severity; low, moderate, and high severity.

3. Account for all 3 burn severities to quantify net fire effects on pyrogenic emission, mortality, C pools, and net ecosystem production.

Our primary hypothesis was that the introduction of low- and moderate-severity fire into the modeling framework would substantially increase pyrogenic C emission but that in contrast, high tree survival in low-severity areas would result in relatively small reductions in C pools, NPP, and NEP.

MATERIALS AND METHODS

Study area

The simulation area is a 244 600 ha landscape including the Metolius River Watershed, located on the east slope of the Oregon Cascades within two major ecoregions: the Cascade Crest (CC) and East Cascades (EC) (Fig. 3.1; Omernik 1987, Griffith & Omernik 2009). East slope vegetation is defined by one of the steepest precipitation gradients in western North America, transitioning from subalpine forests (cool, wet) to *Juniperus* woodlands (warm, dry) within 25 km. The mixed-conifer forests include ponderosa pine *(Pinus ponderosa)*, Douglas-fir *(Pseudotsuga menziesii)*, *Abies spp., Tsuga spp.*, and numerous locally abundant tree species (Swedberg 1973, Griffith & Omernik 2009). Forested elevations range from 600 m to 2000 m, with volcanic peaks reaching up to 3200 m. Slope steepness is generally gradual but increases with topographic complexity at higher elevations. Summers are warm and dry, and most precipitation falls as snow between October and June (Law *et al.* 2001). Mean annual precipitation ranges from 400 to 2300 mm, average minimum January temperature ranges from -6 °C to -3 °C, and average maximum July temperature ranges from 22 °C to 30 °C (Thornton *et al.* 1997; DAYMET 2009). Soils are volcanic (vitricryands and vitrixerands), well-drained sandy loams/loamy sands.

Recent fires are previously described in detail in Chapter 2 of this thesis. The study area spans a wide range of historic fire regimes associated with the climate gradient, from frequent, low-severity fire in ponderosa pine (return interval: 3-38 y; Fitzgerald 2005) to infrequent, high-severity fire in subalpine forests (fire interval: 168 y; Simon 1991). By the late 20th Century, a combination of time since previous fire, fire suppression, anomalous drought (Fig. 3.3), and insect activity generated fuel conditions conducive to large-scale wildfire (Waring *et al.* 1992, Franklin *et al.*1995, Fitzgerald 2005). Since 2002, 10 large (>1000 ha) wildfires have burned across multiple land cover types, yielding a heterogeneous spatial pattern of tree mortality and survival. This study focuses on 4 major fires that burned *ca.* 35% of the watershed in 2002-2003 (Figs. 3.1 and 3.2, Table 3.1).

Biome-BGC model background

Biome-BGC is a widely-used, daily time step ecosystem process model described in numerous publications (*e.g.,* Running & Coughlin 1988, Running & Hunt 1993, White *et al.* 2000, Turner *et al.* 2007) and evaluated previously in the study area (Law *et al.* 2001, Thornton *et al.* 2002, Law *et al.* 2004). Here, we provide a concise overview and highlight details specific to new disturbance parameterizations. The model simulates coupled terrestrial carbon, nitrogen, and water cycle processes, including photosynthesis, respiration (autotrophic and heterotrophic), C allocation, decomposition, plant mortality, nitrogen mineralization, and evapotranspiration (Thornton *et al.* 2002). Key inputs include daily meteorological data and a suite of land cover, soil, age, ecophysiological, and disturbance parameters derived from satellite remote-sensing. We used Biome-BGC version 4.1.1, modified for spatial analysis of Pacific Northwest regional C cycling and variable disturbance severity. We ran the model at a 1 km grain to produce annual maps of disturbance effects on C stocks and fluxes from 1985 to 2004 in the EC and CC ecoregions. A reference model run for hypothetical low-, moderate-, and high-severity fire in 1950 provides an adequate postfire time period to show trajectories of NEP recovery (Figure 3.4).

Principal inputs: land cover, climate, stand age, and ecophysiology

We derived land cover, soils, and climate inputs using the same procedures as Turner *et al.* (2007). Land cover was grouped into 7 classes determined from 2 primary sources: the National Land Cover Data set (Vogelmann *et al.* 2001) and Oregon GAP analysis (Kagan *et al.* 1999). Transitional vegetation in recent clearcuts was reclassified as conifer forest. We identified the EC and CC ecoregions from level III and level IV ecoregion descriptions, respectively (Omernik 1987, Griffith & Omernik 2009), and obtained soils data from U.S. Geological Survey coverages (CONUS, 2009). We used daily, 1 km resolution minimum and maximum temperature, precipitation, humidity, and solar radiation data from 1980-2004 developed with the DAYMET model (Thornton *et al.* 1997, DAYMET 2009) and recycled the 25-y record during model spin-up. We employed an age map based on land cover, remotely-sensed disturbance, and regression

of Forest Inventory and Analysis plot data with Landsat spectral indices. For conifer forest, we assigned the actual age to those pixels identified as stand-replacement disturbance since 1984 by the MTBS and LandTrendr datasets (described below) and grouped all other pixels into four age classes (45, 80, 150, 250 y) using regression-based modeled age (Duane *et al.,* in prep). Deciduous and woodland pixels were assigned ages of 50 y and 70 y, respectively. Landsat-derived variables were resampled to 25 m resolution for scaling with 1 km resolution climate data, and all spatial data were projected in Albers conic equal area NAD 83. We used the same ecophysiological and allometric constants described previously (Turner *et al.* 2007). To minimize bias in the age-specific patterns of live wood mass, we ran a parameter optimization procedure with regional Forest Inventory and Analysis data to determine the fraction of leaf nitrogen as rubisco (FLNR) and annual mortality (%) that best simulated ecoregion live wood mass distributions. FLNR has been used previously in optimization exercises with Biome-BGC because the model NPP is sensitive to it, and its value is poorly constrained by measurements (Thornton *et al*. 2002). Mortality is likewise poorly constrained and it has a strong influence on age-specific wood mass.

Novel disturbance inputs and parameterization

We resolved annual disturbance from fire and timber harvest across the study area using two complimentary Landsat remote-sensing datasets. The MTBS program has mapped all fires >400 ha in western North America from 1984 to present using before-after change detection with Landsat TM and ETM+ imagery (Schwind 2008). MTBS analysts compute the differenced normalized burn ratio (dNBR; Key and Benson 2006), a widely used metric of pre- to post-fire change, and derive 6 burn severity classes (Table 3.2). For this analysis, we accounted for low-, moderate-, and high-severity fire but excluded the unburned-low class, which represents a substantial area within fire perimeters (Fig. 3.5; Schwind 2008; http://mtbs.gov/). To determine if the severity proportions in our study area were representative of regional patterns and to assess the importance of non-stand-replacing fire across the region, we used the MTBS database to

investigate the patterns of burned area and severity classes across the Pacific Northwest, comparing states, ecoregions, and two 11-y time periods (1984-1994, 1995-2005).

LandTrendr is a new change detection technique that leverages a set of segmentation algorithms to identify salient trends and events in a time-series of Landsat imagery, enabling capture of slow disturbances (*e.g.,* insect defoliation) and partial disturbances (*e.g.,* thinning, prescribed fire) at an annual time-step (Kennedy *et al.* 2007, Kennedy *et al.*, in prep). We extracted all LandTrendr disturbances with a duration of 1-2 y and relative magnitude >15% cover change from 1985-2004, excluded pixels within MTBS-identified fires, and assumed that all other disturbances were clearcut timber harvests. We also used LandTrendr data to fill in low-, moderate-, and high-severity fire pixels within MTBS non-processing mask areas (defined in Table 3.2). In these areas, we extracted LandTrendr disturbance data within one year of the fire occurrence and classified low, moderate, and high severity with cover change relative magnitudes of 15-30%, 30-50%, and 50-100%, respectively.

We accounted for the 2 most recent disturbances. If less than 2 disturbances occurred after 1984, we assumed that age represented time since disturbance and that stands less than and greater than 75 y old were initiated by clearcut harvest and high-severity fire, respectively. We estimated pyrogenic C emission with severity- and biomass pool-specific combustion factors from published measurements in western Oregon conifer forests (Table 3.3; Campbell *et al.* 2007). To estimate tree mortality (transfer from live to dead tree pools), we used mid-range values from MTBS severity classes of percent tree mortality: 12.5%, 50%, 95% respectively for low-, moderate-, and high-severity fire and subtracted prefire from postfire pixels. We assumed that clearcut harvest resulted in 100% tree mortality and removed 75% of live tree mass from stands and that no disturbance occurred in non-forested pixels (Turner *et al.* 2007).

Biome-BGC simulations

To isolate the effects of low- and moderate-severity fire on C pools and fluxes, we ran 3 burn severity scenarios: high severity only; moderate and high severity; low, moderate, and high severity. Because of computational limitations from the number of

pixels at 25 m resolution ($n \approx 4000\ 000$), we ran the model for the 5 most prevalent combinations of land cover and disturbance history within each 1 km pixel ($n = 2446$; Turner *et al.* (2007). This approach captured >80% of the 25 m resolution variability for 93% of the simulation landscape (data not shown). There were 395 unique combinations of land cover and disturbance history (10 most frequent combinations shown in Table 3.4). Following model spin-up, including a dynamic mortality model (Pietsch & Hasenauer 2006), we simulated all disturbance scenarios to the year 2004 (the last year of available DAYMET climate data). After area-weighting to the 1 km resolution, the data were assembled into spatial surfaces of key response variables.

Data and uncertainty analysis

We calculated summary statistics (mean, spatial SD of 1 km cells) for mapped pre- and post-fire C metrics among the 3 severity scenarios described above. We computed annual NEP as the difference between NPP and heterotrophic respiration and quantified NEP, pyrogenic C emission, and harvest removals separately rather than combining them into a single metric (*i.e.,* net ecosystem carbon balance; Chapin *et al.* 2006). After we determined the differences between severity scenarios, we focused on the "all severities" scenario (low + moderate + high severity) to assess net fire effects on C pools and fluxes.

Previous studies have evaluated the Biome-BGC model across this landscape and region (Thornton *et al.* 2002, Law *et al.* 2004, Turner *et al.* 2007), but the new remote-sensing datasets described above provided an opportunity to investigate the uncertainty due to disturbance extent and severity. As such, we held other model parameters constant between burn severity scenarios. To assess the accuracy of the MTBS severity classification, we compared the severity classes with ground-based measurements of burn severity (% tree basal area mortality) from an independent dataset of field plots within the study area ($n = 24$), described in detail in Chapter 2 of this thesis.

We evaluated Biome-BGC outputs of annual NEP with field measurements 4-5 y postfire at a subset of ponderosa pine plots ($n = 15$). The DAYMET climate record (1980-2004) did not coincide with field measurements of NEP (2007), precluding a direct

comparison. We therefore simulated fire events in 1995 in order to estimate NEP 5 y postfire in the year 2000, the climate year most similar to the year when field plots were surveyed, thereby minimizing the confounding influence of interannual climatic variability on NEP (Fig. 3.3). We simulated low, moderate, and high severity according to the MTBS classes and compared measured and predicted values at individual sites and within severity classes. We estimated stand age by matching modeled live tree stem mass to field-measured prefire biomass, calculated as the sum of postfire live tree stem mass and fire-killed standing dead trees. Although few trees had fallen at the time of sampling, this approach likely underestimated actual prefire live tree mass because of infrequent snag fall and mass loss due to charring (Donato *et al.* 2009). We were unable to determine the extent of complete combustion of small trees across the landscape and among different severities. For the purposes of this prefire live tree reconstruction, we assumed that this pool was negligible relative to prefire aboveground biomass of large overstory trees (*i.e.,* one large overstory tree is equivalent to 60 small understory trees; Fellows & Goulden 2008).

We performed an additional analysis of remotely-sensed disturbance inputs, comparing the spatial extent and severity resolution of 5 different, readily-available datasets. In addition to MTBS, we used the stand-replacement disturbance map from Turner *et al.* (2007), two Landsat-based fire maps obtained directly from the Deschutes National Forest, and the MODIS MCD45A1 global burned area product (Roy *et al.* 2008), filtered to avoid double-counting of burned pixels. Other model uncertainties, including spatial inputs (*e.g.,* land cover, stand age, soils) and long-term postfire responses, are beyond the scope of this study.

RESULTS

Burned area and severity patterns across the region and simulation landscape

The 22 y MTBS record (1984-2005) provides a regional context for the large fires simulated in the current study and demonstrates the prevalence of low- and moderate-severity fire throughout the Pacific Northwest, as well as important ecoregional and temporal trends (Fig. 3.5). Averaged across all years and forested ecoregions in Oregon, low- and moderate-severity fire accounted for the largest proportions of annual burned area (42% and 30%, respectively, of total low-, moderate-, and high-severity area), whereas high-severity fire averaged 28% (*i.e.,* moderate and high severity totaled 58%. Burned area increased substantially between the two intervals (1984-1994, 1995-2005), more than doubling in all ecoregions except the Blue Mountains and Coast Range. In addition, there was a marked increase in the proportion of high-severity fire in the Cascade Crest, East Cascades, and Klamath Mountains ecoregions (Fig. 3.5). These trends were partially driven by the large fires assessed in this study, particularly in the Cascade Crest ecoregion, which exhibited the highest proportion of high-severity fire.

At the Metolius landscape scale, the large fires in 2002 and 2003 yielded a complex spatial mosaic of burn severity. Most of the burned landscape exhibited high heterogeneity from pixel to pixel, with low-, moderate-, and high-severity areas frequently co-occurring within 1 km pixels (Fig. 3.2). Although the 3 severity levels were generally interspersed, there was an increase in burn severity and patch size at higher elevations on the western portion of the landscape (Cascade Crest Ecoregion). Clearcut harvest was pervasive throughout burned and unburned forests on both sides of the Cascade Crest, but fire was the predominant recent disturbance in the Metolius Watershed (Fig. 3.2).

Sensitivity of simulated carbon cycle impacts to burn severity characterization

This section reports the relative differences between simulated severity scenarios, and the following section presents results from the "all severities" disturbance parameterization only. Despite the relatively high proportion of high-severity fire in the Cascade Crest Ecoregion, this condition accounted for less than half of the total burned

area across the 4 large fires in 2002 and 2003 (44%; Table 3.1, Fig. 3.2). Inclusion of low- and moderate-severity fire more than doubled the simulation burned area (127% increase from high only scenario). High-severity fire disproportionately impacted carbon pools and fluxes, but moderate- and low-severity fire substantially increased estimated pyrogenic emission and tree mortality and decreased postfire NEP. The effects of moderate- and low-severity fire on C responses was remarkably consistent, respectively contributing 25% and 11% of pyrogenic emission, 23% and 5% of tree mortality, and 26% and 8% of fire-reduced NEP (Table 3.5, Fig. 3.6). Although the % differences for tree mortality were smaller than the results for pyrogenic emission, the magnitude of C mortality was larger (Fig. 3.6). For simulated NEP one year postfire, the inclusion of moderate-severity fire resulted in a 39% decrease in mean NEP, and low-severity fire further reduced NEP by 11%; low- and moderate-severity combined reduced stand- and landscape-scale NEP by 50% (Fig. 3.7).

Fire effects on carbon pools, pyrogenic emission, and NEP

The largest overall C transfer was tree mortality, reflected in the change in live wood mass across the simulation landscape (Fig. 3.8). Fire-induced mortality created large swaths of very low live wood mass (<3000 g C m^{-2}), reducing high-severity areas to values well below adjacent unburned forest, woodlands, and shrublands (Figs. 3.8a and 3.8b). The simulated reduction in live mass was greater than 8000 g C m^{-2} (equivalent to 80 Mg C ha^{-1}) in many high-severity pixels, a function both of fire effects and prefire fuel mass (Fig. 3.8a). Across the burned landscape, we estimate that total tree mortality (transfer from live to dead wood pools) was 2.00 Tg C (weighted mean: 56 Mg C ha^{-1}). Based on published negative exponential decomposition constants for two dominant conifers (*Pinus ponderosa*: 0.011, *Abies grandis*: 0.038; Harmon *et al.* 2005), it would take 18-63 years for fire-killed necromass to lose 50% of its mass (*i.e.,* half-life) and substantially longer for full transfer to the atmosphere, particularly given that these published decomposition constants are from down woody detritus and standing dead trees decay at a much slower rate until they fall (M. Harmon, Oregon St. Univ., 2009, personal communication). We expect that NPP of surviving and regenerating vegetation will

offset these decomposition losses which are fundamentally different from the immediate combustion release (this thesis, Chapter 2).

Total simulated pyrogenic C emission was 0.66 Tg C, with a severity-weighted mean of 19 Mg C ha^{-1} (Table 3.5), one-third of the C transfer due to tree mortality. The landscape pattern of pyrogenic emission paralleled the burn severity mosaic and demonstrated the pervasive influence of low- and moderate-severity fire as well as the spatial heterogeneity in prefire C pools (*i.e.*, fuels; Figs. 3.8 and 3.9). Total simulated emission from the 2002-2003 fires was 2.2% of Oregon statewide anthropogenic CO_2 emissions equivalent for the 2-y period 2002-2003 (30.6 Tg C equivalent; http://oregon.gov/energy/gblwrm/docs/ccigreport08web.pdf).

The prefire landscape exhibited interannual variability in NEP with climate and localized disturbances (mostly patch clearcuts). In areas that eventually burned in 2002 and 2003, simulated NEP was close to C neutral throughout the study period, before changing to a large source in 2003 (Fig. 3.10). NEP across the entire simulation landscape averaged 19 g C m^{-2} y^{-1} (spatial SD = 67) from 1997-2001 (averaged from Fig. 3.11a.). Across burned areas, postfire (2004) NEP averaged -123 g C m^{-2} y^{-1} (spatial SD = 110). The spatial pattern of negative postfire NEP was highly variable, however, linked to prefire C pools, NEP, and burn severity (Fig. 3.11b). Much of the simulated postfire landscape was a strong C source (lower than -50 g C m^{-2} y^{-1}) immediately postfire, and some high-severity areas exhibited a net decrease in NEP of > 250 g C m^{-2} y^{-1} (Fig. 3.11c), driven largely by reductions in NPP. Summed across the burned landscape, total simulated NEP in 2004 was -0.065 Tg C y^{-1}, a large reduction from a prefire net C exchange (1997-2001 mean: -0.003 Tg C y^{-1}). Net C exchange across the entire landscape declined from the prefire to postfire period, but despite the large-scale wildfires, the simulation landscape remained a small C sink (prefire: 0.046 Tg C y^{-1}; postfire: 0.018 Tg C y^{-1}; postfire mean NEP ± SD: 7 ± 111 g C m^{-2} y^{-1}).

Uncertainty analysis

   Remote-sensing dataset comparison. The 5 readily-available remote-sensing datasets diverged widely in total burned area, as well as the level of precision and severity-specific coverage (Fig. 3.12). The MTBS dataset increased burned area by 43% compared to the Landsat stand replacement map (Turner *et al.* 2007), and the combination of MTBS moderate- and high-severity areas was similar to the stand replacement area. Conversely, the MTBS area was 29% less than the fire perimeters, and the MTBS burned area was very similar to the Burned Area Emergency Rehabilitation (BAER) map. Finally, the MODIS MCD45A1 global burned area product (500 m resolution, based on spectral change detection like Landsat; Roy *et al.* 2008) dramatically underestimated burned area (27% of the MTBS burned area). The MODIS product detected fire at 7 out of 48 randomly-located, independent field plots (Fig. 3.13). We further assessed the MODIS product, comparing it to MTBS for the Biscuit Fire in SW Oregon, and the MODIS underestimation was more extreme (*ca.* 5% of the burned area, Figs. 3.12b, 3.14).

   Evaluation of modeled severity effects on C uptake. Modeled annual NEP values were not strongly correlated with measured NEP 4-5 y postfire (Fig. 3.16a). The model tended to overestimate NEP, and there was only a weak linear trend ($R^2 = 0.05$). Comparison of modeled and observed NEP at the severity class level did not show improved correlations (Fig. 3.16b), although the model did correlate well with field measurements of NEP in unburned ponderosa pine forest in 2001 when multiple plots were aggregated for each data point in the correlation (Appendix 5).

DISCUSSION

Importance of low- and moderate-severity fire across the landscape and region

It is clear from both the regional trends in burn severity (Fig. 3.4) and the distribution of severity classes across the simulation landscape (Table 3.1, Fig. 3.2) that low- and moderate-severity fire influence C dynamics at multiple scales. Averaged across the total burned area, low- and moderate-severity fire decreased stand-scale (average per unit area) pyrogenic emission but increased landscape-scale pyrogenic emission by 57% (Table 3.5). High- and moderate-severity fire are clearly the principal drivers of C responses, but in the case of pyrogenic emission, the omission of low-severity would lead to the underestimation of fire emissions by 11%. Part of the underlying mechanism is the high combustion of the forest floor relative to other pools (Table 3.3), wherein tree survival can be relatively high despite substantial pyrogenic emissions (Campbell *et al.* 2007). These results support the approach of previous studies limited to stand-replacement disturbance (Law *et al.* 2004, Turner *et al.* 2007) but also underscore the value of accounting for the incremental effects of moderate- and low-severity fire for specific C responses. Because the fires in our simulation landscape included some of the largest proportions of high-severity fire in the Pacific Northwest, the C impacts of low- and moderate-severity fire would be more pronounced in other ecoregions and at the regional scale.

The prevalence of low- and moderate-severity fire across forested ecoregions of Oregon (72% of the mean total from 1984-2005) is consistent with our expectations of fire behavior and effects for temperate forests in this region (Agee 1993). Other biomes, however, may diverge widely from this pattern, notably boreal (Bond-Lamberty *et al. 2007*) and chaparral systems (Keeley & Zedler 2009). Because the Cascade Crest includes subalpine forest with fire regimes (Simon 1991) similar to boreal forest or other high-elevation forests in the conterminous US (*e.g.,* lodgepole pine ecosystems in Yellowstone National Park; Smithwick *et al.* 2009), it is not surprising that this ecoregion exhibited the highest proportion of high-severity fire of all the Oregon ecoregions. The large increase in burned area and severity between time intervals could be a function of

time since previous fire, fire suppression, and climate, or it may also be linked to widespread insect-caused tree mortality in the area that subsequently burned in the B & B Complex fire (Waring *et al.* 1992, Franklin *et al.*1995). The potential interactive effects of insects and wildfire merit further study (see Kurz *et al.* 2008) but are outside the scope of the current study.

The substantial increase in annual burned area and proportion of high-severity fire revealed by the MTBS record (Fig. 3.5) supports the findings of other studies documenting the widespread increase in fire extent and severity in western North America (Westerling *et al.* 2006, Miller *et al. 2*009). Using the same MTBS dataset, Schwind (2008) did not find similar patterns across a larger region (including parts of the Intermountain West and California), but our analysis focused solely on forested ecoregions at a finer spatial resolution. Miller *et al.* (2009) used an independent Landsat dataset and the RdNBR continuous burn severity index to quantify increasing burn severity in the Sierra Nevada, although they also documented substantial low- and moderate-severity proportions across all fires. We recognize that two decades is an inadequate reference period to assess large-scale changes in fire activity. Current fire extent is far less than historic levels (Stephens *et al.* 2007, Keeley & Zedler 2009), and continued increases in burned area thus appear likely even without climate change feedbacks. Nevertheless, in the context of continued increases in fire activity (Balshi *et al.* 2009), explicitly accounting for the effects of variable burn severity will become more important. By integrating new disturbance detection technologies like MTBS and LandTrendr, modelers can substantially increase both the areal coverage and precision of disturbance parameterization. Ignoring low- and moderate-severity fire is no longer necessary, and studies that exclude these areas will continue to underestimate fire effects, particularly pyrogenic emissions and tree mortality.

Landscape simulation of fire effects in the context of previous studies

Landscape-scale simulation was particularly effective for quantifying total C transfer due to mortality and pyrogenic emission, the two principal mechanisms of fire-induced C loss. By including low- and moderate-severity fire, our simulated estimates of

tree mortality are substantially higher than previous analyses (Turner *et al.* 2007). Although the magnitude of C transfer from live to dead pools exceeded the one-time loss through combustion (2.00 vs. 0.66 Tg C, respectively), these fire-killed pools will decay over many decades (coarse woody detritus half-life: 18-63 y). In addition, the decay of standing dead wood is substantially slower (5-20% of down woody detritus) in this seasonally-moisture-limited system (M. Harmon, Oregon St. Univ., 2009, personal communication), and the rapid growth of surviving and regenerating vegetation will likely offset respiratory losses from these necromass pools in the next 20 years (Law *et al.* 2003, this thesis, Chapter 2). In the short-term, however, most of the burned landscape remains a substantial C source (negative NEP), consistent with the controlling influences of soil heterotrophic respiration on postfire NEP (Irvine *et al.* 2007, this thesis, Chapter 2). Long-term monitoring of decomposition and soil processes is essential to elucidate pulses and time lags in these principal C sources.

Our simulated estimates of pyrogenic C emissions represent a substantial improvement from previous analyses, which focused on high-severity fire only and systematically underestimated emissions (Turner *et al.* 2007). On a per unit area basis, the total emissions of 0.66 Tg C from 35 723 ha is identical to the 3.8 Tg C estimated for the 200 000 ha Biscuit Fire (19 Mg C ha^{-1}, Campbell *et al.* 2007), suggesting that average prefire fuel accumulations were similar between these two western Oregon landscapes. Our finding that the one-time pulse from pyrogenic emission is equivalent to 2.2% of Oregon statewide anthropogenic CO_2 emissions provides an important constraint for C policies, and it is much lower than a published estimate that the B & B Complex Fire released 6 times the average Oregon statewide fossil fuel emissions (OFRI 2006). The contrast between infrequent pyrogenic vs. annual anthropogenic emissions also calls into question the notion of "catastrophic carbon release" from large wildfires (*sensu* Hurteau *et al.* 2008).

Because our Biome-BGC framework accumulates its own fuels at the pixel scale and accounts for variable fire effects, this approach enables spatially-heterogeneous, stand-scale precision. The high spatial resolution (25 m grain) enables linkages with

other fuel maps such as the FCCS (McKenzie *et al.* 2007), enhancing landscape-level analysis. In contrast, a regional to continental scale assessments by Wiedinmyer *et al.* (2006) assumed uniform fire effects (high severity only), that all needle-leaved evergreen fuel types—including open and closed canopy conifer forests—contained 140 Mg C ha^{-1} of fuel, and that a constant 30% of woody fuel was consumed. Although the approach described in the current study is an improvement over earlier efforts, many uncertainties remain due to the transient nature of pyrogenic emissions and lack of field measurements of prefire fuel mass and combustion factors. One crucial uncertainty is that Biome-BGC does not account for belowground C loss due to combustion, erosion, or other fire effects, which can be substantial (Bormann *et al.* 2008). In the fire studied here, however, an analysis of soil C and depth showed no significant differences among severities in this study area (this thesis, Chapter 2, Appendix 4).

These simulated C pools and fluxes before and after fire are largely consistent with previous studies in the area and provide an improved understanding of landscape gradients compared to stand-scale measurements. The range and distribution of simulated prefire aboveground live wood mass (Fig. 3.8a) is encompassed by C pool estimates from a ponderosa pine chronosequence (Law *et al.* 2003), and simulated postfire values (Fig. 3.8b) are similar to quantities measured in burned ponderosa pine (Irvine *et al.* 2007) and mixed-conifer forest (this thesis, Chapter 2). The simulated change from pre- to post-fire NEP (Fig. 3.11c) was consistent with these studies, although postfire NEP was generally lower, as demonstrated by the high-severity fire comparison in Table 3.6. One limitation of current Biome-BGC parameterization is the tendency for simulated NEP of older forests to approach C neutrality (Fig. 3.10), despite evidence that these forests can remain important C sinks both locally (Law *et al.* 1999, Anthoni *et al.* 2002) and globally (Luyssaert *et al.* 2008). This model bias could result in artificially reduced NEP, particularly in semi-arid systems (Mitchell *et al.*, in review).

Uncertainty analysis

Remote-sensing dataset comparison. Because disturbance is a crucial control on ecosystem processes (Law *et al.* 2004), the choice of remotely-sensed disturbance inputs is a principal driver of modeling uncertainty. The 43% increase in burned area and specific severity classes represent a large improvement over the previous disturbance map. The MTBS burned area reduction compared to fire perimeters demonstrates the important role of unburned and very low-severity islands across postfire landscapes and shows that modelers could substantially overestimate fire effects (*i.e.,* pyrogenic emissions) by using fire perimeters alone. The similarity between MTBS and BAER is logical because a dNBR image was the precursor to both maps, but the dramatic divergence in severity proportions highlights the uncertainty in the project-specific severity classification and soil burn severity focus of BAER analyses (Safford *et al.* 2008). Our finding that the MODIS burned area product was very low relative to other disturbance maps is consistent with the MODIS product's potential limitations for detection of variable-severity fire in dense forests at sub-regional scales (Roy *et al.* 2008). In contrast to the fire perimeters, modelers would drastically underestimate fire effects with the MODIS product. Although MODIS is fully automated and independent of subjective classification (MTBS limitations described below), Landsat appears to be a more appropriate sensor when targeting specific fire events, given its higher spatial resolution and established methods for determining burn severity thresholds in this region. In addition to increasing the area affected by fire, the MTBS archive enables the parameterization of low- and moderate-severity, thereby reducing uncertainty in both disturbance extent and magnitude.

Limitations of the MTBS archive. Although MTBS appears to be the best currently available remote-sensing fire dataset, several key uncertainties remain. First, the MTBS database is not exhaustive and to our knowledge, landscape-level accuracy assessment has not been conducted. It excludes fires <400 ha in western North America, ignoring a substantial number of smaller fires. In our study area, MTBS captured all major fires, but multiple fires burned together and were grouped, mislabeled, and double-

counted (in the case of the Cache Mt. Fire). Second, classification of the continuous variable dNBR image is an inherently subjective process that varies among technicians, management agencies, and regions (Schwind 2008). For this reason, results from the current study should not be extrapolated to other regions where the MTBS classes may reflect different fire effects and C responses. Third, the dNBR index has both known and unknown limitations (Roy *et al.* 2006). Like other remote-sensing indices, the dNBR calculation describes changes in spectral data, not tangible biological factors such as vegetation mortality, although it is strongly correlated with vegetation and soil effects and can be tuned with standardized ground measurements (Key & Benson 2005). Our comparison of field-measured tree mortality with the MTBS classes yielded mixed results (Fig. 3.15). Although the three MTBS severity classes captured a gradient of increasing tree mortality, there was substantial overlap between classes, and six plots with >25% mortality were classified as unburned to low-severity. This class accounts for a large portion within fire perimeters (Fig. 3.5), suggesting the need for further refinement in MTBS thresholds and model parameterization. Finally, the non-processing mask area can reduce MTBS coverage substantially, as in the B & B Complex fire. These limitations underscore the value of combining the MTBS data with continuous variable products like LandTrendr and the unclassified dNBR or RdNBR indices, as well as independent measures of burn severity (*e.g.,* field and aerial surveys).

Evaluation of modeled severity effects on C uptake. There are many sources of variability in simulated NEP, particularly in the underlying surfaces of age, land cover, and climate. Similarly, field-based estimates depend on numerous measurements and scaling assumptions (Campbell *et al.* 2004). Based on previous studies (*e.g.,* Law *et al.* 2003), we expected NEP to be most negative in high-severity stands and closest to C neutral in low-severity stands, but neither measured nor modeled NEP estimates followed this trend. The temporal mismatch between modeled and observed NEP precluded direct comparison in this study. This early stage of NEP in the first years after major disturbances is difficult to capture in forest growth models, which require further improvements based on field observations.

CONCLUSION

A period of anomalously dry years was a primary driver of recent fires across the Metolius Watershed (Fig. 3.3; Thomas *et al.* 2009), and although predictions of future climate are highly uncertain, the influence of wildfires on the terrestrial carbon balance will likely increase (Balshi *et al.* 2009). Modeling the full gradient of fire effects will thus become increasingly important. The novel disturbance simulation framework illustrated in this study increased the area affected by wildfire by 43% compared to previous studies and enabled severity-specific model parameterization. High-severity fire disproportionately impacted carbon pools and fluxes, but moderate- and low-severity fire substantially increased estimated pyrogenic emission and tree mortality and decreased postfire NEP. Moderate- and low-severity fire respectively contributed 25% and 11% of pyrogenic emission, 23% and 5% of tree mortality, and 26% and 8% of fire-reduced NEP. By accounting for all 3 severity classes, we estimated that the 2002-2003 fires released 0.66 Tg C through combustion (2.2% of statewide anthropogenic CO_2 emissions equivalent from the same 2-year period) and transferred 2.00 Tg C from live to dead wood pools.

Satellite remote-sensing has enabled unprecedented coverage of disturbance extent and severity. The MTBS database showed that low- and moderate-severity fire accounted for *ca.* 70% of the area burned from 1984 to 2005 in forested ecoregions of Oregon and that the burned area and proportion of high-severity fire increased in the last decade in parts of the Pacific Northwest, including the recent large wildfires on the East Slope of the Oregon Cascades. With these currently available remote-sensing approaches, researchers can achieve a more complete accounting of disturbance controls on landscape and regional C cycling. Future research should further reduce uncertainties associated with the MTBS database and explore the application of continuous variable change detection indices, including RdNBR and LandTrendr. Expanding on this active frontier, longer-term studies can further elucidate postfire trajectories, interannual climatic variability, multiple disturbance interactions (*e.g.*, insect defoliation, salvage harvest, and reburn), and future climate change scenarios.

REFERENCES

Agee JK (1993) *Fire ecology of Pacific Northwest forests.* Island Press, Washington, D.C.

Amiro BD, Todd JB, Wotton BM, *et al.* (2001) Direct carbon emissions from Canadian forest fires, 1959-1999. *Canadian Journal of Forest Research*, **31**, 512-525.

Anthoni PM, Unsworth MH, Law BE, Irvine J, Baldocchi DD, Van Tuyl S, Moore D (2002) Seasonal differences in carbon and water vapor exchange in young and old-growth ponderosa pine ecosystems. *Agricultural and Forest Meteorology,* **111**, 203-222.

Balshi MS, McGuire AD, Zhuang Q*, et al.* (2007) The role of historical fire disturbance in the carbon dynamics of the pan-boreal region: A process-based analysis. *Journal of Geophysical Research-Biogeosciences,* **112**.

Bond-Lamberty B, Peckham SD, Ahl DE, Gower ST (2007) Fire as the dominant driver of central Canadian boreal forest carbon balance. *Nature,* **450**, 89-93.

Bormann BT, Homann PS, Darbyshire RL, Morrissette BA (2008) Intense forest wildfire sharply reduces mineral soil C and N: the first direct evidence. Canadian Journal of Forest Research, **38**, 2771-2783.

Bowman D, Balch JK, Artaxo P*, et al.* (2009) Fire in the Earth System. *Science,* **324**, 481-484.

Campbell JL, Alberti G, Martin JG, Law BE (2009) Carbon dynamics of a ponderosa pine plantation following a thinning treatment in the northern Sierra Nevada. *Forest Ecology and Management,* **257**, 453-463.

Campbell JL, Donato DC, Azuma DL, Law BE (2007) Pyrogenic carbon emission from a large wildfire in Oregon, United States. *Journal of Geophysical Research,* **112**.

Campbell JL, Sun OJ, Law BE (2004) Disturbance and net ecosystem production across three climatically distinct forest landscapes. *Global Biogeochemical Cycles,* **18**.

CCAR (2007) Forest sector protocol version 2.1. California Climate Action Registry (CCAR). http://www.climateregistry.org/tools/protocols/industry-specific-protocols.html.

Chapin FS, III, Woodwell GM, Randerson JT*, et al.* (2006) Reconciling carbon-cycle concepts, terminology, and methods. *Ecosystems,* **9**, 1041-1050.

Cohen WB, Harmon ME, Wallin DO, Fiorella M (1996) Two decades of carbon flux from forests of the Pacific northwest. *Bioscience,* **46**, 836-844.

CONUS (2009) Conterminous United States multi-layer soil characteristics dataset for regional climate and hydrology modeling. http://www.soilinfo.psu.edu/index.cgi?index.html

Cope MJ, Chaloner WG (1985) Wildfire: An interaction of biological and physical processes. In: *Geological factors and the evolution of plants* (ed Tiffney BH), pp. 257-277. Yale University Press, New Haven.

DAYMET (2009) Distributed climate data, http://www.daymet.org/.

Donato DC, Campbell JL, Fontaine JB, Law BE (2009) Quantifying char in postfire woody detritus inventories. *Journal of Fire Ecology*, in press.

Duane M, Cohen WB, Campbell JL, *et al.* (In prep) Implications of two different field sampling designs on local accuracy and estimate distributions in mapping forest biophysical attributes from Landsat data.

Fellows AW, Goulden ML (2008) Has fire suppression increased the amount of carbon stored in western US forests? *Geophysical Research Letters,* **35.**

Fitzgerald SA (2005) Fire ecology of ponderosa pine and the rebuilding of fire-resilient ponderosa pine ecosystems. In: *Proceedings of the Symposium on Ponderosa Pine: Issues, Trends, and Management, 2004 October 18-21, Klamath Falls, OR*. USDA Forest Service, Pacific Southwest Research Station, PSW-GTR-198. Albany, CA.

Franklin SE, Waring RH, McCreight RW, Cohen WB, Fiorella M (1995) Aerial and satellite sensor detection and classification of western spruce budworm defoliation in a subalpine forest. *Canadian journal of remote sensing,* **21**, 299-308.

Giglio L, Loboda T, Roy DP, Quayle B, Justice CO (2009) An active-fire based burned area mapping algorithm for the MODIS sensor. *Remote Sensing of Environment,* **113**, 408-420.

Goward SN, Masek JG, Cohen WB*, et al.* (2008) Forest disturbance and North American carbon flux. *Eos, Transactions, American Geophysical Union,* **89**, 105-116.

Griffith G, Omernik JM (2009) Ecoregions of Oregon (EPA) In: *Encyclopedia of Earth* (eds McGinley M, Cleveland CJ). Environmental Information Coalition, National

Council for Science and the Environment, Washington, D.C. http://www.eoearth.org/article/Ecoregions_of_Oregon_(EPA)

Harmon ME, Fasth B, Sexton JM (2005) Bole decomposition rates of seventeen tree species in Western U.S.A.: A report prepared for the Pacific Northwest Experiment Station, the Joint Fire Sciences Program, and the Forest Management Service Center of WO Forest Management Staff. http://andrewsforest.oregonstate.edu/pubs/webdocs/reports/decomp/cwd_decomp _web.htm.

Hessburg PF, Salter RB, James KM (2007) Re-examining fire severity relations in pre-management era mixed conifer forests: inferences from landscape patterns of forest structure. *Landscape Ecology,* **22**, 5-24.

Hurteau MD, Koch GW, Hungate BA (2008) Carbon protection and fire risk reduction: toward a full accounting of forest carbon offsets. *Frontiers in Ecology and the Environment*, **6**, 493-498.

IPCC (2007) Climate Change 2007: The physical science basis: Contribution of Working Group I to the Fourth Assessment Report of the Intergovernmental Panel on Climate Change (IPCC) In: *IPCC Fourth Assessment Report* (eds Solomon S, Qin D, Manning M, Chen Z, Marquis M, Averyt KB, Tignor M, Miller HL). Cambridge University Press, Cambridge, United Kingdom and New York, NY, USA. http://www.ipcc.ch.

Irvine J, Law BE, Hibbard KA (2007) Postfire carbon pools and fluxes in semiarid ponderosa pine in Central Oregon. *Global Change Biology,* **13**, 1748-1760.

Kagan JS, Hak JC, Csuti B, *et al.* (1999) Oregon gap analysis project final report: A geographic approach to planning for biological diversity.

Kang S, Kimball JS, Running SW (2006) Simulating effects of fire disturbance and climate change on boreal forest productivity and evapotranspiration. *Science of the Total Environment,* **362**, 85-102.

Keeley JE, Zedler PH (2009) Large, high-intensity fire events in southern California shrublands: debunking the fine-grain age patch model. *Ecological Applications,* **19**, 69-94.

Kennedy RE, Cohen WB, Schroeder TA (2007) Trajectory-based change detection for automated characterization of forest disturbance dynamics. *Remote Sensing of Environment,* **110**, 370-386.

Kennedy RE, Yang Z, Cohen WB (In prep) Detecting trends in disturbance and recovery using yearly Landsat Thematic Mapper stacks: 1. Processing and analysis algorithm.

Key CH, Benson NC (2006) Landscape assessment: Ground measure of severity, the Composite Burn Index; and remote sensing of severity, the Normalized Burn Ratio. In: *FIREMON: Fire effects monitoring and inventory system.* USDA Forest Service, Rocky Mountain Research Station, RMRS-GTR-164-CD, Fort Collins, CO.

Körner C (2003) Slow in, rapid out - Carbon flux studies and Kyoto targets. *Science*, **300**, 1242-1243.

Kurz WA, Dymond CC, Stinson G*, et al.* (2008) Mountain pine beetle and forest carbon feedback to climate change. *Nature,* **452**, 987-990.

Law BE, Sun OJ, Campbell JL, Van Tuyl S, Thornton PE (2003) Changes in carbon storage and fluxes in a chronosequence of ponderosa pine. *Global Change Biology,* **9**, 510-524.

Law BE, Thornton PE, Irvine J, Anthoni PM, Van Tuyl S (2001) Carbon storage and fluxes in ponderosa pine forests at different developmental stages. *Global Change Biology,* **7**, 755-777.

Law BE, Turner D, Campbell JL, Sun OJ, Van Tuyl S, Ritts WD, Cohen WB (2004) Disturbance and climate effects on carbon stocks and fluxes across Western Oregon USA. *Global Change Biology,* **10**, 1429-1444.

Luyssaert S, Schulze ED, Borner A*, et al.* (2008) Old-growth forests as global carbon sinks. *Nature,* **455**, 213-215.

Mäkela A, Landsberg J, Ek AR, *et al.* (2000) Process-based models for forest ecosystem management: current state of the art and challenges for practical implementation. *Tree Physiology,* **20**, 289-298.

McKenzie D, Raymond CL, Kellogg LKB*, et al.* (2007) Mapping fuels at multiple scales: landscape application of the Fuel Characteristic Classification System. *Canadian Journal of Forest Research,* **37**, 2421-24

Meigs GW, Donato DC, Campbell JL, *et al.* (2009) Influence of mixed-severity wildfires on pyrogenic carbon transfers, postfire carbon balance, and regeneration trajectories in the Eastern Cascades, Oregon. *Ecosystems*, in press.

Miller JD, Safford HD, Crimmins M, Thode AE (2009) Quantitative evidence for increasing forest fire severity in the Sierra Nevada and Southern Cascade Mountains, California and Nevada, USA. *Ecosystems,* **12**, 16-32.

OFRI. 2006. Forests, Carbon, and Climate Change: A Synthesis of Science Findings. Oregon Forest Resources Institute (OFRI). Portland, OR.

Omernik JM (1987) Ecoregions of the conterminous United States. Map (scale 1:7,500,000). *Annals of the Association of American Geographers,* **77**, 118-125.

Pietsch SA, Hasenauer H (2006) Evaluating the self-initialization procedure for large-scale ecosystem models. *Global Change Biology,* **12**, 1658-1669.

Potter C, Tan PN, Steinbach M, Klooster S, Kumar V, Myneni R, Genovese V (2003) Major disturbance events in terrestrial ecosystems detected using global satellite data sets. *Global Change Biology,* **9**, 1005-1021.

Powell SL**,** Healey SP, Cohen WB, *et al.* (In prep) Quantification of live aboveground forest biomass dynamics with Landsat time-series and field inventory data: A comparison of empirical modeling approaches.

Roy DP, Boschetti L, Justice CO, Ju J (2008) The collection 5 MODIS burned area product - Global evaluation by comparison with the MODIS active fire product. *Remote Sensing of Environment,* **112**, 3690-3707.

Roy DR, Boschetti L, Trigg SN (2006) Remote sensing of fire severity: Assesing the performance of the normalized Burn ratio. *Ieee Geoscience and Remote Sensing Letters*, **3**, 112-116.

Running SW (2008) Ecosystem disturbance, carbon, and climate. *Science,* **321**, 652-653.

Running SW, Coughlan JC (1988) A general model of forest ecosystem processes for regional applications: 1. Hydrologic balance, canopy gas-exchange and primary production processes. *Ecological Modelling,* **42**, 125-154.

Running SW, Hunt ER (1993) Generalization of a forest ecosystem process model for other biomes, BIOME-BGC, and an application for global scale models. In: *Scaling physiological processes: leaf to globe* (eds Ehleringer JR, Field CB), pp. 141-157. Academic Press, San Diego.

Safford HD, Miller J, Schmidt D, Roath B, Parsons A (2008) BAER soil burn severity maps do not measure fire effects to vegetation: A comment on Odion and Hanson (2006). *Ecosystems,* **11**, 1-11.

Schoennagel T, Veblen TT, Romme WH (2004) The interaction of fire, fuels, and climate across Rocky Mountain forests. *Bioscience,* **54**, 661-676.

Schwind B (Compiler) (2008) Monitoring Trends in Burn Severity: Report on the Pacific Northwest and Pacific Southwest fires -- 1984 to 2005. Available online: http://mtbs.gov.

Simon SA (1991) Fire history in the Jefferson Wilderness area of east of the Cascade Crest. A final report to the Deschutes National Forest Fire Staff.

Smithwick EAH, Ryan MG, Kashian DM, Romme WH, Tinker DB, Turner MG (2009) Modeling the effects of fire and climate change on carbon and nitrogen storage in lodgepole pine (*Pinus contorta*) stands. *Global Change Biology,* **15**, 535-548.

Stephens SL, Martin RE, Clinton NE (2007) Prehistoric fire area and emissions from California's forests, woodlands, shrublands, and grasslands. *Forest Ecology and Management,* **251**, 205-216.

Swedberg KC (1973) Transition coniferous forest in the Cascade Mountains of Northern Oregon. *American Midland Naturalist,* **89**, 1-25.

Thomas CK, Law BE, Irvine J, *et al.* (2009) Seasonal hydrology explains inter-annual and seasonal variation in carbon and water exchange in a semi-arid mature ponderosa pine forest in Central Oregon. *Journal of Geophysical Research, Biogeosciences,* in press.

Thornton PE, Law BE, Gholz HL*, et al.* (2002) Modeling and measuring the effects of disturbance history and climate on carbon and water budgets in evergreen needleleaf forests. *Agricultural and Forest Meteorology,* **113**, 185-222.

Thornton PE, Running SW, White MA (1997) Generating surfaces of daily meteorological variables over large regions of complex terrain. *Journal of Hydrology,* **190**, 214-251.

Turner DP, Ritts WD, Law BE*, et al.* (2007) Scaling net ecosystem production and net biome production over a heterogeneous region in the western United States. *Biogeosciences,* **4**, 597-612.

Vogelmann JE, Howard SM, Yang LM, Larson CR, Wylie BK, Van Driel N (2001) Completion of the 1990s National Land Cover Data set for the conterminous United States from Landsat Thematic Mapper data and Ancillary data sources. *Photogrammetric Engineering and Remote Sensing,* **67**, 650-662.

Waring RH, Savage T, Cromack K, Jr., Rose C (1992) Thinning and nitrogen fertilization in a grand fir stand infested with western spruce budworm. Part IV: An ecosystem management perspective. *Forest Science,* **38**, 275-286.

Westerling AL, Hidalgo HG, Cayan DR, Swetnam TW (2006) Warming and earlier spring increase western US forest wildfire activity. *Science,* **313**, 940-943.

Wiedinmyer C, Quayle B, Geron C, *et al.* (2006) Estimating emissions from fires in North America for air quality modeling. *Atmospheric Environment,* **40**, 3419-3432.

White MA, Thornton PE, Running SW, Nemani RR (2000) Parameterization and sensitivity analysis of the BIOME–BGC terrestrial ecosystem model: net primary production controls. *Earth Interactions,* **4**, 1-85.

FIGURES AND TABLES
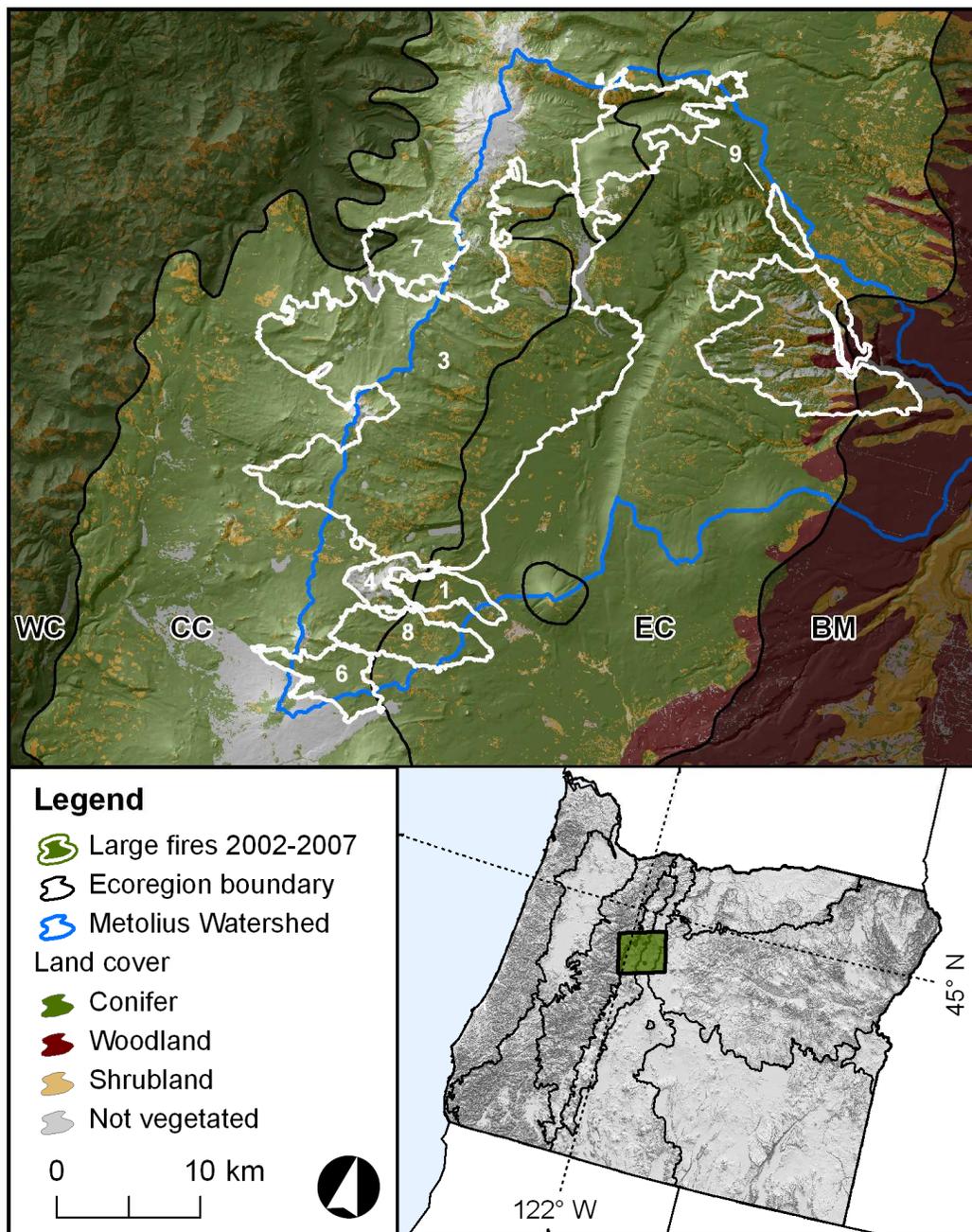
Figure 3.1. Biome-BGC simulation landscape. Ecoregion codes: WC: West Cascades; CC: Cascade Crest; EC: East Cascades; BM: Blue Mountains. Other ecoregions described in Turner *et al.* 2007. Fire reference numbers in Table 3.1. Inset map: location within Oregon ecoregions and topographic gradients. Data sources: Ecoregions: Omernik 1987, Griffith *et al.* 2009. Landcover: Kagan *et al.* 1999, Vogelmann *et al.* 2001. Fire perimeters: Deschutes National Forest. Spatial grain: 25 m. Projection: Albers Equal Conic Area NAD83.
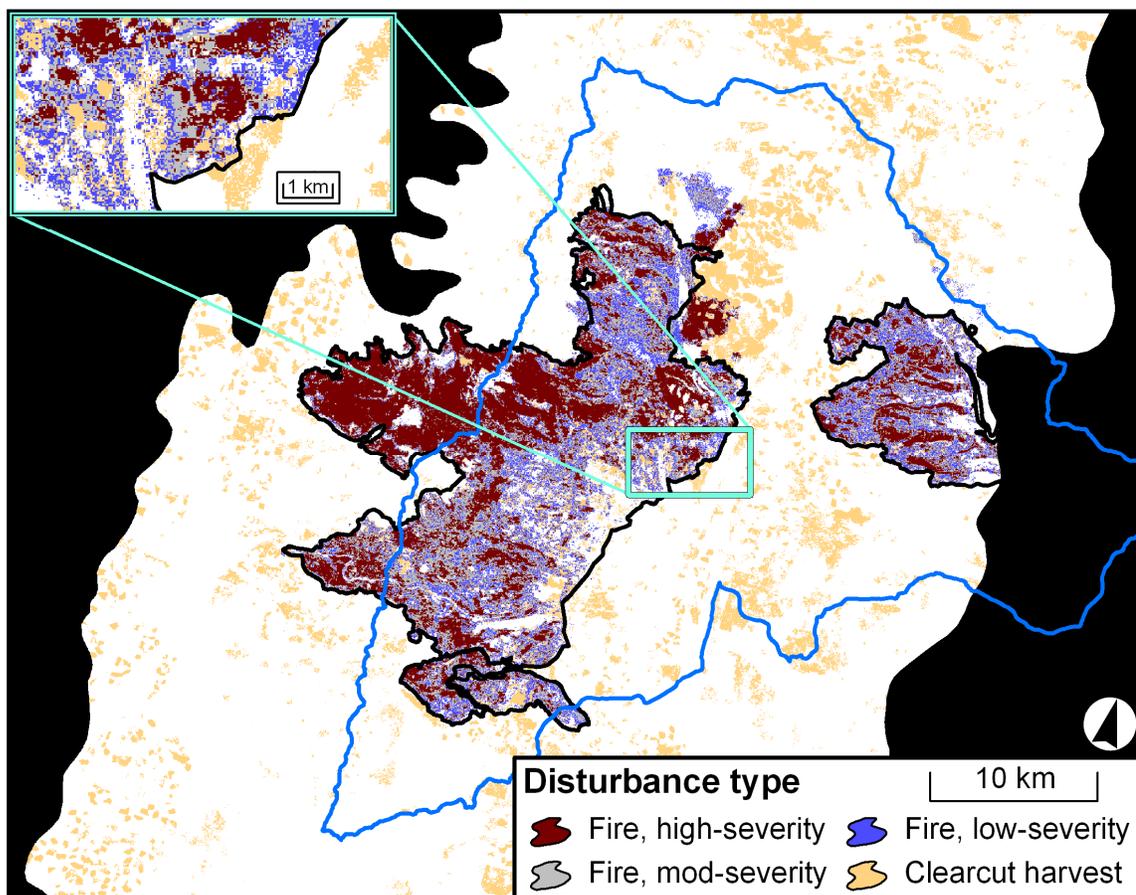
Figure 3.2. Distribution of disturbance inputs across the simulation landscape. White areas assumed undisturbed since 1984. Burn severity classes from MTBS (http://mtbs.gov). Timber harvest data from LandTrendr (Kennedy *et al.*, In prep). Inset map: zoomed view of spatial mosaic. Same spatial data sources as Fig. 3.1. Spatial grain: 25 m. Projection: Albers Equal Conic Area NAD83.
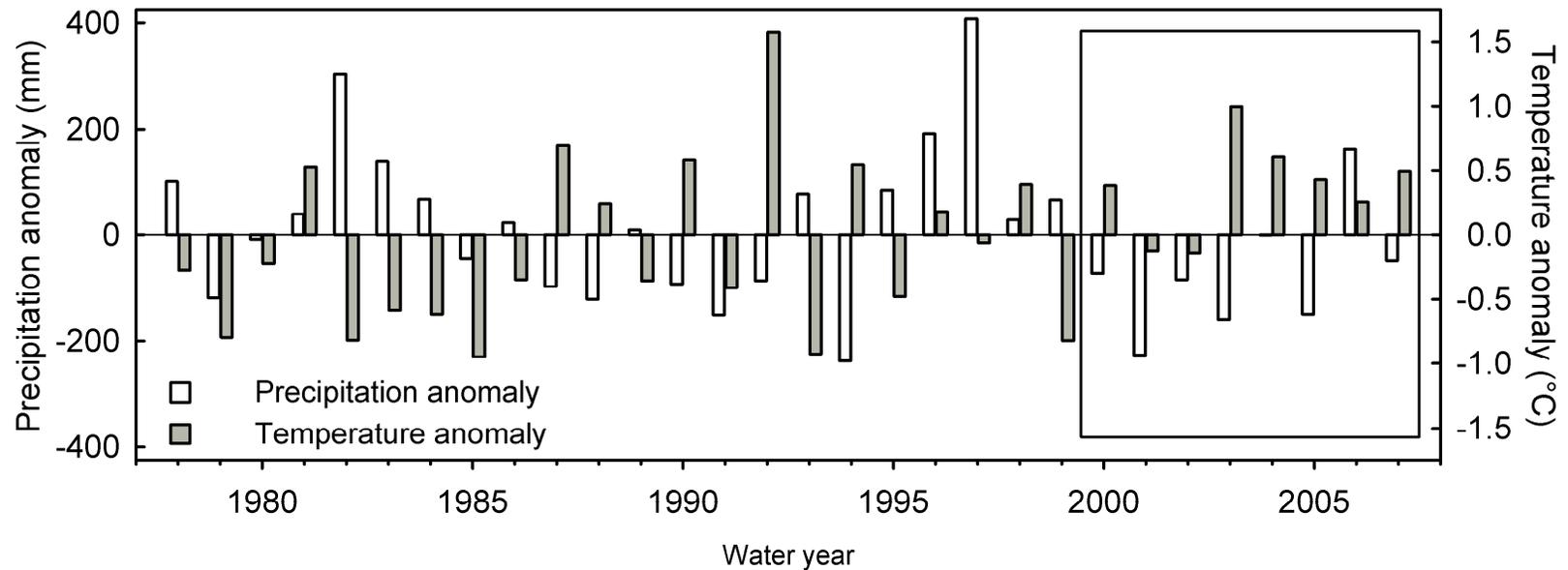
Figure 3.3. Climate anomalies in the Metolius Watershed. Anomalies in precipitation (mm) and temperature (°C) are in reference to the 30-y mean (1978-2007) from PRISM data (prismclimate.org) extracted at a central location in the watershed (described by Thomas *et al.*, 2009). Water year is defined as the 12-mo period from October-September. The 2000 water year marked the beginning of an anomalously warm and dry period, coincident with a positive phase of the Pacific Decadal Oscillation (Thomas *et al.*, 2009). These anomalies contributed to drought stress and set the stage for wildfires and potentially harsh conifer regeneration conditions.

[Figure created for previous manuscript (this thesis, Chapter 2). Used with permission of *Ecosystems.*]
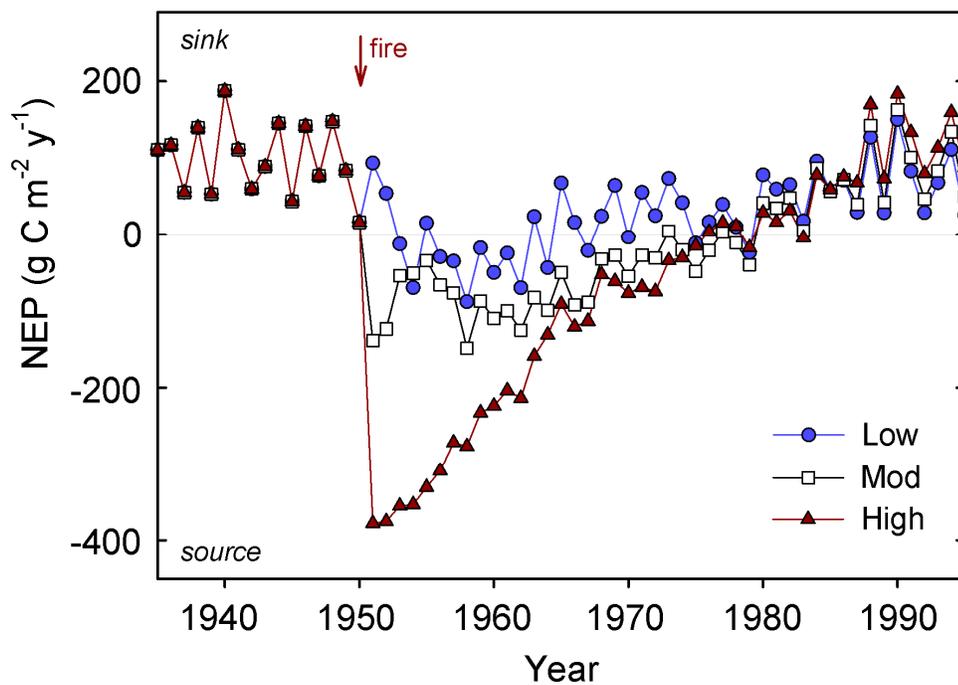
Figure 3.4. Biome-BGC simulation of low-, moderate-, and high-severity fire effects on mean annual NEP, based on mortality thresholds from MTBS (Tables 3.2 and 3.3). Example model runs from a representative ponderosa pine site with fire occurring in 1950, an arbitrary year that provides a reference for model behavior several decades following fire. Note the high interannual variability due to climate and dramatic NEP decline due to high-severity fire (and relatively small declines due to low- and moderate-severity fire).
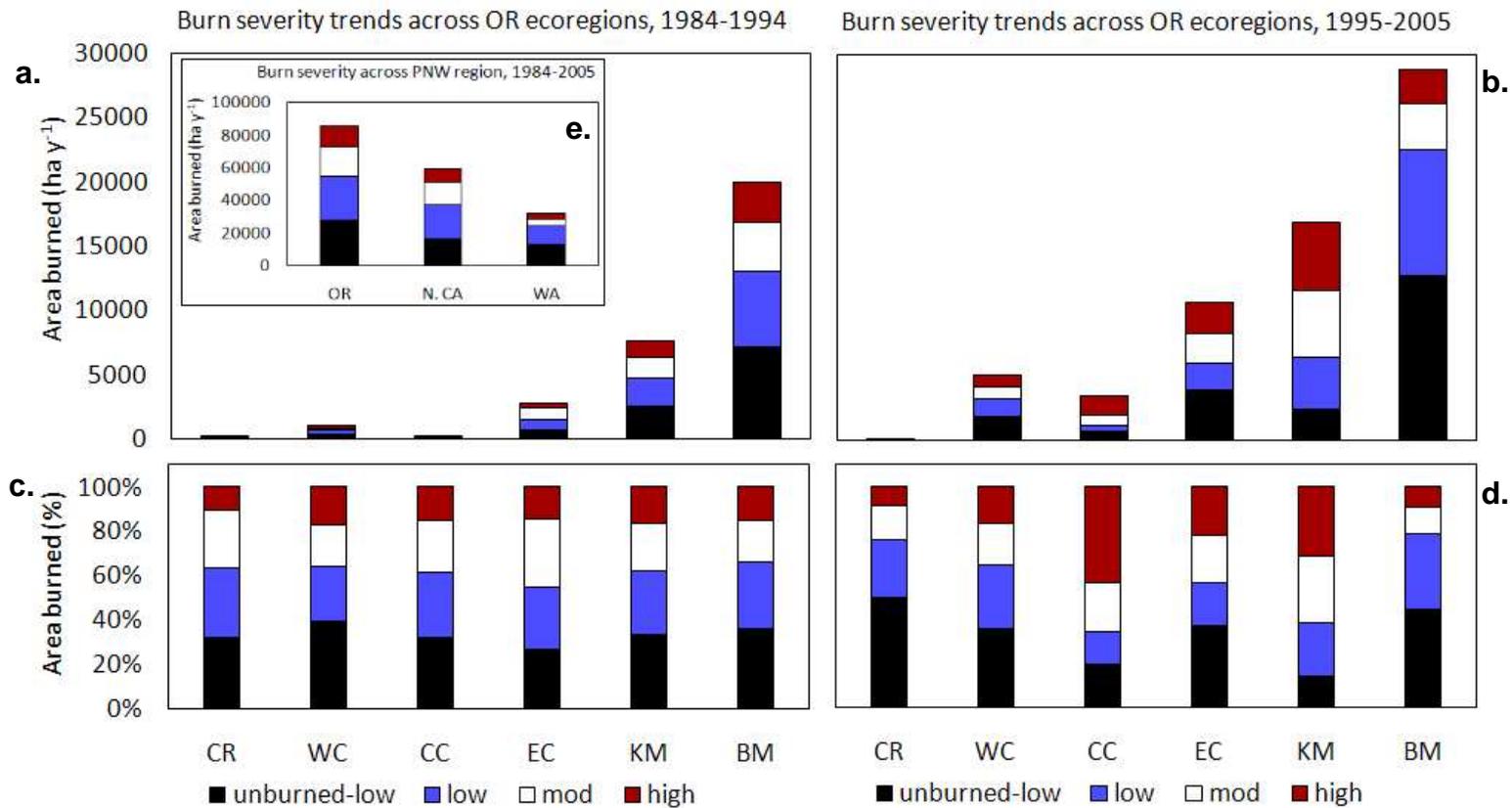
Figure 3.5. Burn severity trends across the PNW region and Oregon ecoregions for two time periods:1984-1994 and 1995-2005. Severity classes from MTBS (http://mtbs.gov), defined in Table 3.2. Forested ecoregions shown for Oregon: CR: Coast Range; WC: West Cascades; CC: Cascade Crest; EC: East Cascades; KM: Klamath Mountains; BM: Blue Mountains. State averages in (e) include forested and non-forested regions: OR: Oregon; N. CA: Northern California; WA: Washington. Panels (a) and (b) are mean annual burned area. Panels (c) and (d) are the same data on % scale.
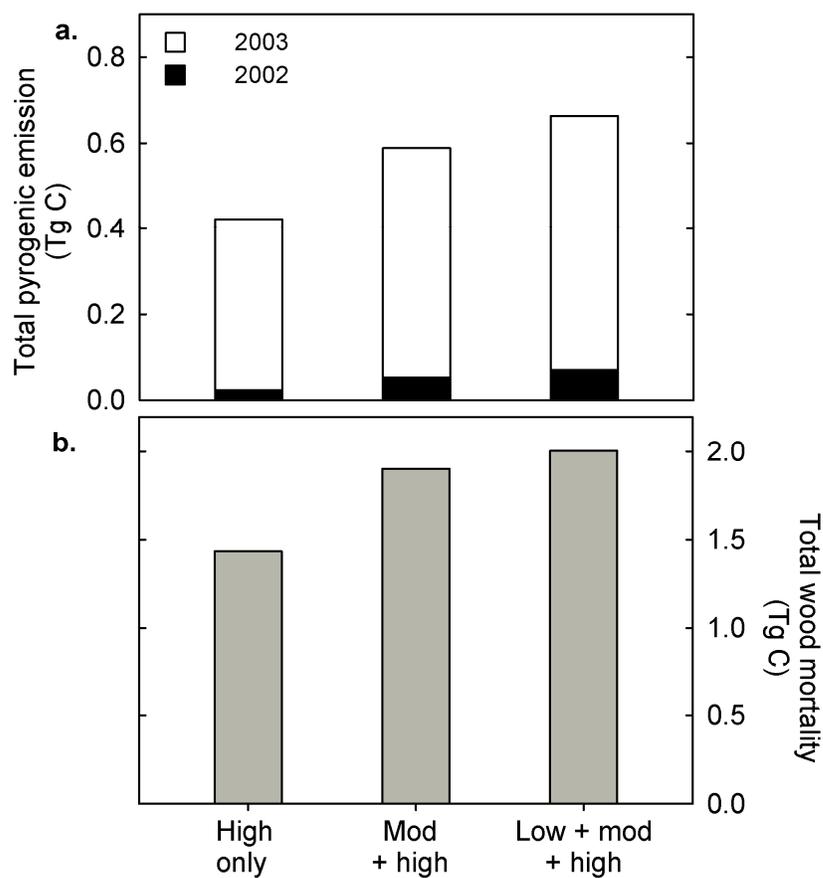
Figure 3.6. (a) Pyrogenic C emission and (b) total wood mortality across 3 severity detection scenarios. Scenario description and area given in Table 3.5. Pyrogenic emission computed directly from Biome-BGC outputs. Wood mortality computed as the difference between prefire (2001) and postfire (2004) values within pixels that burned in the "all severities" scenario. Note the different y-axis scales, showing that mortality transfers are *ca.* 3-fold higher than pyrogenic emission.
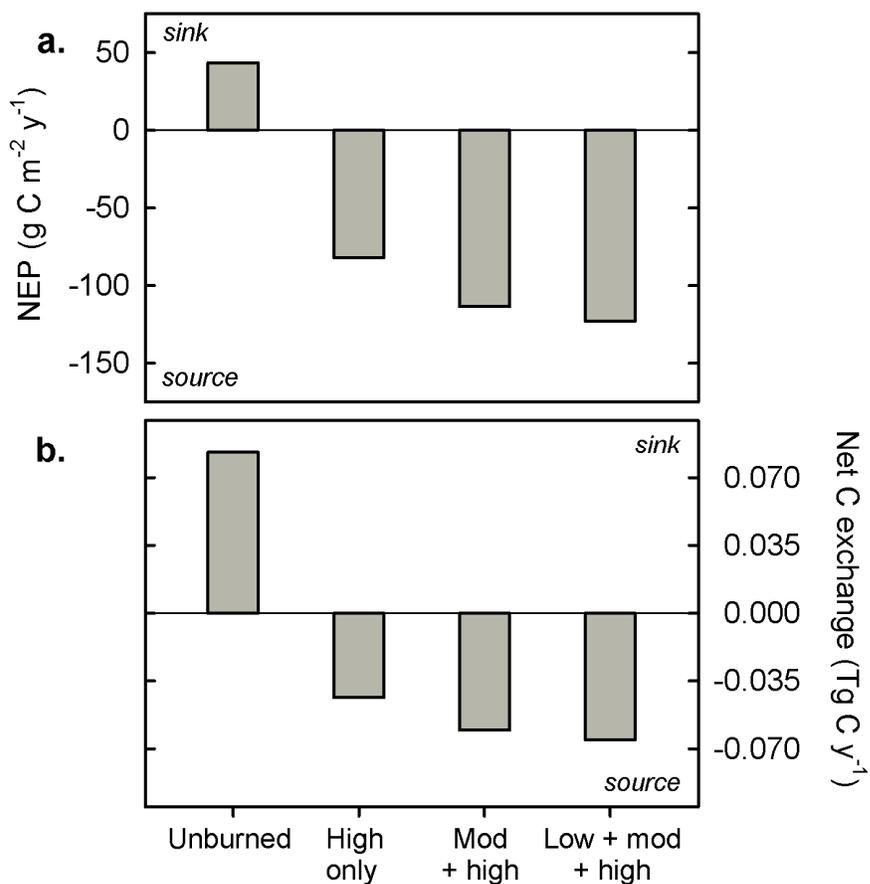
Figure 3.7. (a) Mean annual net ecosystem production (NEP) and (b) total net C exchange across 3 severity detection scenarios one year following large wildfires (2004). NEP in all 3 scenarios derived from the same area (affected by the low + mod + high scenario); Unburned results are from all other 1 km pixels.
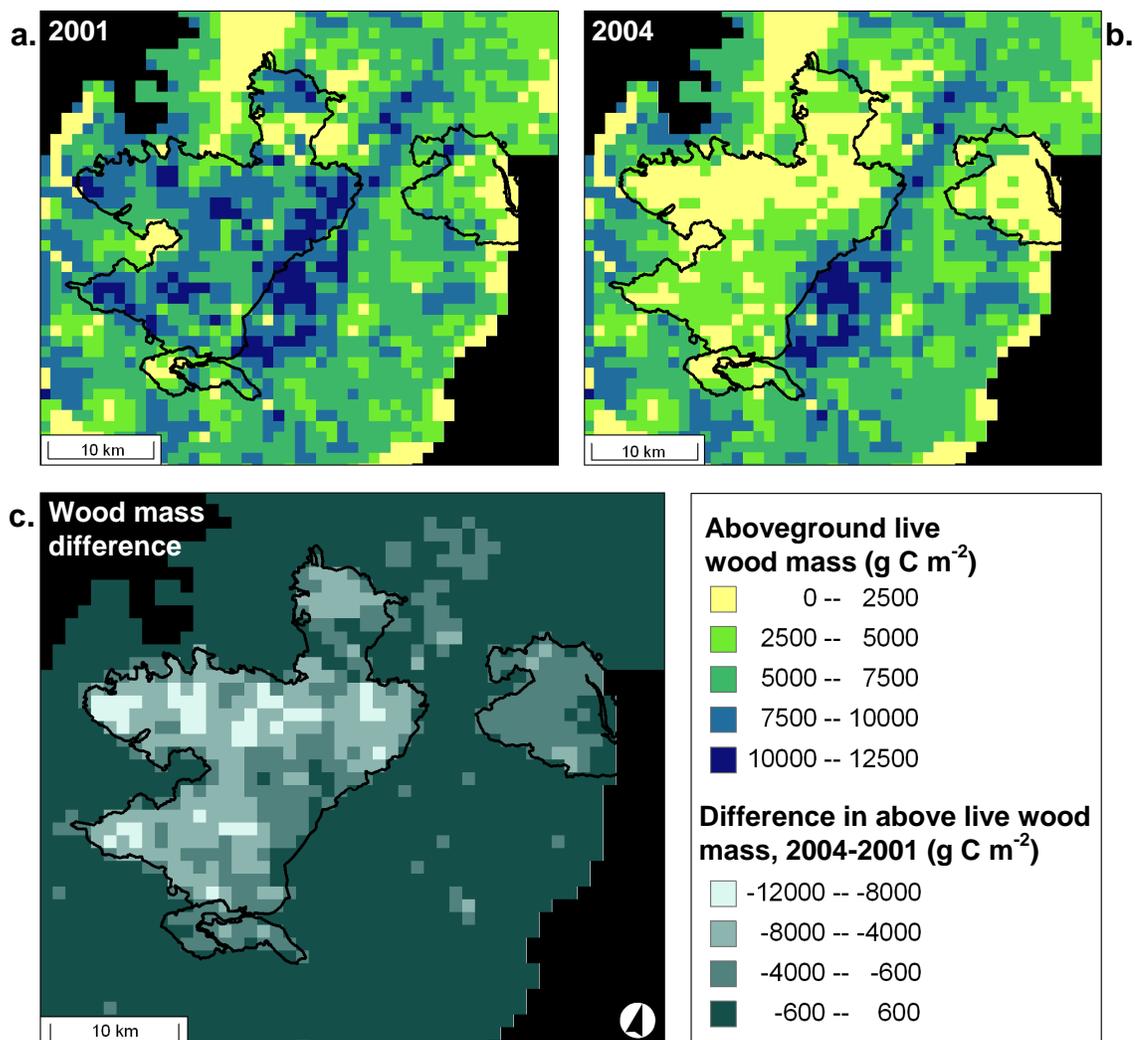
Figure 3.8. Live aboveground wood mass (a) before and (b) after large wildfires and (c) fire-induced differences. Difference in (c) produced by subtracting 2001 from 2004 pixel values. Values are from simulation including low-, moderate-, and high-severity fire. Spatial grain: 1 km. Projection: Albers Equal Conic Area NAD83.
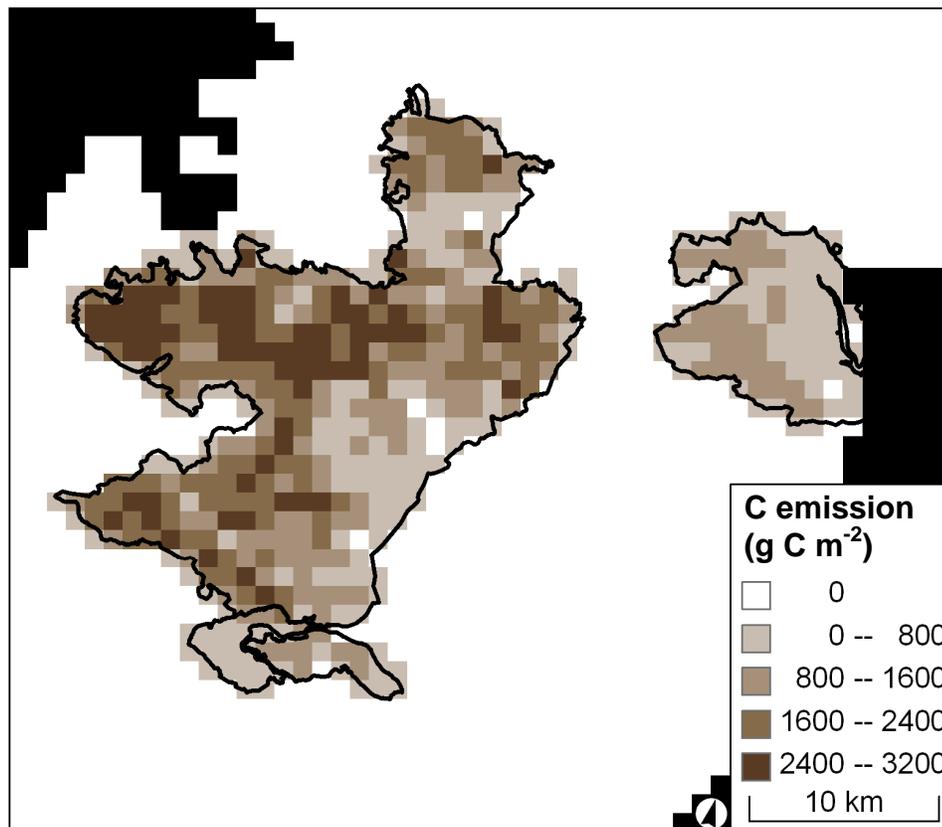
Figure 3.9. Pyrogenic C emission from 2002-2003 fires based on Biome-BGC simulated prefire fuel loading and field-measured combustion factors from western Oregon (Table 3.3; Campbell *et al.* 2007). Divide by 100 for Mg C ha^{-1}. Total emissions = 0.66 Tg C. Values are from simulation including low-, moderate-, and high-severity fire. Spatial grain: 1 km. Projection: Albers Equal Conic Area NAD83.
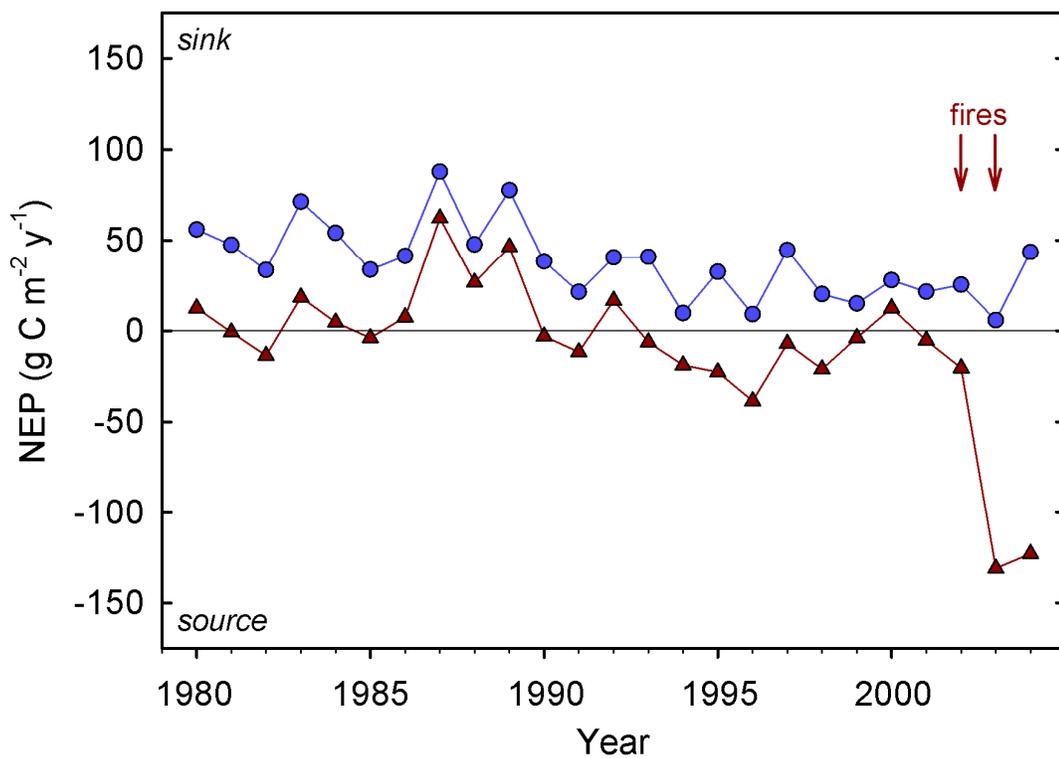
Figure 3.10. Mean annual net ecosystem production (NEP) for all 1 km pixels that eventually burned (red triangles) or did not burn (blue circles) in 2002 and 2003 ($n = 531$ and 1915, respectively). Note the parallel trend and consistent difference between burned and unburned pixels (due to the burned pixels being generally higher elevation, older forests closer to zero NEP). Points denote the spatial mean of annual NEP.
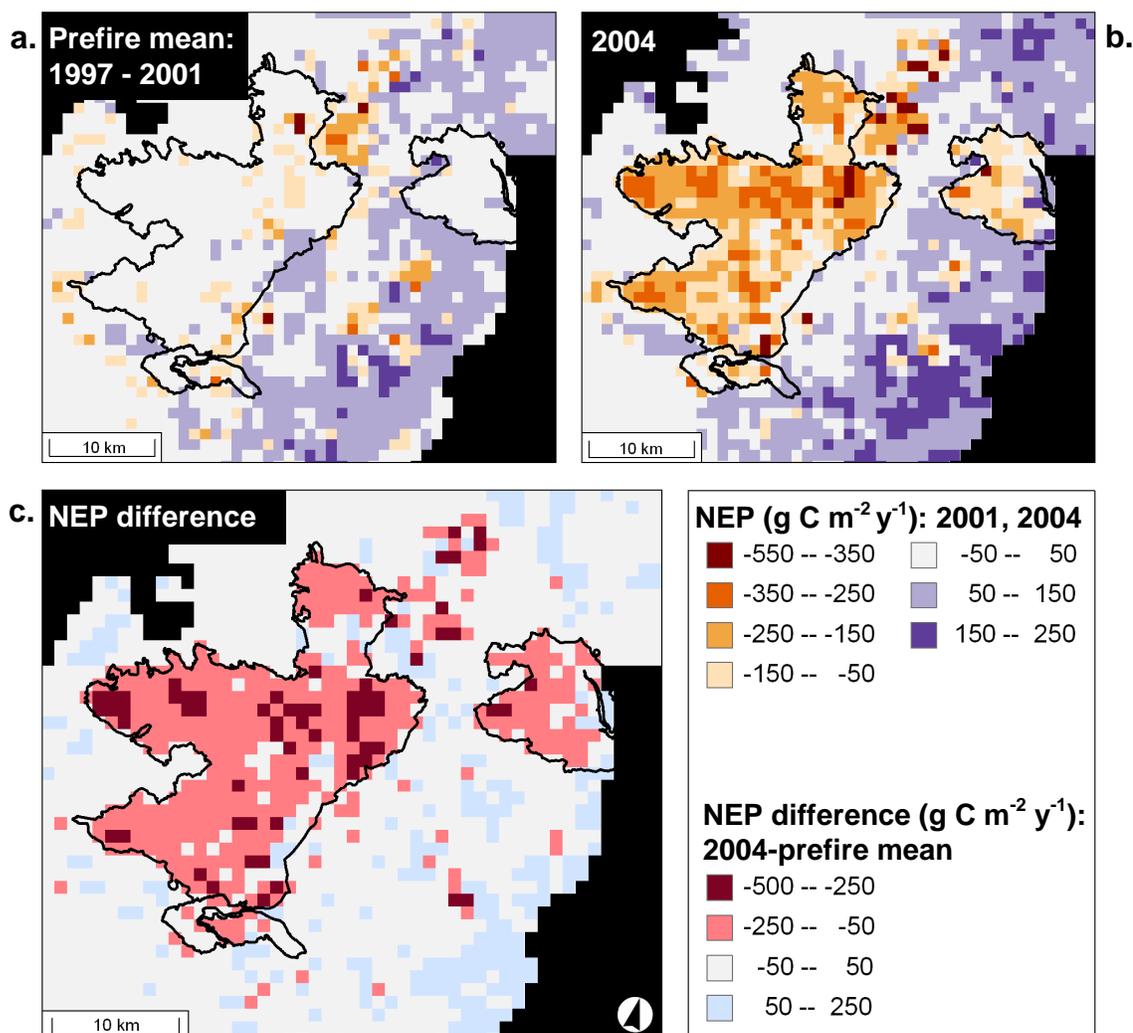
Figure 3.11. Annual net ecosystem production (a) before and (b) after large wildfires. Difference in (c) produced by subtracting 2001 from 2004 pixel values. Note the relatively small changes in unburned forest vs. the large reductions within fire perimeters. Values are from simulation including low-, moderate-, and high-severity fire. Spatial grain: 1 km. Projection: Albers Equal Conic Area NAD83.
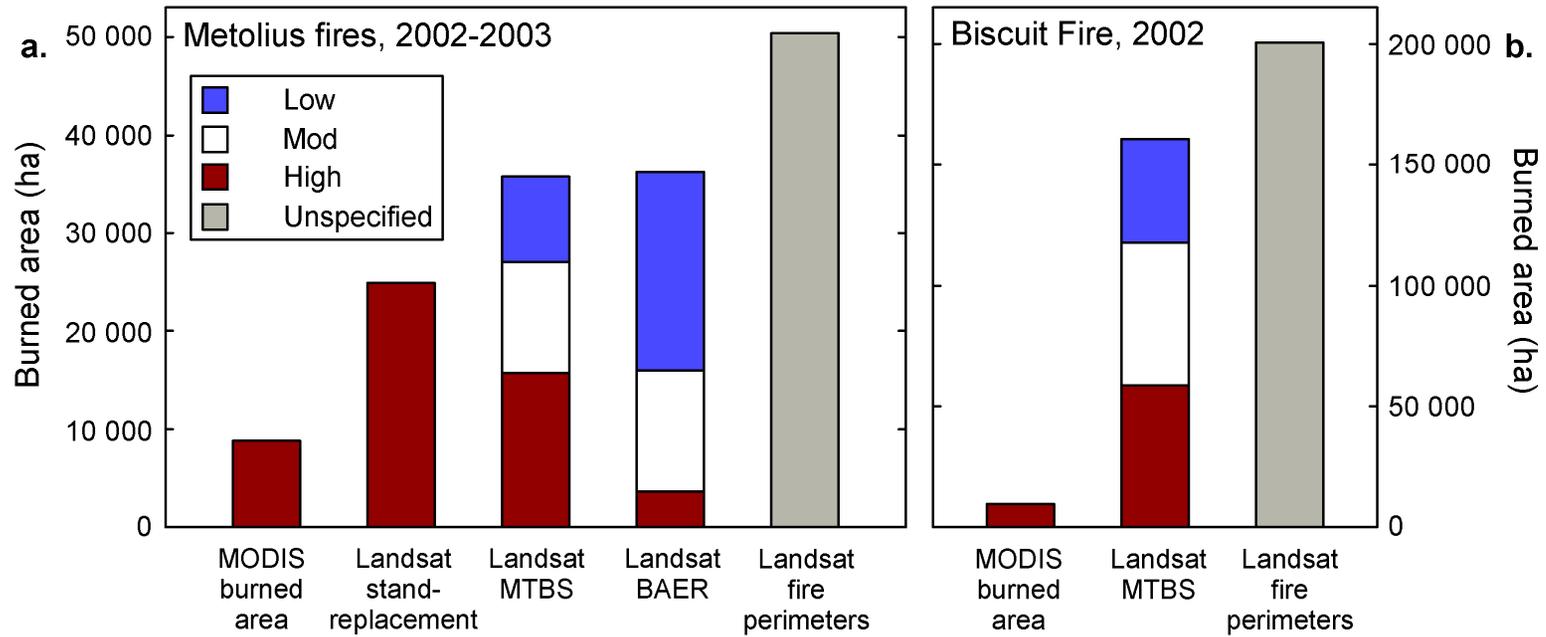
Figure 3.12. Burned area from 5 available disturbance datasets within (a) Metolius fires, 2002-2003 (Table 3.2) and (b) Biscuit Fire, 2002. Data sources: MODIS burned area product (MCD45A1; Roy *et al.* 2008); Landsat stand replacement disturbance map used in Turner *et al.* (2007); MTBS low, moderate, and high severity only: http://mtbs.gov; BAER: Burned Area Emergency Rehabilitation team, Deschutes National Forest; fire perimeters from MTBS database, derived from Landsat imagery.
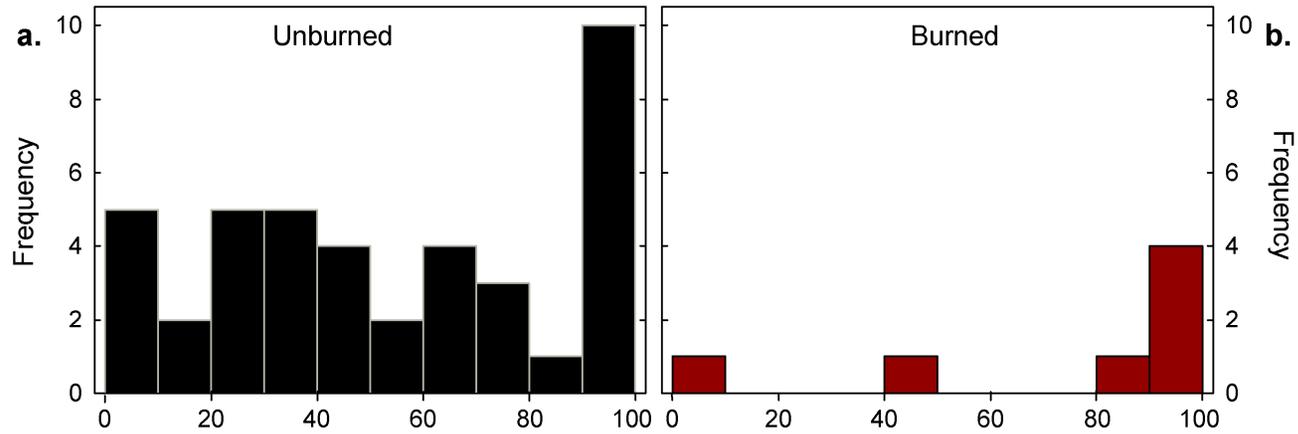
Figure 3.13. Evaluation of MODIS burned area product (MCD45A1; Roy *et al.* 2008) with field observations of tree basal area mortality within the 2002-2003 fire perimeters (*n* = 48 randomly located plots). (a) shows burned plots where MODIS did not detect fire. (b) shows the 7 burned plots that fell within fire pixels detected by the MODIS product. Field plots described in this thesis, Chapter 2.
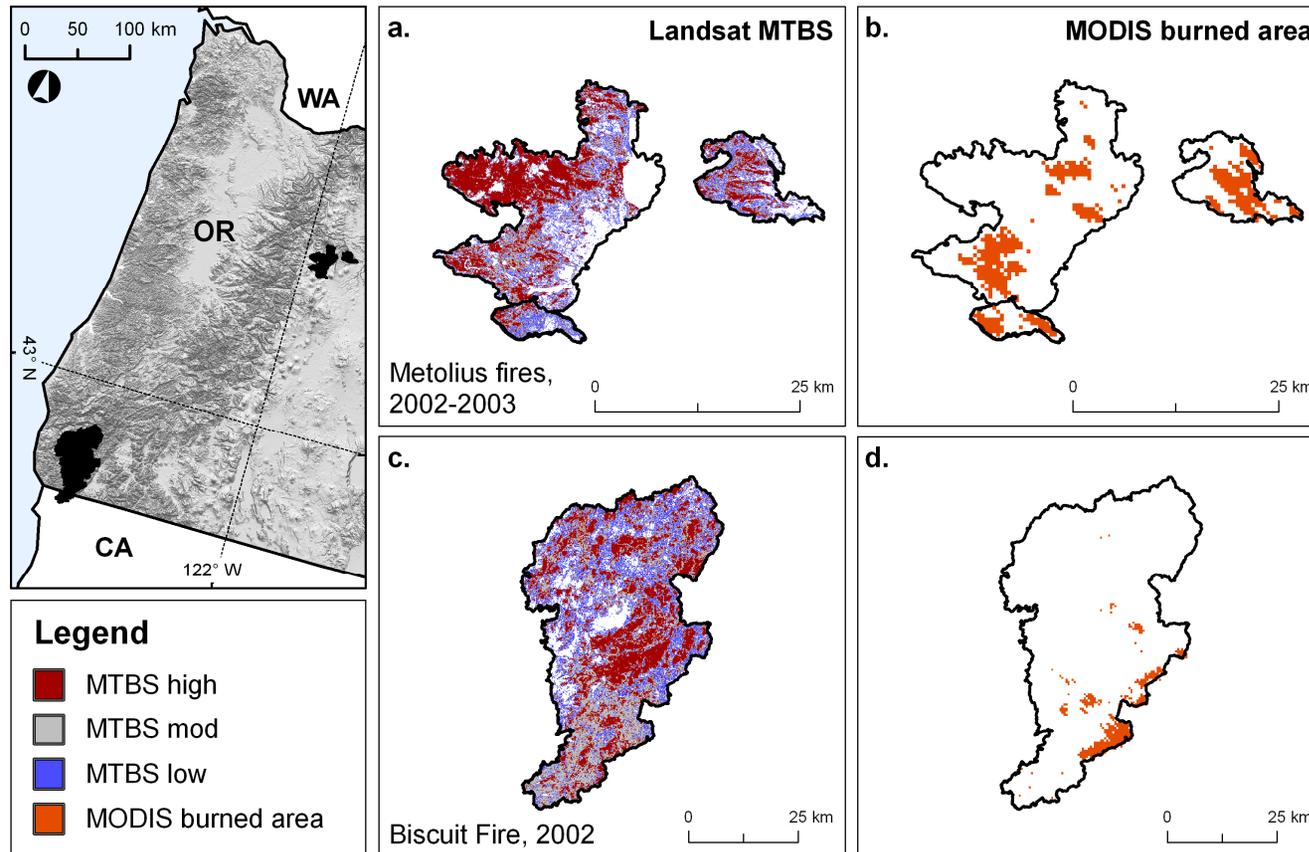
Figure 3.14. Comparison of MTBS (Monitoring Trends in Burn Severity) and MODIS (Moderate Resolution Imaging Spectroradiometer) burned area (MCD45A1) across sample fires in Western Oregon. (a) Metolius MTBS (b) Metolius MODIS (c) Biscuit MTBS (d) Biscuit MODIS. Inset shows fire size and location across Western Oregon topographic gradients. Fire perimeters from MTBS database (http://mtbs.gov). MTBS classes include low, moderate, and high severity only (disturbance inputs for Biome-BGC analysis [Chapter 3]). MODIS burned area product (MCD45A1) described by Roy *et al.* (2008). MTBS spatial grain: 30 m. MODIS spatial grain: 463 m. Projection: Albers Equal Conic Area NAD83.
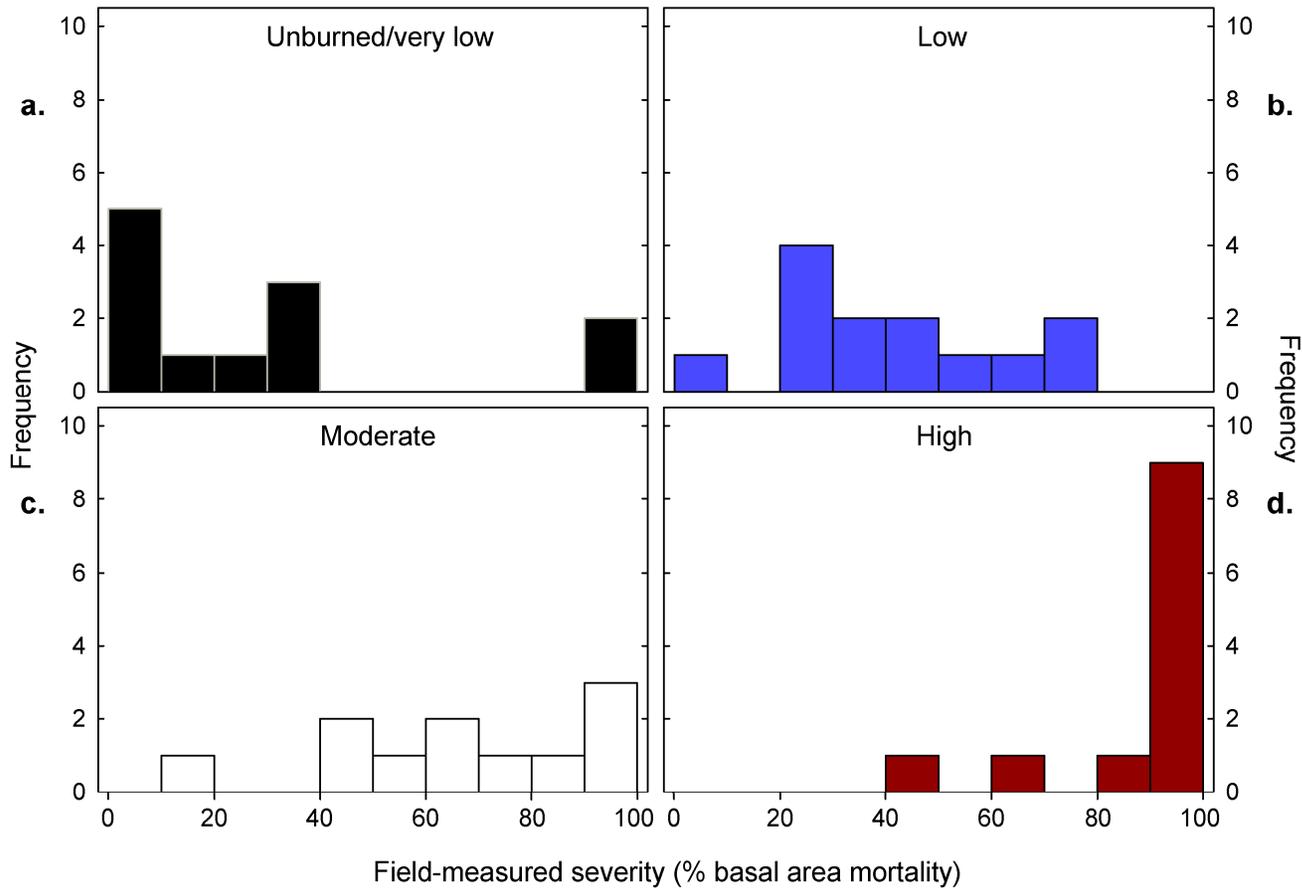
Figure 3.15. Evaluation of MTBS severity classes with field observations of tree basal area mortality within the 2002-2003 fire perimeters (*n* = 48). Frequency distributions show general agreement but substantial variability within MTBS severity classes: (a) Unburned/very low; (b) low; (c) moderate; (d) high. Note the overall increase in mean tree mortality in the moderate- and high-severity classes and the substantial overlap of ranges between severity bins. Unburned to low-severity class included 12 out of 48 total plots. MTBS classes defined in Table 3.2. Field plots described in this thesis, Chapter 2.
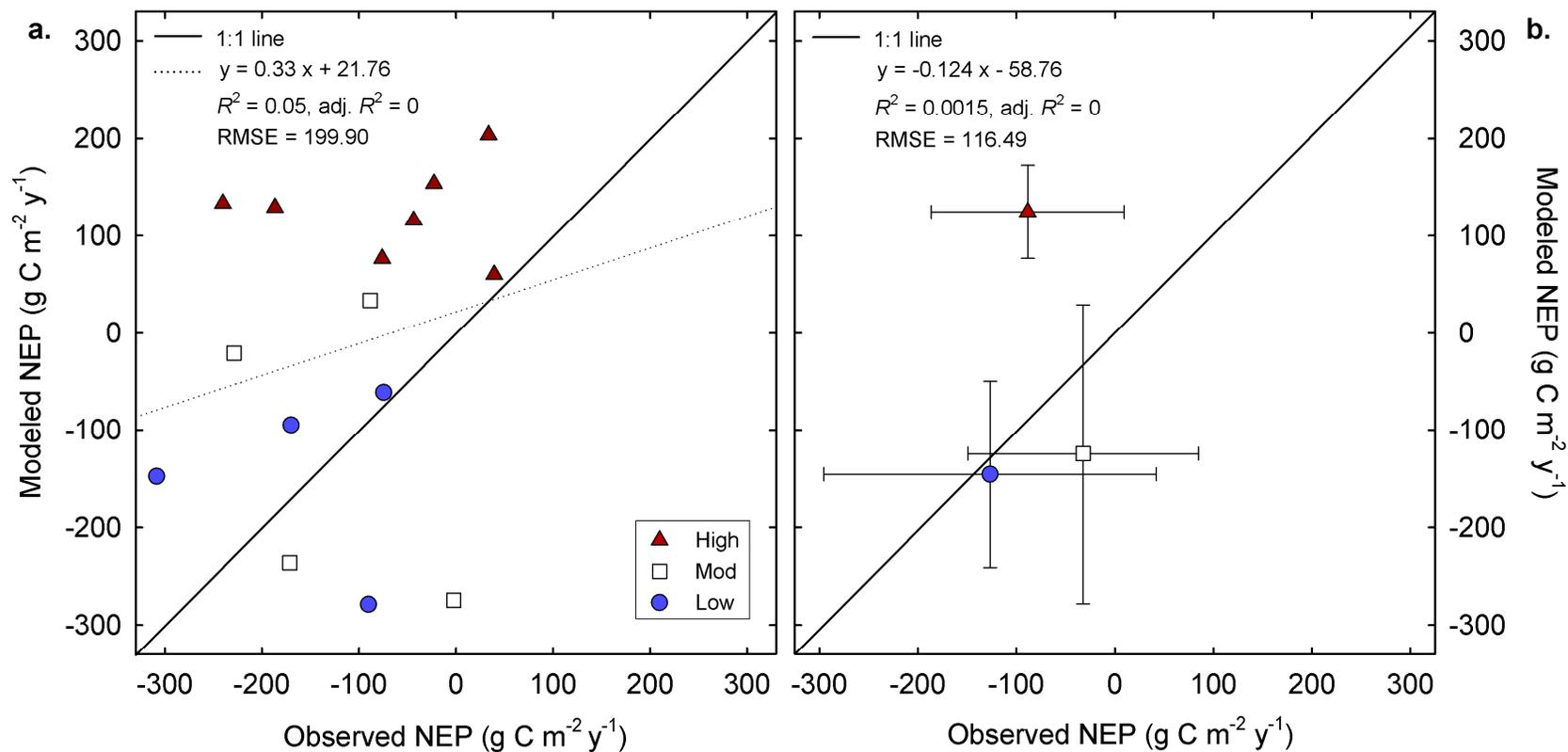
Figure 3.16. Modeled vs. observed NEP (g C m^{-2} y^{-1}) for burned plots. Observations from field measurements 5 y postfire in 2007 in ponderosa pine stands that burned across a range of severities in 2002. Model results from simulated fire year of 1995 to enable 5 y postfire NEP comparison between 2000 (simulated) and 2007 (measured) because 2000 was the climate year most similar to 2007 [Fig. 3.3]). DAYMET climate data were available through 2004 only. Plot (b) shows the mean and SE of points in (a). See Appendix 5 for evaluation of BGC results at unburned ponderosa pine stands measured in 2001.

Table 3.1. Large fires in the greater Metolius Watershed, 2002-2007.

Fire name	Fire size (ha)[a]	Year	Ignition source	Reference number[b]	% severity of burned area[c]		
					Low	Mod	High
Cache Mt	1417	2002	lightning	1	39	42	19
Eyerly Complex	9366	2002	lightning	2	32	35	33
B&B Complex[d]	36 717	2003	human	3	22	30	48
Link	1453	2003	lightning	4	26	39	35
Total, 2002-2003	48 953				24	32	44
Black Crater[e]	3800	2006	lightning	5			
Lake George	2240	2006	lightning	6			
Puzzle	2562	2006	lightning	7			
GW	2971	2007	lightning	8			
Warm Springs Lightning Complex	5283	2007	lightning	9			
Total, 2002-2007	65 809						

Notes:
Large fires: >1000 ha
[a] Based on fire perimeter GIS data from Deschutes National Forest.
[b] For study area map labels (Fig. 3.1).
[c] Percentage from MTBS (http://mtbs.gov) severity classes (Table 3.2, Fig. 3.2), extracted in GIS for portions of 2002-2003 fires that burned with low, moderate, and high severity. Mod: moderate severity.
[d] Booth and Bear Butte Complex: two large fires that merged into one.
[e] Black Crater fire burned on southern edge of simulation landscape and was excluded from Fig. 3.1.

Table 3.2. Monitoring Trends in Burn Severity (MTBS) severity classes.

MTBS class	MTBS description[a]
Unburned to low-severity	within fire perimeter, but either unburned, or visible fire effects occupy <5% of area
Low-severity[b]	all strata altered from prefire state; some strata substantially altered (particularly forest floor and understory vegetation); overstory mortality up to 25%
Moderate-severity[b]	transitional in magnitude and/or uniformity between low- and high-severity; many possible combinations of diverse fire effects
High-severity[b]	uniformly extreme, generally long-lasting effects across strata; overstory tree mortality typically >75%; understory vegetation and forest floor mostly consumed; >50% newly exposed mineral soil
Increased greenness	fire-induced increase in vegetation cover, density, and/or productivity (usually herbaceous or shrub)
No data/non-processing mask	missing data due to sensor problems or interference (clouds, smoke, shadow, snow); filled in with LandTrendr data in this study

Notes:
Source: Schwind 2008, http://mtbs.gov
[a] Based on forested sites in general.
[b] Classes used in this study; other classes assumed unburned.

Table 3.3. Combustion factors for pyrogenic C emission estimates.

Burn severity	Live stem	Foliage[a]	Dead stem	Forest floor[b]	Woody detritus[c]
Low	0.02	0.125	0.11	0.66	0.17
Moderate	0.03	0.50	0.14	0.66	0.22
High	0.05	0.95	0.18	1.00	0.39

*Notes***:**
Proportions are mean combustion factors, weighted by severity class area, derived from field-measurements in western Oregon conifer forests (Campbell *et al.* 2007), except foliage.
[a] Foliage proportion from MTBS (http://mtbs.gov) burn severity classes for percent tree mortality, the same value for transfer from live to dead tree pools.
[b] Weighted mean of litter and duff.
[c] Weighted mean of coarse woody and fine woody detritus.
Due to model logic, live fine and coarse roots incur same effects as foliage and live stem, respectively.

Table 3.4. Top 10 combinations of land cover and disturbance history across the simulation landscape.

Number	Land cover	Last disturbance type	Last disturbance year[a]	First disturbance type	First disturbance year[a]	Area (ha)	Frequency
1	Conifer	clearcut harvest	1959	fire, high severity	1759	65 986	0.18
2	Conifer	fire, high severity	1854	fire, high severity	1654	59 322	0.17
3	Conifer	fire, high severity	1754	fire, high severity	1554	47 483	0.13
4	Woodland	fire, high severity	1934	fire, high severity	1734	36 477	0.10
5	Shrubland[b]	na	na	na	na	35 660	0.10
6	Conifer	fire, high severity	1924	fire, high severity	1724	31 197	0.09
7	Non-vegetated[b]	na	na	na	na	17 713	0.05
8	Conifer	fire, high severity	2003	fire, high severity	1803	12 095	0.03
9	Conifer	fire, mod. severity	2003	fire, high severity	1803	6713	0.02
10	Conifer	fire, low severity	2003	fire, high severity	1803	4342	0.01

Notes:
Top 10 combinations account for 88% of the simulation landscape (total area: 360 400 ha, the rectangular frame in Fig. 3.1).
[a] Disturbance year before 1984 is based on stand age (stand initiating fire) for conifer pixels and assumed age of 70 y for woodlands.
[b] No age assigned for shrubland and non-vegetated pixels.

Table 3.5. Pyrogenic C emission across three burn severity detection scenarios.

Severity scenario[a]	Burned area (ha)[a]	% increase in burned area from high only scenario	Mean PE (Mg C ha^{-1})[b]	Total PE (Tg C)[b]	% increase in total PE from high only scenario
High only	15 704	0	26.94	0.423	0
Mod + high	27 079	72	21.73	0.588	39
Low + mod + high[c]	**35 723**	**127**	**18.56**	**0.663**	**57**

Notes:
[a] Severity scenarios and area burned from MTBS classes (http://mtbs.gov) within 2002-2003 fires combined (Table 3.1, Fig. 3.1). Bold indicates scenario including all severities.
[b] Weighted mean and total PE both based on area burned in each severity class.
[c] Includes low-, moderate-, and high-severity classes.

CHAPTER 4 || CONCLUSION

Synthesis

This thesis quantifies the carbon consequences of wildfire severity across the Metolius Watershed and demonstrates the importance of accounting for the full range of disturbance effects on carbon pools and fluxes. At stand- and landscape-scales, the severity mosaic resulted in diverse fire impacts (pyrodiversity) and some surprising overall effects (pyrocomplexity). The 2002-2003 fires released an estimated 0.66 to 0.74 Tg C through combustion (depending on simulation approaches), equivalent to *ca.* 2% of statewide anthropogenic CO_2 emissions from the same 2-year period, and transferred 2.00 Tg C from live to dead wood pools. Despite these dramatic short-term impacts, the rapid response of early successional vegetation offset potential declines in NPP and NEP, reducing long-term fire effects on stand and landscape C storage. This apparent ecosystem resistance was bolstered by belowground components (soil C, soil heterotrophic respiration, and belowground NPP) and the lagged decomposition of aboveground necromass. Mean annual NEP was highly variable and declined with increasing burn severity, resulting in a substantial C source in high-severity stands. NEP simulations indicated that although burned areas were a large C source in 2004 (net C exchange across 53 000 ha: -0.065 Tg C y^{-1}), the overall landscape remained a small C sink (net C exchange across *ca.* 250 000 ha: 0.018 Tg C y^{-1}). Conifer and shrub regeneration was variable and generally abundant. Conifer seedlings were negatively correlated with overstory mortality, whereas shrub biomass showed the opposite response, indicating a wide range of potential carbon trajectories.

As expected, high-severity fire exerted disproportionate C effects, including pyrogenic emission, tree mortality, NEP, and understory regeneration. The majority of burned area across the Metolius landscape and PNW region, however, experienced low- and moderate-severity fire. The stand-scale impacts of this non-stand-replacement wildfire were reduced compared to high-severity fire but accounted for *ca.* 30% of overall fire-induced C responses. With the disturbance datasets and methods introduced in this thesis, researchers can achieve a more complete accounting of disturbance controls on C cycling from local to global scales.

Global change context

Large, infrequent disturbances like the landscape fires described here appear to be on the rise regionally and globally with climate change, and it is likely that fire activity will continue to increase (Balshi *et al.* 2009). Positive feedbacks between disturbance, carbon, and climate change could potentially accelerate ecosystem decline, and some forest landscapes could switch from net carbon sinks to sources (*e.g.,* Kurz *et al.* 2008b). The Metolius fires occurred during anomalously dry years (Thomas *et al.* 2009), and although predictions of future precipitation patterns have high uncertainty, multiple years of prolonged summer drought could yield profound, fire-mediated impacts on C pools and fluxes in these semi-arid forests. Conversely, fire has long played a crucial role in the development and vitality of these forests, and the recent wave of fire may represent the restoration of a crucial historic process.

The results of this thesis, at both the stand and landscape scales, do not indicate a strong climate-induced state change. Recent fires did render unequivocal impacts, including widespread mortality, regionally significant pyrogenic emissions, and declines in NEP. In the case of high-severity fire in ponderosa pine stands, it may take decades to recover prefire stand structure and carbon balance storage. In general, however, the large proportion of low- and moderate-severity fire, vigorous growth response of surviving and new vegetation, and conservation of belowground processes suggest a surprising conservation of ecosystem structure and function. Across the landscape, negative fire impacts were mitigated by the severity mosaic and interspersion of unburned forest patches. The pyrogenic emissions represent an important one-time pulse to the atmosphere, but annual anthropogenic CO_2 emissions from the state of Oregon were *ca.* 45-fold higher over the same time period and continue to increase annually.

Future research

Future studies should extend the spatiotemporal scales investigated here and link fire effects to other disturbance processes. Additional fires since 2003 provide an opportunity to investigate a short-term chronosequence and reduce uncertainties in

immediate postfire C responses, and simulation of future climate and fire scenarios could elucidate probable long-term dynamics. In addition to studies at multiple temporal scales, an explicit analysis of spatial scaling laws would enable the comparison of baseline scenarios with alternate successional trajectories due to variable-severity disturbance (Enquist *et al.* 2009).

This thesis explores the role of wildfire severity, but the effects of other disturbances—and their interactions with fire—remain key scientific frontiers. Specifically in the Metolius Watershed, large-scale tree mortality from insects likely influenced fire behavior and net C effects in many mixed-conifer stands that burned in 2002 and 2003, while postfire salvage harvest removed C from burned stands and likely altered successional pathways. With new approaches (such as MTBS and LandTrendr) that can map previous disturbance interactions and monitor current events, regional C models can better inform emerging policies and detect potential shifts in system behavior. Although the forests investigated here appear relatively buffered to the impacts of recent large fires, subsequent disturbances, including reburn, could push these systems into fundamentally altered states. Long-term field studies will be essential to advance our understanding of this socially-important landscape and the fundamental, dynamic role of wildfire disturbance.

BIBLIOGRAPHY

Agee JK. 1993. Fire ecology of Pacific Northwest forests. Island Press, Washington, D.C.

Amiro BD, Todd JB, Wotton BM, Logan KA, Flannigan MD, Stocks BJ, Mason JA, Martell DL, Hirsch KG. 2001. Direct carbon emissions from Canadian forest fires, 1959-1999. Canadian Journal of Forest Research 31:512-525.

Andersen CP, Phillips DL, Rygiewicz PT, Storm MJ. 2008. Fine root growth and mortality in different-aged ponderosa pine stands. Canadian Journal of Forest Research 38:1797-1806.

Anthoni PM, Unsworth MH, Law BE, Irvine J, Baldocchi DD, Van Tuyl S, Moore D. 2002. Seasonal differences in carbon and water vapor exchange in young and old-growth ponderosa pine ecosystems. Agricultural and Forest Meteorology 111:203-222.

Balshi MS, McGuire AD, Duffy P, Flannigan M, Walsh J, Melillo JM. 2009. Assessing the response of area burned to changing climate in western boreal North America using a Multivariate Adaptive Regression Splines (MARS) approach. Global Change Biology 15:578-600.

Balshi MS, McGuire AD, Zhuang Q, Melillo J, Kicklighter DW, Kasischke E, Wirth C, Flannigan M, Harden J, Clein JS, Burnside TJ, McAllister J, Kurz WA, Apps M, Shvidenko A. 2007. The role of historical fire disturbance in the carbon dynamics of the pan-boreal region: A process-based analysis. Journal of Geophysical Research-Biogeosciences 112.

Barrett JW. 1979. Silviculture of ponderosa pine in the Pacific Northwest: the state of our knowledge. USDA Forest Service General Technical Report PNW-97. Portland, OR.

Bond-Lamberty B, Peckham SD, Ahl DE, Gower ST. 2007. Fire as the dominant driver of central Canadian boreal forest carbon balance. Nature 450:89-93.

Bork BJ. 1985. Fire history in three vegetation types on the eastern side of the Oregon Cascades. PhD Thesis. Oregon State University. 94 p.

Bormann BT, Homann PS, Darbyshire RL, Morrissette BA. 2008. Intense forest wildfire sharply reduces mineral soil C and N: the first direct evidence. Canadian Journal of Forest Research 38:2771-2783.

Bowman D, Balch JK, Artaxo P, Bond WJ, Carlson JM, Cochrane MA, D'Antonio CM, DeFries RS, Doyle JC, Harrison SP, Johnston FH, Keeley JE, Krawchuk MA, Kull CA,

Marston JB, Moritz MA, Prentice IC, Roos CI, Scott AC, Swetnam TW, van der Werf GR, Pyne SJ. 2009. Fire in the Earth System. Science 324:481-484.

Bradley BA, Houghton RA, Mustard JF, Hamburg SP. 2006. Invasive grass reduces aboveground carbon stocks in shrublands of the Western US. Global Change Biology 12:1815-1822.

Brown JK. 1974. Handbook for inventorying downed woods material. USDA Forest Service General Technical Report INT-GTR-16. Ogden, UT.

Busse MD, Cochran PH, Barren JW. 1996. Changes in ponderosa pine site productivity following removal of understory vegetation. Soil Science Society of America Journal 60:1614-1621.

Campbell GS, 1991. Application note: canopy LAI from Sunfleck Ceptometer PAR measurements. Decagon Devices, Inc., Pullman, WA.

Campbell JL, Alberti G, Martin JG, Law BE. 2009. Carbon dynamics of a ponderosa pine plantation following a thinning treatment in the northern Sierra Nevada. Forest Ecology and Management 257:453-463.

Campbell JL, Donato DC, Azuma DL, Law BE. 2007. Pyrogenic carbon emission from a large wildfire in Oregon, United States. Journal of Geophysical Research 112.

Campbell JL, Law BE 2005. Forest soil respiration across three climatically distinct chronosequences in Oregon. Biogeochemistry 73:109-125.

Campbell JL, Sun OJ, Law BE. 2004. Disturbance and net ecosystem production across three climatically distinct forest landscapes. Global Biogeochemical Cycles 18.

CCAR. 2007. Forest sector protocol version 2.1. California Climate Action Registry (CCAR). http://www.climateregistry.org/tools/protocols/industry-specific-protocols.html.

Chambers JQ, Fisher JI, Zeng HC, Chapman EL, Baker DB, Hurtt GC. 2007. Hurricane Katrina's carbon footprint on U. S. Gulf Coast forests. Science 318:1107.

Chapin FS III, Matson PA, Mooney HA. 2002. Principles of Terrestrial Ecosystem Ecology. Springer, New York, NY.

Chapin FS III, Woodwell GM, Randerson JT, Rastetter EB, Lovett GM, Baldocchi DD, Clark DA, Harmon ME, Schimel DS, Valentini R, Wirth C, Aber JD, Cole JJ, Goulden ML, Harden JW, Heimann M, Howarth RW, Matson PA, McGuire AD, Melillo JM, Mooney HA, Neff JC, Houghton RA, Pace ML, Ryan MG, Running SW, Sala OE,

Schlesinger WH, Schulze ED. 2006. Reconciling carbon-cycle concepts, terminology, and methods. Ecosystems 9:1041-1050.

Chen H, Harmon ME, Sexton JM, Fasth B. 2002. Fine-root decomposition and N dynamics in coniferous forests of the Pacific Northwest, USA. Canadian Journal of Forest Research 32:320-331.

Cline SP, Berg AB, Wight HM. 1980. Snag characteristics and dynamics in Douglas-fir forests, western Oregon. Journal of Wildlife Management 44:773-786.

Cohen WB, Harmon ME, Wallin DO, Fiorella M. 1996. Two decades of carbon flux from forests of the Pacific northwest. Bioscience 46:836-844.

CONUS. 2009. Conterminous United States multi-layer soil characteristics dataset for regional climate and hydrology modeling. http://www.soilinfo.psu.edu/index.cgi?index.html

Cope MJ, Chaloner WG. 1985. Wildfire: an interaction of biological and physical processes. In: Tiffney, B.H. (Ed.), Geological factors and the evolution of plants. Yale University Press, New Haven, pp. 257-277.

Daly C, Gibson WP, Taylor GH, Johnson GL, Pasteris P. 2002. A knowledge-based approach to the statistical mapping of climate. Climate Research 22:99-113.

DAYMET. 2009. Distributed climate data, http://www.daymet.org/.

DeLuca TH, Aplet GH. 2008. Charcoal and carbon storage in forest soils of the Rocky Mountain West. Frontiers in Ecology and the Environment 6:18-24.

Donato DC, Campbell JL, Fontaine JB, Law BE. 2009a. Quantifying char in postfire woody detritus inventories. Journal of Fire Ecology, in press.

Donato DC, Fontaine JB, Campbell JL, Robinson WD, Kauffman JB, Law BE. 2009b. Early conifer regeneration in stand-replacement portions of a large mixed-severity wildfire in the Siskiyou Mountains, Oregon. Canadian Journal of Forest Research, in press.

Dore S, Kolb TE, Montes-Helu M, Sullivan BW, Winslow WD, Hart SC, Kaye JP, Koch GW, Hungate BA. 2008. Long-term impact of a stand-replacing fire on ecosystem CO2 exchange of a ponderosa pine forest. Global Change Biology 14:1801-1820.

Duane M, Cohen WB, Campbell JL, *et al.* Implications of two different field sampling designs on local accuracy and estimate distributions in mapping forest biophysical attributes from Landsat data. (In prep)

Enquist BJ, West GB, Brown JH. 2009. Extensions and evaluations of a general quantitative theory of forest structure and dynamics. Proceedings of the National Academy of Sciences of the United States of America 106:7046-7051.

Eyre FH (editor).1980. Forest cover types of the United States and Canada. Society of American Foresters, Washington, DC.

Fellows AW, Goulden ML. 2008. Has fire suppression increased the amount of carbon stored in western US forests? Geophysical Research Letters, 35.

Filip GM, Maffei H, Chadwick KL. 2007. Forest health decline in a central Oregon mixed-conifer forest revisited after wildfire: A 25-year case study. Western Journal of Applied Forestry 22:278-284.

Fitzgerald SA. 2005. Fire ecology of ponderosa pine and the rebuilding of fire-resilient ponderosa pine ecosystems. Proceedings of the Symposium on Ponderosa Pine: Issues, Trends, and Management, 2004 October 18-21, Klamath Falls, OR. USDA Forest Service General Technical Report PSW-GTR-198. Albany, CA.

Franklin JF, Dyrness CT. 1973. Natural vegetation of Oregon and Washington. USDA Forest Service General Technical Report PNW-GTR-8. Portland, OR.

Giglio L, Loboda T, Roy DP, Quayle B, Justice CO. 2009. An active-fire based burned area mapping algorithm for the MODIS sensor. Remote Sensing of Environment 113:408-420.

Goward SN, Masek JG, Cohen WB, Moisen G, Collatz GJ, Healey SP, Houghton RA, Huang C, Kennedy RE, Law BE, Powell SL, Turner DP, Wulder MA. 2008. Forest disturbance and North American carbon flux. Eos, Transactions, American Geophysical Union 89:105-116.

Gough CM, Vogel CS, Harrold KH, George K, Curtis PS. 2007. The legacy of harvest and fire on ecosystem carbon storage in a north temperate forest. Global Change Biology 13:1935-1949.

Griffith G, Omernik JM. 2009. Ecoregions of Oregon (EPA) In: *Encyclopedia of Earth* (eds McGinley M, Cleveland CJ). Environmental Information Coalition, National Council for Science and the Environment, Washington, D.C. http://www.eoearth.org/article/Ecoregions_of_Oregon_(EPA)

Harmon ME, Bible K, Ryan MG, Shaw DC, Chen H, Klopatek J, Li X. 2004. Production, respiration, and overall carbon balance in an old-growth *Pseudotsuga-tsuga* forest ecosystem. Ecosystems 7:498-512.

Harmon ME, Fasth B, Sexton JM. 2005. Bole decomposition rates of seventeen tree species in Western U.S.A.: A report prepared for the Pacific Northwest Experiment Station, the Joint Fire Sciences Program, and the Forest Management Service Center of WO Forest Management Staff. http://andrewsforest.oregonstate.edu/pubs/webdocs/reports/decomp/cwd_decomp_web.htm.

Harmon ME, Sexton JM. 1996. Guidelines for measurements of woody detritus in forest ecosystems. U.S. Long Term Ecological Research Program Network Vol. 20. Albuquerque, NM.

Hessburg PF, Salter RB, James KM. 2007. Re-examining fire severity relations in pre-management era mixed conifer forests: inferences from landscape patterns of forest structure. Landscape Ecology 22:5-24.

Hicke JA, Asner GP, Kasischke ES, French NHF, Randerson JT, Collatz GJ, Stocks BJ, Tucker CJ, Los SO, Field CB. 2003. Postfire response of North American boreal forest net primary productivity analyzed with satellite observations. Global Change Biology 9:1145-1157.

Hudiburg T. 2008. Climate, management, and forest type influences on carbon dynamics of West-Coast US forests. M.S. Thesis. Oregon State University. 86 p.

Hudiburg T, Law BE, Turner DP, Campbell JL, Donato DC, Duane M. 2009. Carbon dynamics of Oregon and Northern California forests and potential land-based carbon storage. Ecological Applications 19:163-180.

Hurlbert, S.H. 1984. Pseudoreplication and the design of ecological field experiments. Ecological Monographs 54:187-211.

Hurteau MD, Koch GW, Hungate BA. 2008. Carbon protection and fire risk reduction: toward a full accounting of forest carbon offsets. Frontiers in Ecology and the Environment 6:493-498.

IPCC. 2007. Climate Change 2007: The physical science basis: Contribution of Working Group I to the Fourth Assessment Report of the Intergovernmental Panel on Climate Change (IPCC) [Solomon S, Qin D, Manning M, Chen Z, Marquis M, Averyt KB, Tignor M, Miller HL. (eds.)]. Cambridge University Press, Cambridge, United Kingdom and New York, NY, USA. http://www.ipcc.ch.

Irvine J, Law BE, Hibbard KA. 2007. Postfire carbon pools and fluxes in semiarid ponderosa pine in Central Oregon. Global Change Biology 13:1748-1760.

Irvine J, Law BE, Martin JG, Vickers D. 2008. Interannual variation in soil CO2 efflux and the response of root respiration to climate and canopy gas exchange in mature ponderosa pine. Global Change Biology 14:2848-2859.

Kagan JS, Hak JC, Csuti B, Kiilsgaurd CW, Gaines EP. 1999. Oregon gap analysis project final report: A geographic approach to planning for biological diversity.

Kang S, Kimball JS, Running SW. 2006. Simulating effects of fire disturbance and climate change on boreal forest productivity and evapotranspiration. Science of the Total Environment 362:85-102.

Kashian DM, Romme WH, Tinker DB, Turner MG, Ryan MG. 2006. Carbon storage on landscapes with stand-replacing fires. Bioscience 56:598-606.

Keane RE, Agee JK, Fule P, Keeley JE, Key C, Kitchen SG, Miller R, Schulte LA. 2008. Ecological effects of large fires on US landscapes: benefit or catastrophe? International Journal of Wildland Fire 17:696-712.

Keeley JE, Zedler PH. 2009. Large, high-intensity fire events in southern California shrublands: debunking the fine-grain age patch model. Ecological Applications 19:69-94.

Kennedy RE, Cohen WB, Schroeder TA. 2007. Trajectory-based change detection for automated characterization of forest disturbance dynamics. Remote Sensing of Environment 110:370-386.

Kennedy RE, Yang Z, Cohen WB. Detecting trends in disturbance and recovery using yearly Landsat Thematic Mapper stacks: 1. Processing and analysis algorithm. (In prep)

Key CH, Benson NC. 2006. Landscape assessment: Ground measure of severity, the Composite Burn Index; and remote sensing of severity, the Normalized Burn Ratio. In FIREMON: Fire effects monitoring and inventory system. USDA Forest Service General Technical Report RMRS-GTR-164-CD. Fort Collins, CO.

Keyes CR, Maguire DA. 2008. Some shrub shading effects on the mid-Summer microenvironment of ponderosa pine seedlings in Central Oregon. Northwest Science 82:245-250.

Körner C. 2003. Slow in, rapid out - Carbon flux studies and Kyoto targets. Science 300:1242-1243.

Kurz WA, Dymond CC, Stinson G, Rampley GJ, Neilson ET, Carroll AL, Ebata T, Safranyik L. 2008a. Mountain pine beetle and forest carbon feedback to climate change. Nature 452:987-990.

Kurz WA, Stinson G, Rampley GJ, Dymond CC, Neilson ET. 2008b. Risk of natural disturbances makes future contribution of Canada's forests to the global carbon cycle highly uncertain. Proceedings of the National Academy of Sciences of the United States of America 105:1551-1555.

Law BE, Arkebauer T, Campbell JL, Chen J, Sun O, Schwartz M, van Ingen C, Verma S. 2009. Terrestrial carbon observations: Protocols for vegetation sampling and data submission. Report 55, Global Terrestrial Observing System. FAO, Rome. 87 pp.

Law BE, Ryan MG, Anthoni PM. 1999. Seasonal and annual respiration of a ponderosa pine ecosystem. Global Change Biology 5:169-182.

Law BE, Sun OJ, Campbell JL, Van Tuyl S, Thornton PE. 2003. Changes in carbon storage and fluxes in a chronosequence of ponderosa pine. Global Change Biology 9:510-524.

Law BE, Thornton PE, Irvine J, Anthoni PM, Van Tuyl S. 2001a. Carbon storage and fluxes in ponderosa pine forests at different developmental stages. Global Change Biology 7:755-777.

Law BE, Turner D, Campbell JL, Sun OJ, Van Tuyl S, Ritts WD, Cohen WB. 2004. Disturbance and climate effects on carbon stocks and fluxes across Western Oregon USA. Global Change Biology 10:1429-1444.

Law BE, Van Tuyl S, Cescatti A, Baldocchi DD. 2001b. Estimation of leaf area index in open-canopy ponderosa pine forests at different successional stages and management regimes in Oregon. Agricultural and Forest Meteorology 108:1-14.

Lentile LB, Smith FW, Shepperd WD. 2005. Patch structure, fire-scar formation, and tree regeneration in a large mixed-severity fire in the South Dakota Black Hills, USA. Canadian Journal of Forest Research 35:2875-2885.

Luyssaert S, Schulze ED, Borner A, Knohl A, Hessenmoller D, Law BE, Ciais P, Grace J. 2008. Old-growth forests as global carbon sinks. Nature 455:213-215.

Mäkela A, Landsberg J, Ek AR, Burk TE, Ter-Mikaelian M, Agren GI, Oliver CD, Puttonen P. 2000. Process-based models for forest ecosystem management: current state of the art and challenges for practical implementation. Tree Physiology 20:289-298.

Martin RE, Sapsis DB. 1991. Fires as agents of biodiversity: pyrodiversity promotes biodiversity. In: Harris RR, Erman DE, Kerner HM, technical coordinators (Ed.), Proceedings of the symposium on biodiversity of northwestern California. Wildland Resources Center, Santa Rosa, CA, pp. 150-157.

Maser, C., Anderson, R.G., Cromack Jr, K., Williams, J.T., Martin, R.E. 1979. Dead and down woody material. Wildlife habitats in managed forests of the Blue Mountains of Oregon and Washington, USDA Forest Service Agriculture Handbook No. 553.

McIver JD, Ottmar RD. 2007. Fuel mass and stand structure after post-fire logging of a severely burned ponderosa pine forest in northeastern Oregon. Forest Ecology and Management 238:268-279.

McKenzie D, Raymond CL, Kellogg LKB, Norheim RA, Andreu AG, Bayard AC, Kopper KE, Elman E. 2007. Mapping fuels at multiple scales: landscape application of the Fuel Characteristic Classification System. Canadian Journal of Forest Research 37:2421-2437.

Means JE, Hansen HA, Koerper GJ, Alaback PB, Klopsch MW. 1994. Software for computing plant biomass-BIOPAK users guide. USDA Forest Service General Technical Report PNW-GTR-340. Portland, OR.

Miller JD, Safford HD, Crimmins M, Thode AE. 2009. Quantitative evidence for increasing forest fire severity in the Sierra Nevada and Southern Cascade Mountains, California and Nevada, USA. Ecosystems 12:16-32.

Mitchell SR, Harmon ME, O'Connell KEB. 2009. Forest fuel reduction alters fire severity and long-term carbon storage in three Pacific Northwest ecosystems. Ecological Applications 19:643-655.

Monsanto PG, Agee JK. 2008. Long-term post-wildfire dynamics of coarse woody debris after salvage logging and implications for soil heating in dry forests of the eastern Cascades, Washington. Forest Ecology and Management 255:3952-3961.

Mutch LS, Swetnam TW. 1995. Effects of fire severity and climate on ring-width growth of giant sequoia after burning. USDA Forest Service General Technical Report INT-GTR-320. Ogden, UT.

OFRI. 2006. Forests, Carbon, and Climate Change: A Synthesis of Science Findings. Oregon Forest Resources Institute (OFRI). Portland, OR.

Omernik JM. 1987. Ecoregions of the conterminous United States. Map (scale 1:7,500,000). Annals of the Association of American Geographers 77:118-125.

Ottmar RD, Sandberg DV, Riccardi CL, Prichard SJ. 2007. An overview of the Fuel Characteristic Classification System - Quantifying, classifying, and creating fuelbeds for resource planning. Canadian Journal of Forest Research 37:2383-2393.

Pierce LL, Running SW. 1988. Rapid estimation of coniferous forest leaf-area index using a portable integrating radiometer. Ecology 69:1762-1767.

Pietsch SA, Hasenauer H. 2006. Evaluating the self-initialization procedure for large-scale ecosystem models. Global Change Biology 12:1658-1669.

Prichard SJ, Ottmar RD, Anderson GK. 2006a. Consume 3.0 user's guide. Pacific Wildland Fire Sciences Laboratory, USDA Forest Service, Pacific Northwest Research Station. Seattle, WA. http://www.fs.fed.us/pnw/fera/research/smoke/consume/index.shtml.

Prichard SJ, Riccardi CL, Sandberg DV, Ottmar RD. 2006b. FCCS user's guide. Pacific Wildland Fire Sciences Laboratory, USDA Forest Service, Pacific Northwest Research Station. Seattle, WA. http://www.fs.fed.us/pnw/fera/fccs/index.shtml.

Potter C, Tan PN, Steinbach M, Klooster S, Kumar V, Myneni R, Genovese V. 2003. Major disturbance events in terrestrial ecosystems detected using global satellite data sets. Global Change Biology 9:1005-1021.

Powell SL, Healey SP, Cohen WB, Kennedy RE, Pierce KB, Moisen GG, Ohmann JL. Quantification of live aboveground forest biomass dynamics with Landsat time-series and field inventory data: A comparison of empirical modeling approaches. (In prep)

Reich, P.B., Bakken, P., Carlson, D., Frelich, L.E., Friedman, S.K., Grigal, D.F. 2001. Influence of logging, fire, and forest type on biodiversity and productivity in southern boreal forests. Ecology 82:2731-2748.

Rorig ML, Ferguson SA. 1999. Characteristics of lightning and wildland fire ignition in the Pacific Northwest. Journal of Applied Meteorology 38:1565-1575.

Roy DP, Boschetti L, Justice CO, Ju J. 2008. The collection 5 MODIS burned area product - Global evaluation by comparison with the MODIS active fire product. Remote Sensing of Environment 112:3690-3707.

Roy DR, Boschetti L, Trigg SN. 2006. Remote sensing of fire severity: Assesing the performance of the normalized Burn ratio. Ieee Geoscience and Remote Sensing Letters 3:112-116.

Running SW. 2008. Ecosystem disturbance, carbon, and climate. Science 321:652-653.

Running SW, Coughlan JC. 1988. A general model of forest ecosystem processes for regional applications: 1. Hydrologic balance, canopy gas-exchange and primary production processes. Ecological Modelling 42:125-154.

Running SW, Hunt ER. 1993. Generalization of a forest ecosystem process model for other biomes, BIOME-BGC, and an application for global scale models. In: Ehleringer, J.R., Field, C.B. (Eds.), Scaling physiological processes: leaf to globe. Academic Press, San Diego, pp. 141-157.

Russell RE, Saab VA, Dudley JG, Rotella JJ. 2006. Snag longevity in relation to wildfire and postfire salvage logging. Forest Ecology and Management 232:179-187.

Safford HD, Miller J, Schmidt D, Roath B, Parsons A. 2008. BAER soil burn severity maps do not measure fire effects to vegetation: A comment on Odion and Hanson (2006). Ecosystems 11:1-11.

Santantonio D, Hermann RK, Overton WS. 1977. Root biomass studies in forest ecosystems. Pedobiologia 17:1-31.

Savage M, Mast JN. 2005. How resilient are southwestern ponderosa pine forests after crown fires? Canadian Journal of Forest Research 35:967-977.

Schoennagel T, Veblen TT, Romme WH. 2004. The interaction of fire, fuels, and climate across Rocky Mountain forests. Bioscience 54:661-676.

Schwind B (Compiler). 2008. Monitoring Trends in Burn Severity: Report on the Pacific Northwest and Pacific Southwest fires -- 1984 to 2005. Available online: http://mtbs.gov.

Shatford JPA, Hibbs DE, Puettmann KJ. 2007. Conifer regeneration after forest fire in the Klamath-Siskiyous: How much, how soon? Journal of Forestry 105:139-146.

Simon SA. 1991. Fire history in the Jefferson Wilderness area of east of the Cascade Crest. A final report to the Deschutes National Forest Fire Staff.

Schwind B (Compiler) 2008. Monitoring Trends in Burn Severity: Report on the Pacific Northwest and Pacific Southwest fires -- 1984 to 2005. Available online: http://mtbs.gov.

Soeriaatmadhe RE. 1966. Fire history of the ponderosa pine forests of the Wam Springs Indian Reservation Oregon. Ph.D. Thesis. Oregon State University.

Stephens SL, Martin RE, Clinton NE. 2007. Prehistoric fire area and emissions from California's forests, woodlands, shrublands, and grasslands. Forest Ecology and Management 251:205-216.

Swedberg KC. 1973. Transition coniferous forest in the Cascade Mountains of Northern Oregon. American Midland Naturalist 89:1-25.

Sun OJ, Campbell JL, Law BE, Wolf V. 2004. Dynamics of carbon stocks in soils and detritus across chronosequences of different forest types in the Pacific Northwest, USA. Global Change Biology 10:1470-1481.

Swedberg, KC. 1973. Transition coniferous forest in the Cascade Mountains of Northern Oregon. American Midland Naturalist 89:1-25.

Tappeiner, JC, Helms JA. 1971. Natural regeneration of Douglas fir and white fir on exposed sites in the Sierra Nevada of California. American Midland Naturalist:358-370.

Thomas CK, Law BE, Irvine J, Martin JG, Pettijohn JC, Davis KJ. 2009. Seasonal hydrology explains inter-annual and seasonal variation in carbon and water exchange in a semi-arid mature ponderosa pine forest in Central Oregon. Journal of Geophysical Research, Biogeosciences, in press.

Thornton PE, Running SW, White MA. 1997. Generating surfaces of daily meteorological variables over large regions of complex terrain. Journal of Hydrology 190:214-251.

Thornton PE, Law BE, Gholz HL, Clark KL, Falge E, Ellsworth DS, Golstein AH, Monson RK, Hollinger D, Falk M, Chen J, Sparks JP. 2002. Modeling and measuring the effects of disturbance history and climate on carbon and water budgets in evergreen needleleaf forests. Agricultural and Forest Meteorology 113:185-222.

Turner DP, Ritts WD, Law BE, Cohen WB, Yang Z, Hudiburg T, Campbell JL, Duane M. 2007. Scaling net ecosystem production and net biome production over a heterogeneous region in the western United States. Biogeosciences 4:597-612.

Thornton PE, Running SW, White MA. 1997. Generating surfaces of daily meteorological variables over large regions of complex terrain. Journal of Hydrology 190:214-251.

Turner MG, Tinker DB, Romme WH, Kashian DM, Litton CM. 2004. Landscape patterns of sapling density, leaf area, and aboveground net primary production in postfire lodgepole pine forests, Yellowstone National Park (USA). Ecosystems 7:751-775.

USDA. 1996. Metolius Watershed Analysis. Deschutes National Forest, Sisters Ranger District. Sisters, OR.

USDA. 2003a. Field instructions for the annual inventory of Washington, Oregon, and California. Forest Inventory and Analysis Program. USDA Forest Service Pacific Northwest Research Station. Portland, OR.

USDA. 2003b. Metolius Basin Forest Management Project FEIS. Deschutes National Forest, Sisters Ranger District. Sisters, OR.

USDA. 2004. Metolius Watershed Analysis – Update. Deschutes National Forest, Sisters Ranger District. Sisters, OR.

Van Tuyl S, Law BE, Turner DP, Gitelman AI. 2005. Variability in net primary production and carbon storage in biomass across Oregon forests: An assessment integrating data from forest inventories, intensive sites, and remote sensing. Forest Ecology and Management 209:273-291.

Van Wagner CE. 1968. The line intersect method in forest fuel sampling. Forest Science 14:20-26.

Vogelmann JE, Howard SM, Yang LM, Larson CR, Wylie BK, Van Driel N. 2001. Completion of the 1990s National Land Cover Data set for the conterminous United States from Landsat Thematic Mapper data and Ancillary data sources. Photogrammetric Engineering and Remote Sensing 67:650-662.

Waring RH, Savage T, Cromack K Jr, Rose C. 1992. Thinning and nitrogen fertilization in a grand fir stand infested with western spruce budworm. Part IV: An ecosystem management perspective. Forest Science 38:275-286.

Weaver H. 1959. Ecological changes in the ponderosa pine forest of the Warm Springs Indian Reservation in Oregon. Journal of Forestry 57:15-20.

Wiedinmyer C, Quayle B, Geron C, Belote A, McKenzie D, Zhang XY, O'Neill S, Wynne KK. 2006. Estimating emissions from fires in North America for air quality modeling. Atmospheric Environment 40:3419-3432.

Westerling AL, Hidalgo HG, Cayan DR, Swetnam TW. 2006. Warming and earlier spring increase western US forest wildfire activity. Science 313:940-943.

White MA, Thornton PE, Running SW, Nemani RR. 2000. Parameterization and sensitivity analysis of the BIOME–BGC terrestrial ecosystem model: net primary production controls. Earth Interactions 4:1-85.

Wirth C, Czimczik CI, Schulze ED. 2002. Beyond annual budgets: Carbon flux at different temporal scales in fire-prone Siberian Scots pine forests. Tellus Series B-Chemical and Physical Meteorology 54:611-630.

Woolley TJ, Harmon ME, O'Connell KB. 2007. Estimating annual bole biomass production using uncertainty analysis. Forest Ecology and Management 253:202-210.

Zavitkovski J, Newton M. 1968. Ecological importance of snowbrush *Ceanothus velutinus* in the Oregon Cascades. Ecology 49:1134-1145.

APPENDICES

APPENDIX 1: WOODY SPECIES LIST.

Table A1. Tree and shrub species encountered in field study (Chapter 2).

Growth form	Code[a]	Common name	Botanical name (*Genus species* authorship)[b]	Forest type presence[c]
tree	ABIGRA	grand fir	*Abies grandis* (Douglas ex D.Don) Lindl.	both, generally MC
tree	CALDEC	incense-cedar	*Calocedrus decurrens* (Torr.) Florin	both
tree	JUNOCC	western juniper	*Juniperus occidentalis* Hook.	PP
tree	LAROCC	western larch	*Larix occidentalis* Nutt.	both, generally MC
tree	PICENG	Engelmann spruce	*Picea engelmannii* Parry ex Engelm.	MC
tree	PINCON	lodgepole pine	*Pinus contorta* Douglas ex Louden	both, generally MC
tree	PINLAM	sugar pine	*Pinus lambertiana* Dougl. ex Taylor & Philips[d]	PP
tree	PINMON	western white pine	*Pinus monticola* Douglas ex D.Don	MC
tree	PINPON	ponderosa pine	*Pinus ponderosa* Douglas ex P.Lawson & C.Lawson	both
tree	PSEMEN	Douglas-fir	*Pseudotsuga menziesii* (Mirb.) Franco	both
tree	THUPLI	western redcedar	*Thuja plicata* Donn ex D.Don[d]	MC
tree	TSUHET	western hemlock	*Tsuga heterophylla* (Raf.) Sarg.	MC
tree	TSUMER	mountain hemlock	*Tsuga mertensiana* (Bong.) Sarg.	MC
both	CASCHR	golden chinkapin	*Castanopsis chrysophylla* A.DC.	MC
both	UNKNOW	unknown	na[e]	both
shrub	ACECIR	vine maple	*Acer circinatum* Pursh	MC
shrub	ACEGLA	Rocky Mountain maple	*Acer glabrum* Torr.	MC
shrub	AMESPP	serviceberry	na[e]	both
shrub	ARCPAT	greenleaf manzanita	*Arctostaphylos patula* Greene	both
shrub	ARCUVA	kinnikinnick	*Arctostaphylos uva-ursi* (L.) Spreng.	MC
shrub	CEAPRO	squaw carpet	*Ceanothus prostratus* Benth.	both, generally PP

shrub	CEAVEL	snowbrush	*Ceanothus velutinus* Douglas ex Hook.[f]	both
shrub	CHIUMB	pipsissewa	*Chimaphila umbellata* (L.) Nutt.	both, generally MC
shrub	CHYVIS	yellow rabbitbrush	*Chrysothamnus viscidiflorus* Nutt.	PP
shrub	CORSPP	dogwood species	na[e]	both
shrub	HOLDIS	oceanspray	*Holodiscus discolor* (Pursh) Maxim.	both, generally MC
shrub	LONINV	twinberry honeysuckle	*Lonicera involucrata* (Richardson) Banks ex Spreng.	MC
shrub	MAHNER	Oregon grape	*Mahonia nervosa* (Pursh) Nutt.[g]	both, generally MC
shrub	PAXMYR	Oregon boxleaf	*Paxistima myrsinites* (Pursh) Raf.	MC
shrub	PRUPEN	pin cherry	*Prunus pensylvanica* L.f.	both
shrub	PURTRI	antelope bitterbrush	*Purshia tridentata* (Pursh) DC.	both, generally PP
shrub	RIBSPP	gooseberry/currant species	na[e]	both, generally MC
shrub	ROSSPP	rose species	na[e]	both, generally MC
shrub	RUBSPP	raspberry species	na[e]	MC
shrub	SALSPP	willow species	na[e]	both
shrub	SORSIT	mountain ash	*Sorbus sitchensis* M.Roem.[d,h]	MC
shrub	SYMALB	common snowberry	*Symphoricarpos albus* (L.) S.F.Blake	both, generally MC
shrub	VACSPP	vaccinium species	na[e]	MC

Notes:
[a] first three letters of genus and species combined.
[b] primary source: International Plant Names Index (http://www.ipni.org).
[c] plant association group: MC = mixed-conifer, PP = ponderosa pine.
[d] only 1 individual observed.
[e] na: identified to genus level only.
[f] source: USDA PLANTS Database (http://plants.usda.gov).
[g] could also be *M. aquifolium.*
[h] could also be *S. scopulina.*

APPENDIX 2: POSTFIRE TREE GROWTH. Influence of burn severity in mixed-conifer forests of the Metolius Watershed, OR

Note: This appendix was derived from an independent project by Lipi Gupta, a student at Crescent Valley High School who processed lab samples including tree cores. Lipi conducted her study during her freshman and sophomore years and won several honors. These included participation in the Central Western Oregon Science Expo (2008, 2009), North West Science Expo(2008, 2009), and Intel International Science and Engineering Fair (2009, Reno, NV), as well as multiple college scholarships and awards. Her final report is available upon request from Garrett Meigs.

Extended abstract

Question
Does tree growth change after fire?

Background
Although post-disturbance tree growth is vitally important for understanding and managing western North American forests, very few studies have quantified tree growth patterns following wildfire. Recent large fires in the Metolius Watershed provided an unusual opportunity to investigate tree growth responses to low- and moderate-severity wildfire. We hypothesized that (1) tree growth would initially decline due to fire damage and then exceed prefire growth due to the release of resources (reduced competition for light, nutrients, water); (2) Fire-resistant species would show positive growth responses whereas fire-sensitive species would show negative growth responses; (3) Growth responses in moderate-severity stands would exceed low-severity stands due to increased stand-level mortality and reduced competition among surviving trees.

Methods
We collected an extensive tree core dataset 4-5 years postfire as part of a broader study of postfire carbon dynamics (this thesis). For the current analysis, we compared 3 tree species—grand fir (*Abies grandis*), ponderosa pine (*Pinus ponderosa*), and Douglas-fir (*Pseudotsuga menziesii*)—across a representative range of tree sizes. We collected 20 cores at each of 16 1-ha plots and pooled data within 2 levels of overstory tree mortality (low and moderate severity) in mixed-conifer stands (number of stands in each condition: $n = 8$; total number of cores: $n = 277$). The 3 target species were evenly-distributed (Table A2.1); other tree species were surveyed but excluded from this analysis. We measured annual ring widths with the WinDendro[TM] program and computed a growth index based on the ratio of postfire growth (fire year and each year postfire) to prefire growth (mean of 6 y prefire), after normalizing for size-dependent growth differences (*i.e.,* converting ring widths [mm] to percentage of the last 10 y).

Results and Discussion

The three species showed surprisingly strong and consistent growth trends in both burn severity classes (Fig. A2.2). Douglas-fir postfire growth was higher than prefire, whereas ponderosa pine postfire growth was lower than prefire, and grand fir growth was generally conserved. The positive Douglas-fir response was especially evident in the low-severity class, and the two other species' responses were consistent between severities (Fig. A2.2).

No clear postfire temporal trends were evident (hypothesis 1 not supported). The positive response of Douglas-fir (fire resistant) supported hypothesis 2, but the negative response of ponderosa pine (fire resistant) and neutral response of grand fir (fire sensitive) were inconsistent with hypothesis 2. The strong response of Douglas-fir in low-severity and similarity between severities for the other two species did not support hypothesis 3.

Possible explanatory factors for species differences include differential damage, differential competitive fitness, or inherent species differences in immediate post-disturbance growth and carbon allocation. For example, Douglas-fir may have suffered less overall damage, responded more rapidly to available resources, allocated photosynthate to stem growth, or may be generally more responsive to sudden environmental changes. Conversely, ponderosa pine may have suffered greater damage to fine roots in the forest floor, may be less competitive in these mixed-conifer stands, or may take several years to exhibit positive growth responses (consistent with Hypothesis 1). Finally, the surprising lack of reduced growth in grand fir may be attributable to the live trees (the ones that were cored) being the survivors, whereas many grand firs died in both low- and moderate-severity fire (*i.e.,* same factors predisposed trees to survival and neutral growth response). The strong Douglas-fir response in low-severity fire suggests that this level of mortality (10-35% basal area mortality) resulted in a pulse of available resources without damaging surviving trees, whereas moderate-severity fire (35-75% basal area mortality) damaged all trees substantially, including survivors.

Conclusions

These results suggest that Douglas-fir was the clear winner in the immediate postfire period, whereas ponderosa pine may not readily recover from recent fires. This study underscores the importance of individual species responses and the variability intrinsic to mixed-severity fire regimes. It also highlights the need for further research in multiple fires, forest types, and climatic conditions, particularly over longer postfire time intervals.

Figures and Tables
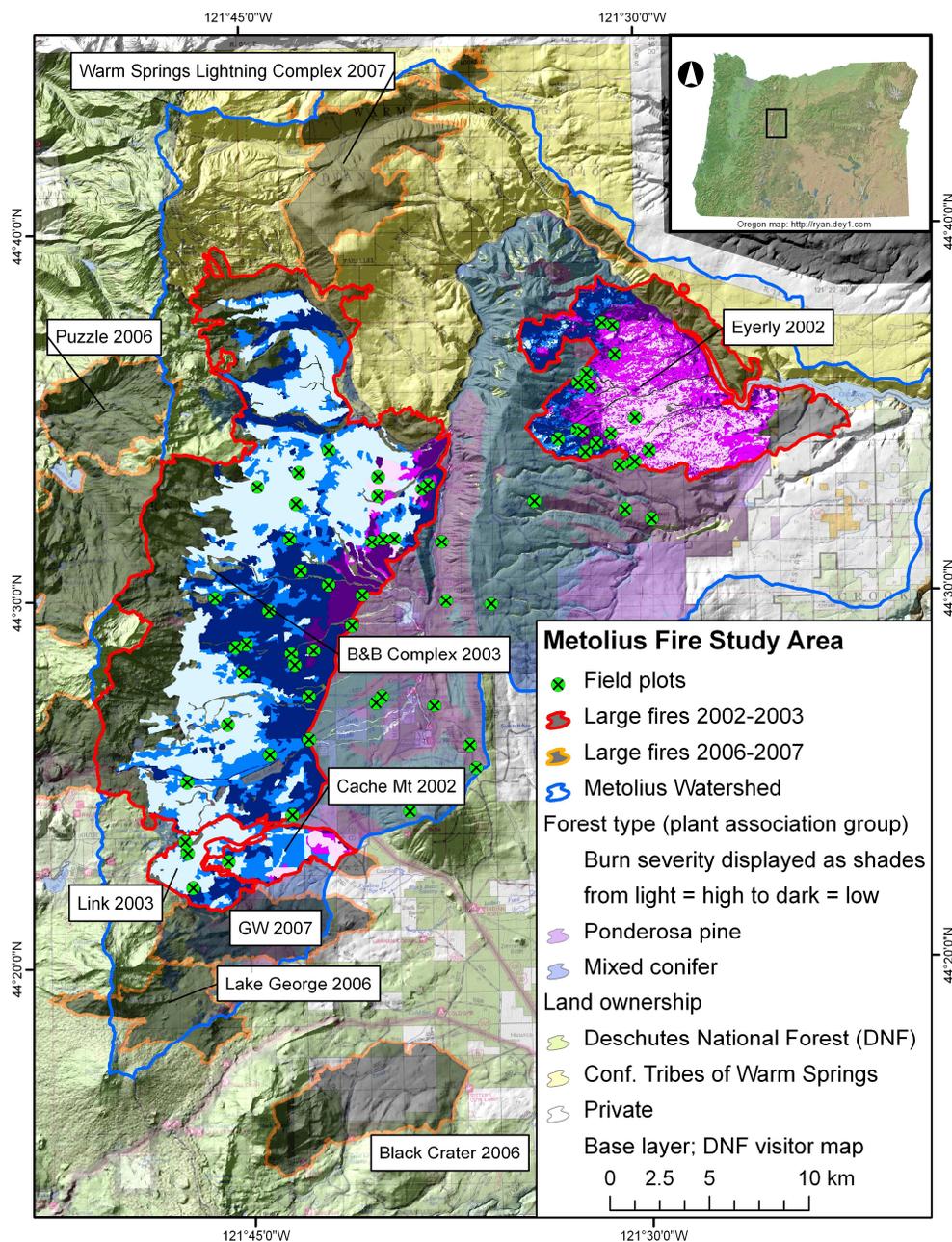
Figure A2.1. Metolius fire study area on the east slope of the Oregon Cascades. Point symbols denote survey plots ($n = 64$). Forest type layer clipped to study scope: two types (MC and PP) on the Deschutes National Forest (DNF) within the Metolius Watershed. Other types (uncolored area within fires) include subalpine forests on the western margin and *Juniperus* woodlands to the east. Inset map shows study area location within Oregon. Fire perimeter and forest type GIS data from DNF. Other GIS data from archives at Oregon State University. See also black and white map in Figure 2.1 (Chapter 2).
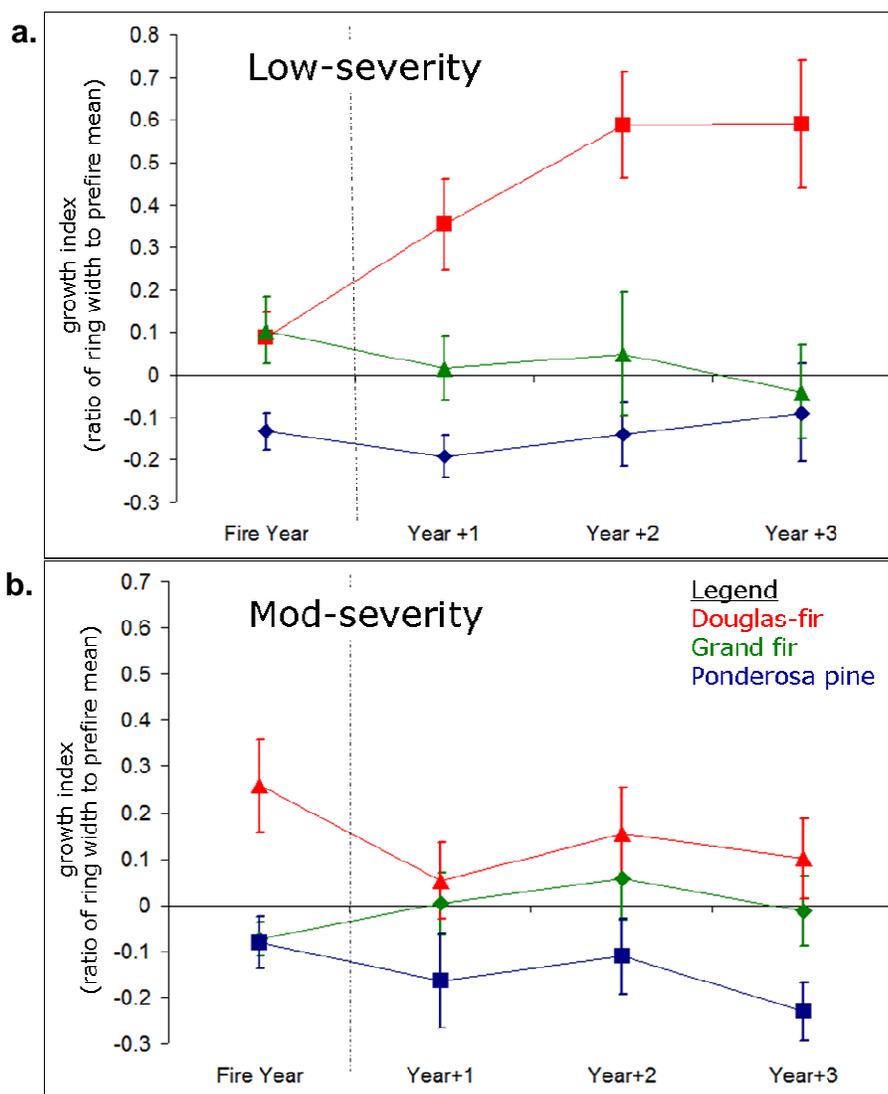
Figure A2.2. Tree growth following (a) low- and (b) moderate-severity fire. Points denote species mean of the growth index (see Appendix text). Error bars denote ±1 SE of the mean. Tree cores collected from live trees ($n = 277$) for NPP computation. Severity classes from Chapter 2. Note the strong positive response of Douglas-fir, neutral response of grand fir, and negative response of ponderosa pine.

Table A2.1. Number of tree core samples by species and severity (Total $n = 277$).

Tree Species	Moderate Severity	Low Severity
Ponderosa pine	49	31
Grand fir	42	42
Douglas-fir	49	64
Total	140	137

APPENDIX 3. SHRUB COMMUNITY RESPONSE TO FIRE. Key figures and tables on shrub community dynamics among forest types and burn severities.

Note: This appendix was derived from an independent project by Adam Pfleeger, an undergraduate student at Western Washington University who worked in the field (2007, 2008) and had a special love for the shrubs. Dan Donato worked closely with Adam on data analysis. Adam's final report is available upon request from Garrett Meigs.
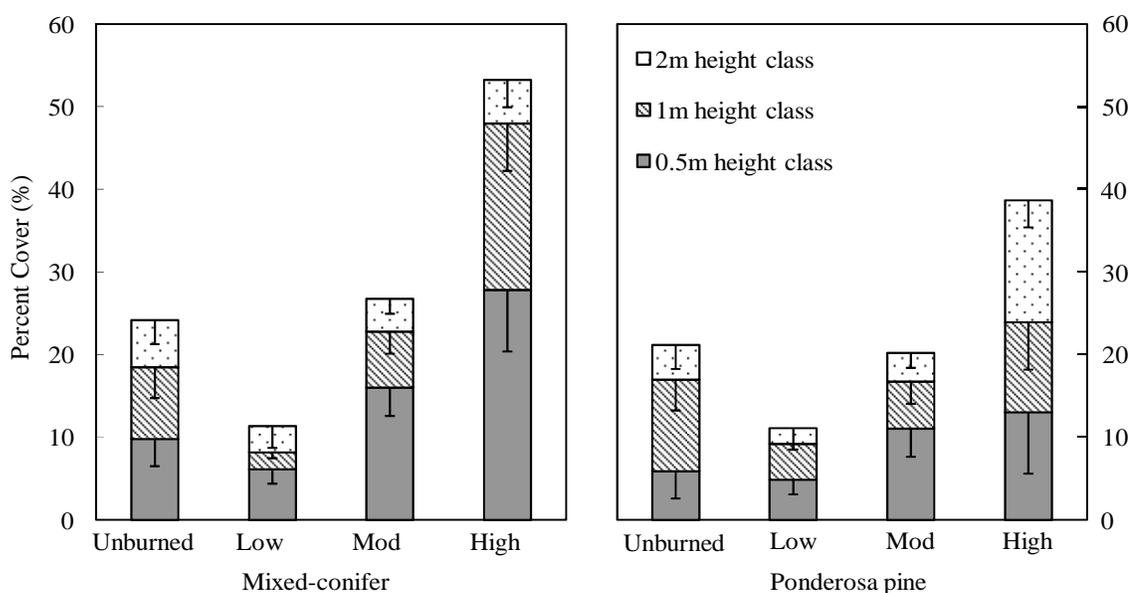
Figure A3.1. Percent cover of live shrubs 4-5 y postfire by forest type, burn severity, and height class. Bars denote means; error bars denote -1 SE from 8 plots in each forest type*burn severity treatment (total *n* = 64). Note that the pattern generally follows the same trend as shrub biomass (Figure 2.5), with declines in shrub cover from unburned to low severity but strong increases with increasing tree mortality.
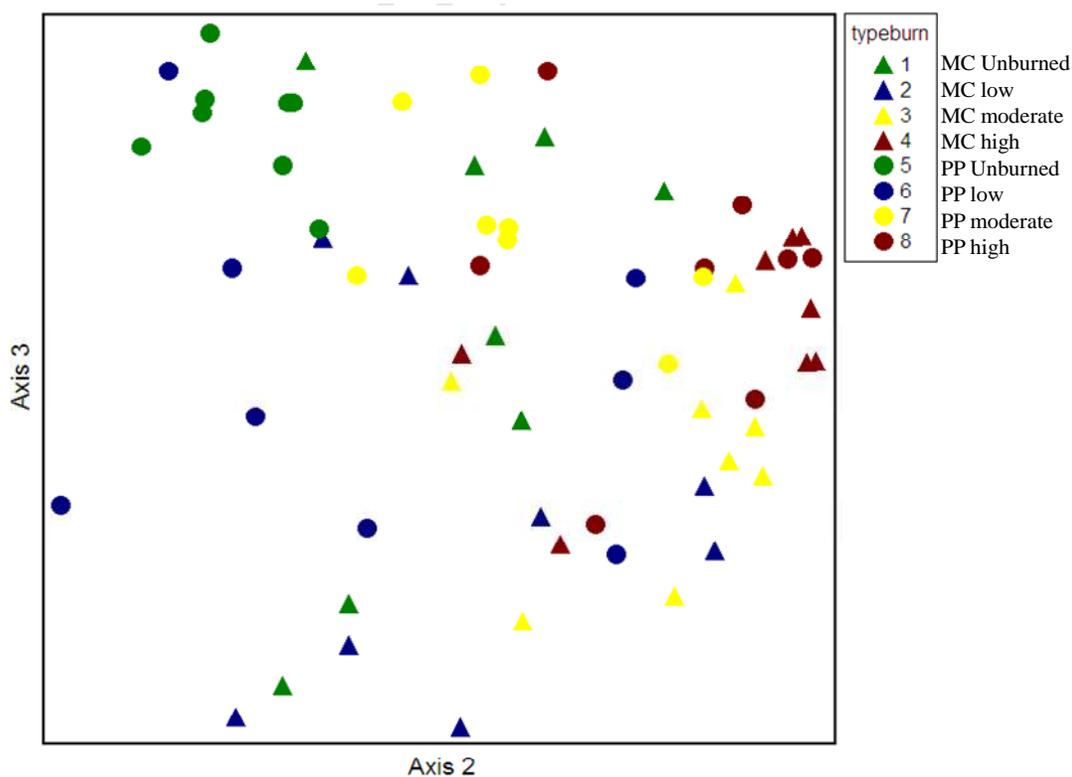
Figure A3.2. Nonmetric multidimensional scaling ordination of shrub species composition across forest type and burn severity gradients 4-5 y postfire. Points close together are more similar compositionally. This figure indicates strong grouping by severity classes, except for low-severity stands, which are widely spaced in this variable space. Forest types are generally similar except for the moderate-severity stands, for which forest types diverge along Axis 3.

Table A3.1. Shrub species and indicator values by forest type and burn severity 4-5 y postfire.

| Species | Indicator value[a] (group) | Mixed-conifer | | | | | | | | Ponderosa pine | | | | | | | |
| | | Unburned | | Low severity | | Mod. severity | | High severity | | Unburned | | Low severity | | Mod. severity | | High severity | |
		% cover (SE)	% freq	% cover (SE)	% freq	% cover (SE)	% freq	% cover (SE)	% freq	% cover (SE)	% freq	% cover (SE)	% freq	% cover (SE)	% freq	% cover (SE)	% freq
Acer circinatum	11.9 MC-U	1.5 (1.5)	13	0.0 (0.0)	0	0.1 (0.0)	25	0.0 (0.0)	13	0.0 (0.0)	0	0.0 (0.0)	0	0.0 (0.0)	0	0.0 (0.0)	0
Acer glabrum	7.1 MC-H	0.0 (0.0)	0	0.1 (0.1)	13	0.1 (0.1)	25	0.3 (0.3)	13	0.0 (0.0)	0	0.0 (0.0)	0	0.0 (0.0)	0	0.0 (0.0)	0
Amelanchier alnifolia	**39.7 MC-U**	1.3 (0.6)	75	0.0 (0.0)	25	0.0 (0.0)	13	0.1 (0.0)	25	0.5 (0.3)	75	0.1 (0.0)	63	0.2 (0.1)	25	0.2 (0.1)	25
Arctostaphylos patula	**29.7 PP-H**	4.2 (3.2)	63	0.6 (0.4)	50	2.1 (1.8)	88	4.3 (1.9)	75	1.2 (0.5)	88	1.4 (0.7)	75	8.6 (1.4)	100	9.5 (3.6)	100
Arctostaphylos uva-ursi	21.7 MC-U	1.6 (1.4)	25	0.0 (0.0)	0	0.3 (0.3)	13	0.0 (0.0)	0	0.0 (0.0)	0	0.0 (0.0)	0	0.0 (0.0)	0	0.0 (0.0)	0
Ceanothus velutinus	**37.8 MC-H**	4.2 (3.1)	50	3.9 (1.8)	100	12.3 (3.3)	100	35.9 (9.0)	100	0.6 (0.3)	50	5.4 (2.9)	75	6.9 (4.1)	75	25.9 (8.5)	88
Chimaphila umbellata	21.8 MC-U	1.1 (0.6)	50	0.7 (0.4)	63	0.3 (0.2)	50	0.2 (0.2)	38	0.2 (0.1)	38	0.0 (0.0)	13	0.0 (0.0)	0	0.0 (0.0)	0
Chrysolepis chrysophylla	12.8 MC-L	0.1 (0.1)	25	2.0 (1.3)	25	0.5 (0.3)	38	1.3 (1.2)	38	0.0 (0.0)	0	0.0 (0.0)	0	0.0 (0.0)	0	0.0 (0.0)	0
Chrysothamnus viscidiflorus	24.0 PP-U	0.0 (0.0)	0	0.0 (0.0)	0	0.0 (0.0)	0	0.0 (0.0)	0	0.3 (0.2)	38	0.0 (0.0)	0	0.1 (0.1)	38	0.0 (0.0)	13
Cornus nuttallii	8.3 MC-M	0.0 (0.0)	0	0.0 (0.0)	0	0.1 (0.1)	13	0.0 (0.0)	0	0.0 (0.0)	0	0.0 (0.0)	0	0.0 (0.0)	13	0.0 (0.0)	13
Holodiscus discolor	11.2 MC-U	1.6 (1.6)	13	0.0 (0.0)	13	0.1 (0.0)	25	0.0 (0.0)	0	0.0 (0.0)	0	0.1 (0.1)	13	0.0 (0.0)	13	0.0 (0.0)	0
Lonicera involucrata	12.5 MC-M	0.0 (0.0)	0	0.0 (0.0)	0	0.1 (0.1)	13	0.0 (0.0)	0	0.0 (0.0)	0	0.0 (0.0)	0	0.0 (0.0)	0	0.0 (0.0)	0

Species	Indicator value / Group	Mean (SE)	%	Mean (SE)	%	Mean (SE)	%	Mean (SE)	%	Mean (SE)	%	Mean (SE)	%	Mean (SE)	%	Mean (SE)	%
Lonicera utahensis	12.5 MC-U	0.0 (0.0)	13	0.0 (0.0)	0	0.0 (0.0)	0	0.0 (0.0)	0	0.0 (0.0)	0	0.0 (0.0)	0	0.0 (0.0)	0	0.0 (0.0)	0
Mahonia nervosa	24.0 MC-H	0.7 (0.5)	38	0.3 (0.3)	25	0.5 (0.3)	50	1.7 (1.0)	50	0.0 (0.0)	0	0.1 (0.1)	25	0.0 (0.0)	0	0.2 (0.1)	25
Paxistima myrsinites	**46.7 MC-H**	0.0 (0.0)	0	0.0 (0.0)	0	0.5 (0.3)	38	1.4 (0.5)	63	0.0 (0.0)	0	0.0 (0.0)	0	0.0 (0.0)	0	0.0 (0.0)	0
Prunus virginiana	15.8 MC-H	0.1 (0.1)	13	0.0 (0.0)	0	0.0 (0.0)	13	0.5 (0.4)	25	0.0 (0.0)	38	0.0 (0.0)	0	0.1 (0.1)	25	0.0 (0.0)	0
Purshia tridentata	**59.5 PP-U**	4.3 (3.1)	50	0.6 (0.5)	25	0.0 (0.0)	0	0.0 (0.0)	0	17.8 (2.3)	100	3.8 (2.2)	88	2.9 (1.0)	100	0.5 (0.2)	50
Ribes spp.	**47.2 MC-H**	0.2 (0.2)	25	0.2 (0.2)	50	1.5 (0.7)	63	2.4 (0.6)	88	0.0 (0.0)	13	0.0 (0.0)	0	0.0 (0.0)	0	0.1 (0.1)	25
Rosa gymnocarpa	**32.2 MC-H**	0.6 (0.3)	63	1.5 (1.5)	38	1.1 (0.4)	88	3.2 (1.4)	75	0.1 (0.1)	13	0.0 (0.0)	0	0.1 (0.0)	25	0.9 (0.4)	50
Salix spp.	**48.7 MC-M**	0.0 (0.0)	0	0.9 (0.6)	63	4.9 (4.6)	88	0.4 (0.2)	50	0.0 (0.0)	13	0.2 (0.1)	50	1.2 (0.8)	63	1.3 (0.6)	50
Sorbus scopulina	12.5 MC-L	0.0 (0.0)	0	0.0 (0.0)	13	0.0 (0.0)	0	0.0 (0.0)	0	0.0 (0.0)	0	0.0 (0.0)	0	0.0 (0.0)	0	0.0 (0.0)	0
Symphoricarpos albus	23.6 MC-U	2.2 (1.2)	63	0.5 (0.4)	50	1.7 (1.3)	38	0.9 (0.3)	63	0.3 (0.2)	38	0.1 (0.1)	25	0.0 (0.0)	13	0.1 (0.1)	25
Vaccinium spp.	15.4 MC-H	0.4 (0.4)	13	0.0 (0.0)	13	0.7 (0.5)	38	0.8 (0.4)	38	0.0 (0.0)	0	0.0 (0.0)	0	0.0 (0.0)	0	0.0 (0.0)	0

Notes:
[a] Indicator value (0-100) indicates species relationship with forest type-burn severity groups ($n = 8$ stands in each group, total $n = 64$). Bold denotes species significantly related to group ($P < 0.05$). Group abbreviations: MC = mixed-conifer, PP = ponderosa pine, U = unburned, L = low severity, M = moderate severity, H = high severity.
See Chapter 2 for methods on overall study design and shrub sampling.

Implications of shrub results

The different burn severities had a major impact on shrub cover and on many individual species. In general, shrubs responded rapidly, and shrub percent cover paralleled burn severity, with higher cover in stands with higher overstory tree mortality). Interestingly, shrub cover in moderate-severity stands was equivalent shrub cover in unburned stands, possibly indicating that low-severity fires are not sufficient to induce rapid shrub growth.

Individual species showed generally low overall percent cover, with the exception of *Arctostaphylos patula, Ceanothus velutinus,* and *Purshia tridentata*, the only species with values >5%. The former two species were the most widespread (highest % frequency) across the study, whereas *Purshia tridentata* was associated with the PP forest type and several species were associated closely with the MC forest type, including *Chimaphila umbellate, Ribes spp., Rosa gymnocarpa,*and *Vaccinium spp.* MC forests also showed generally higher shrub species richness than PP forests (mean richness: 7 vs. 5, respectively). Shrub species diverged in their affinities to varying burn severity. Key species that were positively associated with burn severity include *Arctostaphylos patula, Ceanothus velutinus, Mahonia nervosa, Paxistima myrsinites, Ribes spp., Rosa gymnocarpa* and *Salix spp.* Species that responded negativity to fire (*i.e.,* found in unburned and low-severity stands) were *Amelanchier alnifolia* and *Purshia tridentata.* Species that were generally neutral to burn severity included *Chrysolepis chrysophylla, Holodiscus discolor, Prunus virginiana,* and *Symphoricarpos albus.*

The ecological significance of shrubs in the immediate postfire environment and throughout succession are broad: quick regeneration (sprout or seed), soil stabilization, food and habitat for wildlife, shade for other vegetation (including tree seedlings), and much more. This importance is intensified in high-severity fires, where shrubs can dominate vegetative cover and play a key pioneering role in the sometimes extreme postfire conditions.

APPENDIX 4. SOIL PARAMETERS. Soil nitrogen, pH, texture, and depth by forest type and burn severity 4-5 y postfire.

Table A4.1.

Forest type Burn severity	Soil N to 20 cm (g N m^{-2})		Soil N to 100 cm[a] (g N m^{-2})		pH		% sand[b]		% silt[b]		% clay[b]		Bulk density[c] (g cm^{-3})		Soil depth, shallow[d] (cm)		Soil depth, deep[e] (cm)	
Mixed-conifer[f]	128	(9)	270	(19)	6.48	(0.04)	73.3	(1.3)	22.5	(1.1)	4.2	(0.5)	0.82	(0.02)	19.6	(0.3)	48.8	(3.4)
Low severity	118	(13)	249	(27)	6.51	(0.06)	71.2	(2.6)	23.3	(1.8)	5.5	(1.1)	0.85	(0.03)	19.4	(0.6)	44.8	(6.6)
Mod severity	129	(14)	272	(30)	6.50	(0.07)	73.1	(2.3)	23.1	(2.1)	3.8	(0.8)	0.78	(0.06)	19.4	(0.6)	42.4	(4.3)
High severity	137	(20)	289	(42)	6.43	(0.07)	75.7	(2.0)	21.1	(1.7)	3.2	(0.5)	0.82	(0.04)	20.0	(0)	59.3	(5.4)
Ponderosa pine[f]	120	(6)	253	(13)	6.54	(0.03)	64.2	(1.0)	26.3	(0.6)	9.4	(0.7)	0.95	(0.02)	17.7	(0.7)	40.4	(2.4)
Low severity	118	(9)	248	(19)	6.51	(0.05)	66.1	(1.9)	25.9	(1.4)	8.0	(1.4)	0.91	(0.02)	18.1	(1.3)	42.8	(3.4)
Mod severity	125	(15)	263	(32)	6.56	(0.04)	63.9	(1.4)	26.4	(0.9)	9.7	(0.9)	0.94	(0.03)	16.3	(1.6)	34.6	(4.2)
High severity	118	(7)	247	(15)	6.56	(0.05)	62.7	(1.6)	26.8	(0.5)	10.5	(1.4)	1.00	(0.04)	18.8	(0.8)	43.8	(4.5)

Notes:
Values are the mean of each forest type*severity treatment (*n* = 8 stands per treatment, *n* = 24 stands per forest type). SE of the mean in parentheses.
[a] Soil N to 100 cm depth, modeled from 20 cm depth (study-wide correction factor: 48% [SD = 17] of soil N assumed in top 20 cm). Mass fraction of N from LECO CNS 2000 analyzer, Oregon St. Univ. Central Analytical Laboratory.
[b] Soil texture by hydrometer method, Oregon St. Univ. Central Analytical Laboratory.
[c] Bulk density from mass and volume of mineral soil passed through 2 mm sieve.
[d] Rocky soils at some stands precluded consistent sampling to 20 cm depth, particularly moderate-severity ponderosa pine stands.
[e] One deep core sampled per plot, up to 100 cm.
[f] Italics denote mean and SE from burned plots. Soil not surveyed in unburned stands.

APPENDIX 5. UNBURNED NEP EVALUATION.

Figure A5.1 Modeled vs. observed NEP (g C m^{-2} y^{-1}) at unburned plots in 2001. Observations from field measurements described in Law *et al.* (2003). Plot (b) shows the mean and SE of points in (a).